ABSTRACT

LLOYD, BRIAN JEFFERY. Analysis of radiant heating to produce an alternative frying process. (Under the direction of Brian E. Farkas, Kevin M. Keener, and S. Andrew Hale.)

Immersion frying is one of the most popular methods of preparing foods. Consumers enjoy fried foods due to convenience, low cost, and appealing taste. Sensorial properties include a golden color, crunchy crust, tender and moist core, and a pleasing flavor. Producers of fried products benefit from high throughput and sales of a value-added product.

Unfortunately, there are several disadvantages of immersion frying and fried foods. Product disadvantages include variable oil quality and oil content in the finished material. The high caloric content of fried foods is primarily derived from the high oil content. With billions of pounds of fried foods produced and consumed each year in the United States, oil content in fried foods may be considered to significantly impact consumer health through obesity and obesity related health problems. Other problems associated with immersion frying include cost of waste oil disposal, need for use of caustic cleaning agents, and the large number of accidents associated with immersion fryers each year. An alternative immersion frying process would be beneficial to consumers and producers alike.

The focus of this project was to study radiant heating as an alternative finish frying process. This overall goal was separated into three separate objectives: (1) an analysis of radiant emitters, (2) an analysis of quality indices of radiant heated potatoes, and (3) a numerical simulation of radiant heating of potato.

Radiant emission from short, medium, and long wavelength thermal radiant emitter systems typically used for food processing applications were quantified. Measurements included heat flux intensity, emitter surface temperature, and spectral wavelength

distribution. Heat flux measurements were found highly dependent on the incident angle and the distance from the emitter facing. The maximum flux measured was 5.4 W/cm^2. Emitter surface temperature measurements showed that short wavelength radiant systems had the highest surface temperature and greatest thermal efficiency. The emitter spectral distributions showed that radiant emitter systems had large amounts of far infrared energy emission greater than 3 μm when compared to theoretical blackbody curves. The longer wavelength energy would likely cause increased surface heating for most high moisture content food materials.

The effect of finish heating method: immersion frying, oven heating or dynamic radiant heating was evaluated for texture, color, and sensory properties of par-fried French fries. Peak breaking force was highest for radiant heated French fry samples. Color analysis revealed equivalent b-value (yellowness) of crust color for immersion fried and radiant heated French fries. Sensory evaluation indicated overall acceptability of radiant heated French fries equivalent to traditional immersion fried French fried potatoes.

A numerical simulation of high intensity radiant heating was developed for a potato slab. The simulation predicted the temperature profile throughout in a one-dimensional slab. A surface crust and core region were defined and the increase in crust thickness was tracked during radiant heating. Measured surface and core temperatures showed excellent agreement with simulation results producing an average deviation of less than 3°C during 15,000 and 27,000 W/m^2 constant flux heating. The simulation could be used as a tool to evaluate radiant heating of products to simulate immersion frying and crust formation.

ANALYSIS OF RADIANT HEATING TO PRODUCE AN ALTERNATIVE FRYING PROCESS

by

BRIAN JEFFERY LLOYD

A dissertation submitted to the Graduate Faculty of
North Carolina State University
in partial fulfillment of the
requirements for the degree of
Doctor of Philosophy

FOOD SCIENCE

BIOLOGICAL AND AGRICULTURAL ENGINEERING

Raleigh

2003

APPROVED BY:

_____	_____
_____	_____
Co-chair of Advisory Committee	Co-chair of Advisory Commitee

DEDICATION

To all of my teachers, my personal pursuit of knowledge and understanding has been encouraged, enlightened, nurtured, and challenged by some of the best teachers in the world. I shall never forget your sacrifices of time and energy used to develop my academic skills. For the rest of my life, may my teaching ability to others never lack zeal, uphold the highest standard, and always include loving patience and persistence. I dedicate this work to you as a tribute and thanks to the extra effort put forth to help me learn.

BIOGRAPHY

Brian Jeffery Lloyd was born to Cleo and Beverly Lloyd on November 6, 1974, in Fayetteville, Arkansas. Brian and his brother Brad were raised in rural Washington County near the community of Sonora. He attended elementary, junior, and senior high school at the nearby city of Springdale, Arkansas.

While growing up, Brian was active in agriculture both at home and in school. He assisted in the family's small scale cattle farming operation. He also restored two antique tractors, a John Deere 420 and an International Super W-6. He was an active FFA member in High School, and earned National FFA honors in poultry judging as a member of the top ranking team and overall high individual. Brian was active in the First Baptist Church of Springdale and became a born-again Christian during high school

After graduating from high school in 1993, Brian went on to the University of Arkansas. He earned a Bachelor of Science in Biological and Agricultural Engineering in 1997 graduating Magna Cum Lade. Immediately he began a graduate program under the direction of Dr. Terry Siebenmorgen at Arkansas in the area of food processing. Brian graduated with a Masters of Science in the fall of 1999 then married Alisha Ballard in the winter of 1999. In the fall of 2000, Brian began a USDA doctorate fellowship program at North Carolina State University under Dr. Kevin Keener and Dr. Brian Farkas. In December of 2003, Brian will receive a Doctorate of Philosophy with dual majors in Food Science and Biological and Agricultural Engineering.

ACKNOWLEDGEMENTS

I would like to give my sincere thanks to my graduate committee for their support and guidance through the course of my program. I sincerely appreciate Dr. Kevin Keener's willingness to include me to work on the creation of the Food Sanitation course (FS 592K). This project challenged my computer skills, established my distance education teaching ability, and invoked my overall creativity to rise to a new level. I always appreciate Dr. Keener's positive 'can do' attitude. I would also like to give thanks Dr. Andy Hale for encouragement and critical analysis through some of the more difficult aspects of my research. I also appreciate Dr. Hale representing the Biological and Agricultural Engineering Department with firm support yet fairness during a dual major undertaking. Thirdly, I would like to extend my appreciation to Dr. Lee-Ann Jaykus as the Food Safety minor representative. Thank you Dr. Jaykus for upholding the food safety aspect of my program in a challenging way in light of the fact that my research did not directly involve food safety research. Finally, I would like to warmly express appreciation to Dr. Brian Farkas. Thank you Brian for encouragement, guidance, and grounding me in the floundering times during my program. I have thoroughly enjoyed working with you while co-teaching classes, writing grants and journal articles, or investigating new processing procedures. I cherish the time I have spent with you. It is clear to me that you are the rare breed of academic professor that befriends, mentors, challenges, and finishes students in a professional yet personal manner. Thank you for being a good example and a friend.

I want to also thank the fellow graduate students in the office and the lab that I have learned from and became friends with. Special appreciation to Pablo Coronel for helping me with computer problems or any other task. Pablo, you have become a wonderful friend and

will always be a part of my most cherished graduate school memories at NC State. I also appreciate Jack Canady for helping me with mechanical and electrical aspects of my project. Thank you Jack also for standing for what is right spiritually and politically. I also want to thank Gary Cartwright and the dairy plant workers for befriending me and sharing many great lunchtime stories and laughs. Thank you guys.

Next, my deepest appreciation to my loving wife, Alisha. Thank you for your patience and perseverance during this time. Without your love and unconditional support this work would not have been possible. You have often seen more in me than I saw in myself. It brings me great joy to share this success with you for the rest of my life. I also thank my parents, Cleo and Beverly Lloyd, and brother Brad Lloyd for encouragement and believing in me during this time. I love you all dearly. Most importantly, I would like to acknowledge God's love and encouragement during my academic career. The spiritual refreshment I received in the Bible, from my church family, and especially the Holy Spirit in my heart always brought encouragement, joy, and proper focus at the right times during this project. May my academic accomplishments be used by you Lord Jesus.

TABLE OF CONTENTS

LIST OF TABLES

LIST OF FIGURES

LIST OF APPENDIXES

INTRODUCTION

Americans enjoy fried foods. It is estimated that the fried foods industry is a $75 billion dollar industry in the United States with a value at least double that for the rest of the world (Blumenthal, 1996). Fried foods include a host of products such as corn and potato chips, doughnuts, chicken nuggets, and breaded seafood. The most popular fried food is French fries with over 4 million tons consumed annually in the United States with exports of par-fried French fries over 1 billion pounds and growing (USDA, 2002). The majority of French fries are served in quick serve restaurants (QSR) as a side item. Processors and producers of fried foods benefit from a high throughput and sales of a safe, value-added product. Consumers enjoy fried products such as French fries because of the convenience, low cost, and appealing taste. Sensorial properties include a golden color, crunchy crust, tender and moist core, and a pleasing flavor.

While the process and product are popular, there are several key disadvantages of frying and fried foods. Product disadvantages are principally associated with oil quality and oil content of the final product. The foremost concern is the high caloric content of fried foods, primarily derived from the high oil content. By weight, chips may contain over 40% oil, doughnuts 20%, and French fries 15-20%. A large order of French fries contains, on average, approximately 540 calories and 26 g of fat (McDonalds, 2003). The FDA recommended daily intake (RDI) based on a 2,000 calorie diet is 65 g of fat (USDA, 2003), thus one large order of French fries approaches 45% of the RDI for fat. As billions of pounds of fried foods are produced and consumed each year in the United States alone, oil content in fried foods may be considered to significantly impact consumer health through

obesity and obesity related health problems such as heart disease and high cholesterol (Saguy and Pinthus, 1995; SFA, 1997).

One of the biggest challenges with the frying industry is the control of oil uptake and oil movement within a fried product (Ufheil and Escher, 1996; Moreira et al. 1997). The use of various product coatings have led to decreases in oil uptake (Holownia et al., 2000; Rayner et al., 2000) but the process still suffers from a lack of control of this variable.

Other disadvantages of immersion frying pertain to the use of finish fryers in QSRs. Frying oil degradation reduces oil and product quality as the oil ages and changes in chemical composition (Blumenthal, 1991). Other disadvantages include: initial oil cost, variable oil quality, cost of waste oil disposal, need for use of caustic cleaning agents, and the large number of burn accidents associated with immersion fryers that occur each year (CDC, 1993).

The majority of fryers in QSRs are used for finish frying of par-fried foods such as French fries, chicken strips, and seafood. An estimated 750,000 fryers are used in QSRs nationwide (NAFM, 2002), this figure does not include institutions and wholesale manufacturers. Development of an alternative finish frying process would be of great economic importance to the snack food, food service, and fast food industries. The ideal process would produce the desirable characteristics of fried products, allow controlled oil content of the finished product, and replace the deep fat fryer in the QSR and other food service establishments eliminating or reducing the use of hot oil and hazards associated with its use.

Development of such a process begins with an understanding of the heat transfer during immersion frying. The high rate of heat flux which foods experience during

immersion frying was first proposed by Farkas and Hubbard (2000) to partially govern the unique characteristics of fried foods. Hubbard and Farkas (1999) measured the heat flux at the solid/liquid interface during the boiling regime of immersion frying of Russet potatoes. It was found that frying did not constitute a constant rate heat transfer but a rather a dynamic heating process with initial rates on the order of 30,000 W/m^2.

Alternative methods to mimic immersion frying developed thus far have used convection air heat transfer and/or constant flux radiant heating. Though some success has been met by each process; however, limitations have existed. Convection heating cannot deliver the intense heat flux required for crust development without using high air velocities that dries the product and strips oil out. Radiant heat transfer has been applied only at constant rates that results in a charred surface with an under-heated core unless a microwave radiation is applied. Few studies quantify the engineering properties of radiant energy or the spectral absorption characteristics of the target food material to mimic an immersion frying process.

Reproduction of the dynamic heat transfer rates found in immersion frying is hypothesized to be accomplished by electromagnetic energy in the visible, near, and far infrared wavelengths from approximately 0.4 to 1000 μm. Radiant heat sources (emitters) are capable of generating over 100,000 W/m^2 with precise control of the output (Heraeus Noble Light, 2001). The incident heat flux intensity and spectral distribution affect the ratio and intensity of short and long wavelength radiation and thus the product heating rates and heating profiles.

Study and development devoted to understanding radiant heating and the possibilities of using radiant heat transfer for finish heating products has been limited to simple toasting,

baking, and roasting applications. The demand to develop alternative heating methods of finish frying by the QSR industry require a better understanding of the fundamental interactions involved during thermal radiant energy absorption by food materials. The introduction of new equipment for an alternative finish frying process must be safe, economically feasible to build, have a high product throughput, and require minimal operator attention and control. To meet these demands quantitative information is needed to characterize the engineering properties of radiant emitters, determine the spectral energy absorption into the food material, determine the depth of energy penetration, and measure flux intensity profiles that correctly develop the crust and texture of a fried-like product. Hence, energy absorption at the surface and into the product must be studied and understood to optimize an alternative finish frying technique. Development of a better understanding of crust development and texture retention from radiant finish heating and the interactions that occur as flux intensity changes may aid in the ability to determine optimal degree of initial par-frying or other surface change that deliver flavors and textures of equal consumer acceptance while that the same time reducing fat content of the product. In general, increased understanding of thermal radiant heating of foods at the fundamental levels of engineering, spectroscopy, heat transfer simulation, and desired sensory attributes of a fried-like product will provide processors and equipment manufacturers a foundation knowledge base to fully develop optimized alternative finishing frying systems.

The overall objective of this research was to study radiant heating of potatoes with the overall goal of reproducing heat transfer rates present during immersion frying to produce a fried-like potato product. The approach divided the goal into three areas that each had more defined specific objectives:

(1) characterize engineering and spectral properties of radiant emitters used in food processing equipment;

(2) measure textural, color, and sensory properties of radiant heated par-fried potatoes; and

(3) measure and mathematically simulate the transient temperature response, drying effects, and absorption of radiant energy used to heat raw potatoes.

Layout of Dissertation

This dissertation is based on the following papers, which will be referred to by Roman numerals in the text:

I. Characterization of radiant emitters used in food processing.

II. Comparison of French fried potatoes produced using different finishing methods.

III. Numerical simulation of high intensity radiant heating of potatoes

A comprehensive literature review follows the introduction. Overall conclusions from this research are then discussed. A literature review bibliography and the individual manuscripts listed above immediately follow.

REVIEW OF LITERATURE

Basic Principles of Thermal Radiation

Thermal radiation is one of the three modes of heat transfer along with conduction and convection. All objects emit thermal radiation energy based on the Stefan-Boltzmann law (Siegel and Howell, 2002):

$$E(T) = \sigma T_{abs}^4 \qquad [1]$$

The Stefan-Boltzmann law states that the thermal radiation emissive power (E) emitted by an object increases by the fourth order of the absolute surface temperature. The proportionality constant σ is the Stefan-Boltzmann constant equal to 5.67x10 W/(m^2 K^4). In the simplest form, this law states that the emissive power increases as the temperature of the heated object increases over the emitted entire wavelength range. The distribution of the emitted wavelengths was described by Planck (1901) creating the theory of a blackbody surface. Fundamental radiation heat transfer defines a 'blackbody' surface as an ideal emitter or absorber (Siegel and Howell, 2002). A blackbody surface will absorb all and reflect none of the radiation falling on it. A heated surface that emits thermal radiation in the same wavelength distribution as a blackbody, but at a proportionally lesser amount is called a graybody. Heated objects are assumed to emit or absorb radiation as a graybody. The proportionality constant that equates a blackbody to a graybody is called the emissivity (ε). The emissivity is incorporated into the Stefan-Boltzmann law to determine the emissive power (E) of a graybody.

$$E(T) = \varepsilon\sigma T_{abs}^4 \qquad [1A]$$

The emissivity of a graybody is less than one, while the emissivity of a blackbody is equal to one. Emissivity values for particular surfaces are listed in many heat transfer texts and range between zero and one.

The wavelength distribution of thermal radiation for a blackbody is defined by Planck's distribution. This distribution is defined by Planck's law (Siegel and Howell, 2002):

$$E_{\lambda,b}(\lambda,T) = \frac{C_1\lambda^{-5}}{e^{C_2/\lambda T}-1} \qquad [2]$$

where the first (C_1) and second (C_2) radiation constants have values of $3.742\text{x}10^8$ W $\mu m^4/m^2$ and $1.439\text{x}10^4$ μm K, respectively. Planck's distribution changes dramatically for different surface temperatures. The total emissive power also increases as the temperature of the object increases, which is indicated by the area under the distribution curve. Also, the wavelength distribution shifts to a greater amount of shorter wavelengths as the temperature of the surface increases. The area under the curve of Planck's distribution is proportional to T^4 in accordance with the Stefan-Boltzmann law and is the total emitted energy.

The peak wavelength value of Planck's distribution at a given surface temperature is defined by Wien's law (Siegel and Howell, 2002):

$$\lambda_{peak} = \frac{C_3}{T_{abs}} \qquad [3]$$

where the third radiation constant (C_3) equals 2897.8 μm K. The peak wavelength λ_{max} varies inversely with the absolute temperature of the radiating object.

Characteristics of Thermal Radiation Emitters

Radiant energy is emitted from heated objects, typically referred to as emitters in a thermal oven-type system. Radiant emitters are commonly used in residential and industrial heating applications. Emitters are commercially available in a wide variety of sizes, shapes, and heating capacities. However, there are three basic classes of radiant emitters: short wavelength, medium wavelength, and long wavelength (Bischof, 1990). These classes are categorized based on the peak wavelength emitted, which is usually determined using Wien's law [Eqn. 3] based on the emitter's surface temperature. Short wavelength emitters are generally composed of a tungsten filament enclosed in quartz envelope filled with a halogen gas. These lamps operate by passing an electrical current through the filament wire, which increases in temperature thereby emitting visible and thermal radiation. A regenerative tungsten halide chemical transport cycle prevents buildup of evaporating filament depositions on the quartz wall as long as the wall is above 250°C (Bergmann and Schaeffer, 1999). These lamps operate at temperatures up to 2600°C, with a typical range of 1900 to 2200°C (Heraeus, 2001). The wavelength range of the radiant energy is approximately 0.2 to 14 μm. Barnes and Forsythe (1936) measured the spectral output of tungsten filaments. The peak wavelength of most short wavelength emitters is approximately 1.4 μm. Short wavelength emitters are often used in lighting applications. If the short wavelength emitter is to be used as a lighting source, a mandatory glass covering removes most of the ultraviolet radiation (NEMA, 1999). Short wavelength emitters also have some limited use in industrial heating and have found a relatively new use in residential oven heating applications.

There are several types of medium wavelength emitters. One type is similar to short wavelength lamps in construction and operation, however the filament wire is usually a

larger diameter and made from a nickel chromium or carbon filament wire. The filament may or may not have a glass covering. Another type of medium wavelength emitter is the heated metal sheath. These emitters are composed of tubular high-temperature metal alloy. The metal alloy has a high-melting temperature and is usually made from a combination of iron, nickel, and copper. Inside the metal tube, a nickel chromium resistance wire is surrounded by solid magnesium oxide packing (Chromalox, 2001). Electrical energy heats the internal resistance wire, thus heating the magnesium oxide packing, which in turn heats the outer metal alloy sheath. Metal sheath emitters are commonly used in various electric oven configurations as well as heating in electric stovetop burners. The third type of medium wavelength emitter is a ceramic surface heated by combustion of fossil fuels, such as natural gas. The energy from combustion heats a ceramic plate on one side. The opposite side of the plate emits radiant energy and thus heats the target object(s). Ceramic infrared heaters are often used in gas-fired ovens and furnaces. Medium wavelength emitters operate at approximately 1500°C with a wavelength range of 1 to 14 μm with a peak wavelength of 4.3 μm.

Long wavelength emitters are the lowest temperature emitters. The most common type of commercial long wavelength emitters are composed of woven quartz fabric. The quartz fabric is heated by embedded resistance wires and the surface of the fabric is often coated in heat resistant carbon black paint. The black coating improves the emission with an emissivity of 0.96 (Siegel and Howell, 2002). Long wavelength emitters have a surface temperature range of 600 to 750° C. Hankins (1989) reviewed the classes of infrared emitters and associated equipment as well as safety, maintenance, oven configurations, and several case histories of infrared heating applications. Although radiant emitters are widely

used in commercial heating applications, few published articles present thorough measurements of engineering properties of radiant emitters.

The most complete studies on measurement of engineering properties of radiant energy of commercial emitters focus on heating thermoplastic injection preforms to produce plastic blow-molded bottles. Monteix et al. (2001) measured the radiant intensity of several tubular quartz tungsten filament emitters at different incident angles. These intensity values were incorporated into a three dimensional control-volume mathematical model of the absorption of radiant energy into a PET (polyethylene terephthalate) sheet from a 1700 K tungsten halogen emitter. The authors found that calculated model temperatures agreed with the measured values with respect to time, but only in a single spatial heating plane. Shelby (1991) studied several factors that affect reheat rate of plastic performs such as: emitter lamp filament temperature, lamp power output, and spectral absorption characteristics of the PET preform. The lamp filament temperature was found to have the most significant effect on reheat characteristics of plastic performs due to increased energy and depth of energy penetration. Maoult et al. (1997) also studied the radiant heating of plastic performs. The authors compared the spectral distribution of a theoretical 2100°C blackbody with a tungsten filament enclosed in a quartz envelope. The temperature of the tungsten filament was indirectly determined by measuring the resistivity (Ω) as a function of temperature, Ω(T). The spectral emissivity of the filament was then approximated using the Drude approach (Bergmann and Schaefer, 1999). This method uses wave theory to estimate emissivity of metals from the equation:

$$\varepsilon(\lambda, T) = 36.5\left(\frac{\Omega(T)}{\lambda}\right)^{0.5} - 464\frac{\Omega(T)}{\lambda} \qquad [4]$$

which was stated as accurate for wavelengths greater than 3 μm. The final determined spectral distribution was approximately a graybody with an emissivity of 0.95.

Extinction of Radiation Within a Semi-Transparent Food Material

Once emitted thermal radiation falls upon a surface, it is either reflected, transmitted, or absorbed. The sum of total reflection, transmission, and absorption is unity:

$$\rho + \tau + \theta = 1 \qquad [5]$$

Reflected energy never contributes to increasing the temperature of a food medium. However, reflected radiation is responsible for creating the shapes and colors that comprise the visual image of a surface that is detected by the human eye. The reflected radiation that the human eye can detect occurs in the visible wavelength spectrum of 0.4 to 0.7 μm. Reflection of radiation from a food material's surface is a spectral property (λ) that varies with wavelength. Reflection also occurs outside of the visible spectrum as well. Lammertyn et al. (2000) measured the reflection spectra of apple slices in the wavelength range of 0.5 to 1.9 μm. The authors measured reflection of 65% in the wavelength range of 0.7 to 0.9 μm, while a lower reflection of less than 10% beyond 1.5 μm. Reflection has spectral dependence, thus it is a function of wavelength (λ). Reflection is also dependent other properties such as surface roughness, incident angle, and surface composition (Mohsenin, 1984).

Radiation transmitted through a food material also does not increase the temperature of the food medium. Radiation transmission is also a spectral property of the material, dependent on the composition and structure. The radiation transmitted through the material may not be affected and pass through the food material or may be scattered internally (Birth,

1978) and emerge at a different wavelength and location. When scattering and redirection occurs, it is called diffuse transmission. Birth (1978) measured the transmitted radiation through potato flesh. He found that transmission of radiation transversely propagated had complete diffusion for a sample 3.75 mm thick, measured using a 632 nm laser. This research showed the importance of internal scattering of electromagnetic energy within a semi-transparent material and that the Kubelka-Munk theory (discussed below) was adequate to describe the transmission propagation.

If the incident radiation is neither reflected nor transmitted through the material, then the radiation is considered absorbed [eqn. 5] causing an increase in the temperature of the material. Like reflection and transmission, absorption of thermal radiation is a spectral property of the material. Absorption is highly dependent on the collective spectral absorption distribution of the food material's individual components (Shuman and Staley, 1950). For example, sugars have two strong absorption bands at 3 μm and 7 to 10 μm (Manning, 1956). Lipids are strong absorbers over the entire infrared spectrum with peak bands at 3 to 4, 6, and 9 to 10 μm (Freeman, 1968). Protein has two strong absorption bands localized at 3 to 4 μm and 6 to 9 μm (Schwarz et. al, 1957). However, the most important absorbing component in most food materials is water. The four principle absorption bands of liquid water are 3, 4.7, 6, and 15.3 μm (Hale and Querry, 1973). Many food materials have excess of 75% water, thus effective radiant emitters used for cooking or drying are chosen with the absorbing characteristics of the food components, primarily water, in mind (Shuman and Staley, 1950). Another important absorption characteristic of radiant heating is the penetration depth of the radiant energy within the food material.

Determining the Penetration Depth of Thermal Radiation

The interdependency of reflection, transmission, and absorption within a semi-transparent solid, such as food materials, has been the focus of several classic radiation absorption theories such as Beer's law, the Kubelka-Munk theory, and others. The most commonly used theory of extinction of radiation as it propagates through a medium is Beer's law (Bergmann and Schaefer, 1999).

$$J_\lambda = J_{\lambda o} e^{(-\sigma_\lambda u)} \qquad [6]$$

which states that spectral irradiance $\left(J_\lambda, W/m^2\right)$ incident on a surface decreases exponentially according to the coefficient $\left(\sigma_\lambda, cm^{-1}\right)$ multiplied by the thickness of the absorbing medium (u, m). The spectral irradiance $\left(J_\lambda\right)$ is the sum of direct and reflected radiation incident on the food's surface. The coefficient $\left(\sigma_\lambda\right)$ is referred to as the spectral extinction (or absorption) coefficient. This coefficient is a complex function of the chemical composition of the medium, the physiochemical state of the medium, and physiochemical parameters defining the medium (Sandu, 1986). The spectral extinction coefficient $\left(\sigma_\lambda\right)$ often is simplified to represent a broad range of wavelength values instead of individual wavelengths. Dagerskog and Österström (1979) determined that the exponential decay of thermal radiation could be accurately represented by two coefficient ranges when measuring radiation through slices of pork, wheat bread, and potato. They used a separate extinction coefficient for a short wavelength range of less than 1.25 μm and one for the longer wavelength range of greater than 1.25 μm. They concluded that the sum of the two Beer's law functions for each wavelength range was satisfactory in predicting the penetration and absorption of the radiation for the entire spectrum incident upon the material. Beer's law,

however, only relates the penetrating and transmitting radiation and does not account for any internally reflected and scattered radiation (Bergman and Schaefer, 1999).

The Kubelka-Munk theory or K-M theory was developed in 1931 to quantify the optical characteristics of semi-transparent media (Kubelka and Munk, 1931). This theory defined several coefficients within two linked hyperbolic functions along with measurable values to define the radiation attenuation within a medium. The primary equation (Birth, 1978):

$$S * d = \frac{1}{b}\left(\sinh^{-1}\frac{b}{T} - \sinh^{-1} b\right) \qquad [7]$$

where S was the scatter coefficient (cm^{-1}), d was the material thickness (cm), T was the fraction of incident light transmitted by the sample. The two intermediate constants was defined:

$$b = \sqrt{a^2 - 1} \quad \text{and} \quad a = \frac{1 + R_0^2 - T^2}{2R_0} \quad \text{and} \quad a = \frac{S + \sigma}{S} \qquad [8], [9], [10]$$

where R_0 was the reflectance of the sample with an ideal black background and σ was absorption coefficient previously mentioned. Finally, these equations were linked together by the relationship:

$$\frac{\sigma}{S} = \frac{(1 - R_\infty)^2}{2R_\infty} \qquad [11]$$

which collectively are known as the K-M functions. R_∞ is the reflectance of a sufficiently thick sample that increasing thickness does not change the reflectance. Although related to Beer's law, the K-M theory has the advantage of accounting for internal scattering (Bergmann and Schaefer, 1999). Several researchers have applied the K-M analysis to foods. Francis and Clydesdale (1975) described these applications primarily for food quality

determination and pigmentation applications. Birth (1976) showed that the second hyperbolic term of the K-M theory was not necessary for non-absorbing radiation in select applications of nondestructive quality indices. Kubelka (1948) further expounded on the K-M theory of intensely light-scattering materials.

Another approach to determining the extinction of radiation within a medium has been adopted for internal quality assessment of fruits. Lammertyn et al. (2000) developed a simplified procedure to determine the penetration depth of visible and near infrared radiation in apple tissue. Percent reflection was measured from slices of apples with increasing thicknesses over a wavelength range of interest. When the reflection value became stable with increased slice thickness, then the penetration depth was determined at the mean reflection for each wavelength value. This procedure produced a histogram of penetration depths verses wavelengths for a 0.2 to 2 μm range. Peirs et al. (2002) used this procedure to compare Fourier Transform and Dispersive Near-infrared Reflectance Spectroscopy for nondestructive internal apple quality indices.

Overview of Radiant Heating of Food Materials

Radiant heating of food materials has been the subject of widespread, but primarily application-oriented study. The bulk of radiant food processing literature may be divided into four main categories: infrared drying of agricultural products, novel infrared cooking techniques, infrared baking, and radiant frying devices. Although there have been a number of papers in each of these categories only a few studies, specifically related to infrared baking, have included research on the general principles and fundamental theory of radiant

heating and cooking. The following sections give an overview of the work published in the aforementioned four areas.

Infrared Drying of Agricultural Products

Drying is an inherently slow and expensive process (Barbosa-Canova and Vega-Mercado, 1996). Radiant heating has been applied in a number of studies in an effort to increase drying rate and decrease energy consumption. These studies have been primarily application oriented, applying radiant heating to existing dryers. Fasina et al. (1998) developed coupled heat and mass transfer equations simulating infrared drying of agricultural crops. They found that infrared burner temperature, distance from product to infrared emitter, initial grain moisture content, and heating time affected kernel temperature. Bal et al. (1970) built and tested a radiant rough rice dryer. Theoretical energy transfer to the kernels was calculated as well as the necessary configuration factors (shape factors) for rice falling between two infrared heaters. Fu and Lien (1998) optimized a FIR (far infrared) system for dehydrating shrimp and found that a low air temperature (43°C) in their dehydrator could be used with significant energy savings.

Hashimoto et al. (1994) modeled the drying characteristics of agar gels dried using infrared heat. The gels were formed using either aluminum, silver, or stainless steel powder in the agar allowing variation of the monochromatic surface emissivity. The samples were exposed to a far infrared radiation source (FIR) and a near infrared (NIR) radiation source. It was found that internal scattering in the NIR range lowered the drying rate and thus was an important factor in the development of mathematical models. The use of metal powders

allowed the study of surface emissivity and its effect on absorption of the incident radiant energy.

Several investigators have studied infrared roasting of nuts. Hebbar and Rastogi (2000) modeled unsteady state diffusion of moisture in cashews heated by an infrared heater. The authors assumed an Arrhenius relationship for effective mass diffusion as a function of nut temperature. Kurz (1987) studied penetration of infrared radiation into the interior of organic materials. It was found that penetration depth depends on several factors but primarily wavelengths of maximum absorption of the product's constituents. Sandu (1986) thorough review of infrared radiative food drying. He contrasted radiative drying with conductive and convective drying as well as the importance of penetration of thermal radiation within the food or agricultural material.

Several authors have studied infrared drying of potato. Asselbergs et al. (1960) first saw the potential for high energy infrared emitters to dry and cook a variety of products including French fries. It was found that potatoes cooked using infrared and then finished fried in oil had good quality. Afzal and Abe (1998) studied the moisture diffusion in potatoes as a function of radiation density and slab thickness. Later, Afzal and Abe (1999) reported that radiant drying of potatoes to be a falling rate process and moisture removal could be described by a modified exponential function. Masamura et al. (1988) reported drying of potato using far infrared radiation. Radiant drying was shown to require less energy than the traditional convective drying process.

Infrared Cooking

Although most cooking processes entail a loss of moisture, similar to drying, some investigators have studied radiant heating as a means of replacing traditional convection and/or conduction processes. Sheridan and Shilton (1999) evaluated the cooking time and temperature rise of meat products cooked by medium wavelength gas heated ceramic emitters. The peak wavelengths of the radiant sources were 2.7 and 4.0 μm. The authors found that a short wavelength source allowed a target internal temperature to be achieved at a lower surface temperature with less dependence on the fat content of the meat sample. The longer wavelength source, however, had less surface drying and charring, than a short wavelength source. Fuel consumption was much higher for the short wavelength source. No heat flux measurements for the two emitters were reported. Khan and Vandermey (1985) evaluated an infrared broiler for cooking ground beef patties and compared the finished product to conventionally (gas/flame) cooked patties. Results indicated shorter cooking times for the infrared oven. Sakai et al. (1994) reviewed the uses of far infrared radiation (defined as 2 to 1000 μm) in Japan. It was determined that infrared heat processing reduced processing times and energy consumption, reduced ambient air temperature rise, and provided greater oven uniformity. It was also noted that with increased processing rates came a need for improved (rapid) heating controls.

Infrared Baking

An area that has received the most fundamental research on radiation heating of food products has been infrared baking of bread and bread products. Ginzburg (1969) presented the foundation text in the area of convective-radiative baking. This work established several governing differential equations for radiation heat transfer to bread dough for proper crust

and crumb formation. It also presented fundamental work on determining the density of radiation in infrared ovens using experimental data. Several Soviet Union researchers have investigated infrared baking. Il'yasov and Krasnikov (1991) reviewed optical and thermal characteristics of foodstuffs for several materials including bread dough. Mohsenin (1984) presented an overview of electromagnetic properties of food and agricultural materials primarily for quality measurements.

In the late 1970s into the 1980s, several researchers from the Swedish Institute for Food Research (SIK) published fundamental research in the area of infrared baking and other applications of infrared radiation for food processing (Dagerskog and Österström, 1979; Dagerskog, 1979). Dagerskog and Österström (1979) presented the fundamental optical properties of infrared radiation in the near infrared range. They determined transmission values of infrared radiation for several foods including white bread, pork, and white potato. A 3200° C halogen lamp was used and the transmission broken into two regions a short wavelength (<1. 507 μm) and a long wavelength region (>1.507 μm) based on a transmission filter. Penetration curves for each region were separately determined and calculated by integration of Planck's equation [2] where D was the fraction of energy passing the filter:

$$D = \frac{1}{\sigma T^4} \int_{1.507\mu m}^{\infty} E_\lambda d\lambda \qquad [12]$$

From this work the absorption and reflection characteristics of the model foods showed a strong dependence on wavelength.

Dagerskog (1979) mathematically modeled radiant heating of several food products including bread, pork, and potato. A one dimensional radiant heat transfer equation

for the surface [13] and interior regions [14] was written using finite difference equations (Dagerskog, 1979):

$$T_{1,k+1} = T_{1,k} + \frac{2a\Delta t}{\Delta x^2}\left(T_{2,k} - T_{1,k}\right) + 2a\frac{\alpha\Delta t}{k\Delta x}\left(T_{air} - T_{1,k}\right) + \frac{2a\Delta t}{k\Delta x}\left[PT\left(1 - P_2\right) + RT\left(R_2 - R_1\right)\right] \qquad [13]$$

$$T_{n,k+1} = T_{n,k} + a * \frac{\Delta t}{\Delta x^2}\left(T_{n+1,k} - 2T_{n,k} + T_{n-1,k)}\right) + \frac{a\Delta t}{k\Delta x}\left[PT\left(P_n - P_{n-1}\right) + RT\left(R_{n+1} - R_n\right)\right] \qquad [14]$$

In this approach, mass transfer was ignored, material properties were constant, and no attempt was made to incorporate crust development. This approach addressed development of subsurface radiant dissipation. For each node, an exponential radiation dissipation term was introduced as an internal generation term(s) (PT and RT) by the constant radiant energy flux. Subsurface heating was calculated and used to determine the temperature distribution throughout the food material at any time. The unsteady-state heat transfer problem was assumed a one-dimensional slab and was solved using finite difference techniques. The model included an internal heat generation term with a dissipation coefficient (σ_λ) determined by Dagerskog and Österström (1979). Both convection and conduction terms were included. Although the simulation output was in good agreement with experimental values, the model was not able to describe non-uniform surface heat flux conditions. Also, the surface characteristics of the slab, such as emissivity and penetration coefficient, were considered constants, although these properties are known to change as material properties (thermal, spatial, and physical) change during the process.

Skjöldebrand et al. (1988) developed a method for determining the optical properties of bread. A comparison of bread baked using infrared heating to conventional convection heating was conducted. Analysis of crust formation found that infrared energy supplied superior heat transfer to produce this characteristic property (Skjöldebrand et al., 1989). It

was found that the rate of surface heat transfer, not the oven temperature, controlled bread crust quality. Using an infrared source with a desired penetration, and controlling the power level in an infrared oven allowed the evaporation rate of moisture in the crust to be balanced with internal crumb development (Skjöldebrand and Anderson, 1986). Based on these and other studies, radiant heat transfer was successfully used in Europe to replace a number of traditional, gas-fired convection ovens with purely radiant ovens (Bischof, 1990; Hankins, 1989; Sharples, 1971). Seiler (1978) reviewed radiant energy baking of bread compared with convectional convection ovens.

Recognizing the advantages of penetration properties of shortwave radiation, the Pillsbury company patented a process for baking using filtered short wavelength infrared radiation (Lentz et al., 1993). It was shown that a water jacket encasing an infrared quartz emitter would remove the longer wavelength radiation (>1.3 μm) thereby allowing internal baking without excessive surface browning or development of a crust. It was proposed that ovens equipped with this technology could be used to create pre-baked products such as toaster pasteries and unbrowned pizza crusts. Walsh (2000) and Westerburg (1997) proposed filtering radiant energy for more wavelength ranges that promote desired heating without surface charring.

Wade (1987) used short wavelength (1.2 μm) infrared radiation to bake biscuit and cookie doughs in approximately half the time required by a convectional oven. The transmission of monochromatic infrared radiation was measured by a radiometer after passing through specific bandpass filters. It was found that use of short wavelengths resulted in greater internal heating and a superior quality than that produced via long wavelength radiant heating. Wade (1987) hypothesized that long wavelength radiation was absorbing

primarily at the product surface resulting in charring and a poor appearance. Unklesbay (1985) found that radiant emitter temperature corresponded to final color of pizza crust.

Radiant Frying Devices

Studies directed at development of an alternative frying process have relied primarily on maintaining a constant air temperature process. Alden and Shelburne (1993) used hot air at a constant temperature to heat par-fried products in a batch process. Gaon and Wiedersatz (1993) developed an alternative frying process utilizing a microwave section as well an infrared section to cook potato chips without oil. August (1991) also included radiative heating on each side of a microwave chamber to cook potato chips without oil. Dauliach (1999), Jenicot (1987), and Mestnik and Alexander (1998) developed a cooking apparatus for heating fried products without oil using constant heating. These devices rely on a constant heat flux from an emission source to maintain a set point temperature of the product's environment. The foods cooked in these devices were reported tougher, have a drier mouthfeel, and have little resemblance to their traditionally fried counterpart. The fundamental aspects of frying a product without oil have largely been neglected. It may be said that this approach has yielded 'device' inventions and not process innovations.

The importance of sub-surface heating and crust formation during radiant baking has been shown critical toward proper crumb and crust development. This past research highlights the potential of radiant heating to produce a crust in an infrared fried product. Determination of the necessary wavelengths to promote crusting and browning are critical for successful development of an alternative frying process.

State of Thermal Radiant Heating of Foods Literature

The thermal radiant heating of food products literature reviewed covers little fundamental engineering research of radiant heating. No research studies have examined the application of radiant heating to produce a fried-like food product. Fundamental studies conducted on radiant baking demonstrated the ability of radiant heating to be engineered to produce a desired heating profile with controlled surface browning and crusting to replace traditional convection baking ovens. This same basic approach will be used to lay a foundation of thermophysical properties and data necessary to evaluate the efficacy of using radiant heat transfer as a replacement for immersion frying. The determination of the role of optical properties as well as the knowledge gained in understanding the role of emitter spectral power distribution, incident heat flux, temperature distributions, and moisture loss during radiant heating will aid in the future development of a radiant frying process. These procedures and experiments will further advance fundamental knowledge of radiant heat transfer for food heating applications and more specifically alternative immersion finish frying techniques.

OVERALL CONCLUSIONS

Dynamic radiant heating was shown as a successful candidate for replacement for immersion finish frying. Refinement and optimization is needed to commercialize dynamic radiant heating for French fries but the process showed promise as a successful replacement to immersion finish frying.

Paper I

Thermal radiant emitters were characterized by measuring heat flux intensity, emitter surface temperature, and spectral wavelength distribution. Heat flux intensity (W/m^2) measurements showed that incident angle and distance from the emitter both caused decreases in the flux intensity from the maximum, which was located 90° perpendicular to the emitter face. Heat flux intensity decreased as distance increased following Lambert's law of radiant energy diffusion. Emitter surface temperature measurements indicated that short wavelength radiant systems had the highest surface temperature for the input electrical power. Thus, the short wavelength emitter system produced a greater amount of radiant energy with a higher input-power to emitter-surface temperature-increase efficiency than the lower temperature systems. Fourier transform infrared spectrophotometer measurements of emitter spectral distributions for both the short and medium wavelength emitter systems produced excess far infrared emission compared to theoretical blackbody curves. This energy would be a significant source of surface absorption energy for food processing or other heating applications.

Paper II

Comparison of finish heating methods demonstrated that controlled radiant heated French fries had consistent texture, color, and consumer acceptability when compared to a traditional immersion finished-fried product. The Kramer shear test measured a significantly higher peak force for radiant finished heated product than immersion fried or oven baked. Comparison of color indices indicated that lightness (L-value) was lowest for radiant heated product than the other methods. The degree of yellowness (b-value) was not significantly different between radiant heated or immersion fried samples. Consumer demographic information collected during sensory analysis indicated that consumers were interested in a low/reduced fat French fry as an alternative to traditional immersion fried French fries. Improving crispness intensity is needed for the dynamically heated French fry product. The overall acceptability of radiant heated French fries was not statistically different than traditional immersion finish frying. Radiant finish heating of par-fried French fries showed promise to produce a lower fat product, as well as an alternative process to traditional immersion finish frying.

Paper III

Predicted and measured temperature profile of raw potato was modeled using one dimensional radiant heat transfer and moisture evaporation equations. High intensity radiant heat transfer was simulated by separating the potato into a crust and core region and tracking the development of the crust as surface moisture was evaporated. Measured surface and core temperatures at 15,000 and 27,000 W/m^2 showed excellent agreement with simulation results producing an average deviation of less than 3°C.

Several input variables of the model were also tested for influence on predicted surface and core temperature. Doubling the impinging radiant flux intensity predicted an exponential decrease in the time required to reach T_{bp}. Crust thickness was predicted to increase by an average of 0.24 mm as radiant flux intensity doubled. The dissipation coefficient σ caused a greater change in core temperature as shorter wavelength radiant energy (low σ value) penetrated deeper within the product. Finally, the drying rate of raw potato was measured as a constant rate process with flux intensities of 15,000 and 27,000 W/m^2 producing nearly identical drying rates.

The characterization of radiant emitters used in food processing as well as the knowledge gained from the numerical simulation of radiant heating may aid in process optimization of an alternative immersion frying process. French fry texture, color, and consumer sensory attributes in comparison with other traditional methods of finish heating clearly indicated that dynamic high intensity radiant heat treatment showed many equivalent quality indices of traditional immersion frying and could serve as an alternative finish frying process.

Further research in this area should focus on more specific analyses of process parameters to determine their effects on French fry quality attributes, primarily crust texture as well as increasing processing speed. Critical process parameters that should be addressed include:

- The effect of different heat flux intensity profiles beyond those studied here such as linear and exponentially decreasing flux intensity profiles.
- The influence of altering the emission output spectra of the emitter that impinges on the product. Filtering techniques that allow more subsurface, penetrating

wavelengths with less surface-only absorption wavelengths would likely improve subsurface heating. Filtering techniques include metallic thin film filters, water or other chemical liquid filters, water vapor, or screen filters.

- Coupling radiant heating with microwave heating to increase internal heating rate while still retaining the controlled radiant surface treatment for proper crust development.

Research should also focus on the effect of changes to the starting French fry material that affect final quality attributes. Suggested product characteristics that should be explored include:

- The influence of degree of par-fry and oil content of the initial product.
- The influence of product thickness and other geometrical features.
- The influence of pre-surface treatments to improve textural characteristics such as the addition of surface coatings or altering the initial surface moisture content.

The numerical simulation provided an accurate transient temperature profile as high intensity radiant energy created a crust region. Improvements to the numerical simulation include:

- Transformation from one to two dimensions.
- The addition of a mathematical moving boundary that will always fall on the crust (I) core (II) interface to eliminate discontinuity during the transition as each node switches from core to crust, which changes the thermal and physical properties.
- The program using a more user friendly platform such as Visual Basic. Input parameters could be user interfaced in a Windows format. Automatic temperature

and crust thickness plots could be graphed in separate windows as the simulation is executed.

More accurate physical properties data on potato would also improve the numerical simulation. Specifically, the optical properties of par-fried potato should be studied to determine the spectral dissipation coefficient, σ_λ, for raw and par-fried potato or other target products.

REFERENCES

Afzal, T.M. and T. Abe. 1998. Diffusion in potato during far infrared radiation drying. J. of Food Eng. 37: 353-365.

Afzal, T.M. and T. Abe. 1999. Some fundamental attributes of far infrared radiation drying of potato. Drying Technol. 17(1,2): 137-155.

Alden, L.B. and V. Shelburne. 1993. Method for cooking food in an infrared conveyor oven. U.S. Patent No. 5,223,290.

Anon. 1971. For crisper French fries. J. of Fruits, Vegetables, and Nuts. 19(8): 7.

Asselbergs, E.A., Mohr, W.P., and J.G. Kemp. 1960. Studies on the application of infrared in food processing. Food Technol. (14):449-453.

August, J.R. 1991. Apparatus for preparing snack food products. U.S. Patent No. 5,049,711.

Bal, S., Wratten, F.T., Chesness, J.L., and M.D. Faulkner. 1970. An analytical and experimental study of radiant heating of rice grain. Trans. of the ASAE. 13: 644-647.

Barbosa-Cánovas, G.V. and H. Vega-Mercado. 1996. Dehydration of foods. New York, Chapman & Hall.

Barnes, B.T. and W.E. Forsythe. 1936. Spectral radiant intensities of some tungsten filament incandescent lamps. J. of the Optical Society of America. 26: 313-315.

Bergmann, L. and C. Schaefer. 1999. Optics of Waves and Particles. Walter de Gruyter, Berlin.

Birth, G.S. 1978. The light scattering properties of foods. J. of Food Science 43: 916-925.

Bischof, H. 1990. The answer is electrical infrared. J. of Microwave Power and Electromagnetic Energy. 25(1): 425(1): 47-52.

Blumenthal, M.M. 1996. Frying technology. In Edible Oil and Fat Products: Products and Application Technology. Pp. 429-481. in Y.H. Hui (ed.) Bailey's Industrial Oil and Fat Products, 5th Ed. Wiley and Sons, Inc. New York, Vol. 3.

Blumenthal, M.M. 1991. A new look at the chemistry and physics of deep-fat frying. Food Technol. 45(2): 68-71, 94.

CDC. 1993. Morbidity and Mortality Weekly Report. 42(37):1-4.

Chromalox, 2001. Precision heating and control. Emerson Electric Co. Pittsburgh, PA.

Dagerskog, M. 1979. Infra-red radiation for food processing II. Calculation of heat penetration during infra-red frying of meat products. Lebensmittel Wissenschaft Technologie 12(4): 252-257.

Dagerskog, M. and L. Österström. 1979. Infra-red radiation for food processing I. A study of the fundamental properties of infra-red radiation. Lebensmittel Wissenschaft Technologie 12(4): 237-242.

Dauliach, M.H. 1999. Electrical cooking apparatus for cooking precooking, deep frozen or fresh food, of the fryer type, with no oil bath. U.S. Patent No. 5,910,264.

Farkas, B.E. and Hubbar, L.J. 2000. Analysis of convective heat transfer during immersion frying. Drying Technol. 18(5):

Fasina, O.O., Tyler, R.T., and M.D. Pickard. 1998. Modeling the infrared radiative heating of agricultural crops. Drying Technol. 16 (9&10): 2065-2082.

Francis, F.J. and F.M. Clydesdale. 1975. Food Colorimetry: Theory and Applications. AVI Publishing. Westport, Connecticut.

Freeman, N.K. 1968. Applications of infrared absorption spectroscopy in the analysis of lipids. J. Am. Oil Chem. Soc. 45: 798-809.

Fu, W. and W. Lien. 1998. Optimization of far infrared heat dehydration of shrimp using RSM. J. of Food Science. 63(1): 80-83.

Ginzburg, A.S. 1969. Application of Infra-red Radiation in Food Processing. Cleveland: CRC Press.

Hale, G.M. and M.R. Querry. 1973. Optical constants of water in the 200 nm to 200 μm wavelength range. Applied Optics 12(3): 555-563.

Hankins, W. 1989. Infrared process heating in the U.K. J. of Microwave Power and Electromagnetic Energy. 24(4): 236-246.

Hashimoto, A., Yamazaki, Y., Shimizu, M., and S. Oshita. 1994. Drying characteristics of gelatinous materials irradiated by infrared radiation. Drying Technol. 12(5): 1029-1052.

Hebbar, H.U. and N.K. Rastogi. 2001. Mass transfer during infrared drying of cashew kernel. J. of Food Eng. 47(1): 1-5.

Heraeus Noblelight. 2001. Technical information of halogen infrared emitters. Technical Publication, Heraeus Noblelight, Atlanta, GA.

Holownia, K.I., Chinnan, M.S., Erickson, M.C., and P. Mallikarjunan. 2000. Quality evaluation of edible film-coated chicken strips and frying oils. J. Food Sci 65(6): 1087-1090

Hubbard, L.J. and B.E. Farkas. 1999. A method for determining the convective heat transfer coefficient during immersion frying. J. of Food Process Engr. 22: 201-214.

Gaon, D. and J. Wiedersatz. 1993. Process for preparing fat free snack chips. U.S. Patent No. 5,202,139.

Il'yasov, S.G. and V.V. Krasnikov. 1991. Physical Principles of Infrared Irradiation of Foodstuffs. New York: Hemisphere Publishing Corp.

Jenicot, J. 1987. Electric fryer. U.S. Patent No. 4,636,618.

Khan, M.A. and P.A. Vandermey. 1985. Quality assessment of ground beef patties after infrared heat processing in a conveyorized tube broiler for foodservice use. J. of Food Science 50: 707-709.

Kubelka, P. 1948. New contributions to the optics of itensely light-scattering materials. Part 1. J. Opt. Soc. Amer. 38:448

Kubelka, P. and F. Munk. 1931. Ein Beitrag zur Optik der Farbanstriche. Z. techn. Phys. 12: 593-601.

Kurz, M. 1987. Infrared roasting of seed kernel. Food Trade Review 57(2): 13-15.

Lammertyn, J., Peirs, A., De Baerdemaeker, J., and B. Nicolaï. 2000. Light penetration properties of NIR radiation in fruit with respect to non-destructive quality assessment. Postharvest Biology and Technology. 18: 121-132.

Lentz, R.R., Pesheck, P.S., Anderson, G.R., DeMars, J., and T.R. Peck. 1995. Method of processing food utilizing infrared radiation. U.S. Patent No. 5,382,441.

Manning, J.J. 1956 Applications of infrared absorption spectroscopy of sugars. Applied Spectroscopy 10: 85.

Maoult, Y. Le, Schmidt, F.M., Laborde, V., El Hafi, M., and P. Lebaudy. 1997. Measurement and calculation of perform infrared heating: a first approach. Proceeedings of the Fourth International Workshop on Advanced Infrared Technology and Applications. Firenze, Sept. 1997: 321-331.

Masamura, A., Sado, H., Honda, T., Shimizu, M., Nabetani, H., Nakajima, M., and A. Watanabe. 1988. Drying of potato by far infrared radiation. Nippon Shokuhin Kogyo Gakkaishi. 35(5): 309-314.

McDonalds Corp. June 8, 2003. McDonald's USA nutrition facts for popular menu items. Oak Brook , IL.

Mestnik, F.G. and B.J. Alexander. 1998. Oil-free fryer, food cooker. U.S. Patent No. 5,780,815

Mohsenin, N. 1984. Electromagnetic properties of foods and agricultural products. Gordon and Breach Publ., New York.

Monteix, S., Schmidt, F., Le Maoult, Y., Ben Yedder, R., Diraddo, R.W., and D. Laroche. 2001. Experimental study and numerical simulation of perform or sheet exposed to infrared radiative heating. J. of Materials Processing Technol. 119: 90-97.

Moreira, R.G., Sun, X.Z., and Y.H. Chen. 1997. Factors affecting oil uptake in tortilla chips in deep-fat frying. J. of Food Engr. 31(4): 485-498.

NAFEM. 2002. North American Association of Food Equipment Manufacturers 1989. Industry Survey, source: Ms. Lori Carey, Market Research Group Manager, NAFEM, Chicago, IL.

Peirs, A., Scheerlinck. N., Touchant, K., and B.M. Nicolaï. 2002. Comparison of fourier transform and dispersive near-infrared reflectance spectroscopy for apple quality measurements. Biosystems Engineering. 81(3): 305-311.

Planck, M. 1901. Distribution of energy in the spectrum. Ann. Phys. 4(3): 553-563.

Rayner, M., Ciolfi, V., Maves, B., Stedman, P., and G.S. Mittal. 2000. Development and application of soy-protein films to reduce fat intake in deep-fried foods. J. of the Science of Food and Agriculture 80(6): 777-782.

Saguy, I.S. and E.J. Pinthus. 1995. Oil uptake during deep fat frying: factors and mechanisms. Food Technol. 49(4): 142-145, 152.

Sakai, N., Fuji, A., and T. Hanzawa. 1994. Applications and advances in far-infrared heating in Japan. Trends in Food Science and Technol. 5(11): 357-362.

Sandu, C. 1986. Infrared radiative drying in food engineering: a process analysis. Biotechnology Progress 2(3): 109-119.

Schwartz, H.P., Dreisbach, L., Childs, R., and S.V. Mastrangelo. 1957. Infrared absorption spectroscopy of proteins. Annuals of the New York Academy of Sciences 69:116.

Seiler, K. 1978. Baking with high frequency. CCB-Review for Chocolate, Confectionary, and Baking. 3(3): 34-38.

SFA. 1997. State of the Snack Food Industry Report. Snack Food Association Alexandria, VA.

Sharples, J.T. 1971. Electroheat in food processing. British Food Journal. Jan./Feb: 14-56.

Shelby, M.D. 1991. Effects of infrared lamp temperature and other variables on the reheat rate of PET. Proceedings of ANTEC '91: 1420-1424.

Sheridan, P. and N. Shilton. 1999. Application of far infra-red radiation to cooking of meat products. J. of Food Engr. 41: 203-208.

Shuman, A.C. and C.H. Staley. 1950. Drying by Infra-Red Radiation. Food Technol. 481-484.

Siegel, R. and J.R. Howell. 2002. Thermal Radiation Heat Transfer, 4th Ed. Taylor & Francis Publ. New York.

Skjöldebrand, C., Ellbjär, C., and C.G. Andersson. 1988. Optical properties of bread in the near-infrared range. J. of Food Engr. 8: 129-139.

Skjöldebrand, and C.G. Andersson. 1989. A comparison of infrared bread baking and conventional baking. J. of Microwave Power and Electromagnetic Energy. 24(2): 91-101.

Skjöldebrand, and C.G. Andersson. 1986. Baking using short wave infra-red radiation. In Proc. 1st Europ. Conf. On Food Science and Technol., ed I.D. Morton, 364-372. New York, NY.

Ufheil, G. and F. Escher. 1996. Dynamics of oil uptake during deep-fat frying of potato slices. Food Sci. and Technol.- Lebensmittel-Wissenschaft & Technologie 29(7): 640-644.

Unklesbay, N.F. 1985. Effect of dough temperature and infrared radiation on crust color of pizzas. J. of Foodservice Systems 3(4): 243-249.

USDA. 2003. Code of Federal Regulations, Nutrition labeling of food. Title 21. Section 101.9.

Wade, P. 1986. Biscuit baking by near-infrared radiation. J. of Food Eng. 6: 165-175.

Walsh, B.C., Kester, J.J., Corrigan, P.J., and J.J. Elsen. 2000. Process for preparing frozen par-fried potato strips having deep fried texture when oven-finished. U.S. Patent No. 6,042,870.

Westerberg, E. 2000. Apparatus and method for cooking food in a controlled spectrum. U.S. Patent No. 6,069,345.

I

Characterization of Radiant Emitters Used in Food Processing

Lloyd, B.J., Farkas, B.E.[1] and K.M. Keener

[1]Corresponding Author

Authors are Brian J. Lloyd, Graduate Assistant; Brian E. Farkas[1], Associate Professor; and Kevin M. Keener, Associate Professor; all from the Department of Food Science, North Carolina State University, Raleigh, NC 27695.

Submitted to the Journal of Microwave Power and Electromagnetic Energy

ABSTRACT

Radiant emission from short, medium, and long wavelength thermal radiant emitter systems typically used for food processing applications were quantified. Measurements included heat flux intensity, emitter surface temperature, and spectral wavelength distribution. Heat flux measurements were found highly dependent on the incident angle and the distance from the emitter facing. The maximum flux measured was 5.4 W/cm^2. Emitter surface temperature measurements showed that short wavelength radiant systems had the highest surface temperature and greatest thermal efficiency. The emitter spectral distributions showed that radiant emitter systems had large amounts of far infrared energy emission greater than 3 μm when compared to theoretical blackbody curves. The longer wavelength energy would likely cause increased surface heating for most high moisture content food materials.

INTRODUCTION

Thermal radiant energy falls into the electromagnetic wavelength spectrum between ultraviolet and microwave energy, approximately 0.4 to 1000 μm. Infrared (IR) energy comprises the bulk of thermal radiant energy spectra and is often subdivided into near IR (NIR), mid-IR (MIR), and far-IR (FIR). Radiant energy causes a temperature increase in a receiving object by inducing thermal molecular vibration (Siegel and Howell, 2002).

Radiant heating has become an important processing tool for many commercial heating applications including curing of paint and powder coatings, bonding of rubber products, and curing of adhesive binders (Hankins, 1989). Bischof (1990) found that infrared heating is well suited for high intensity surface heating applications. One application of radiant heating is thermal processing of food materials.

Radiant heating of food products has been an important means of cooking, drying, baking, and holding food and food ingredients at a desired temperature. Sharples (1971) reviewed radiant heating of food products and compared it to other conventional heat transfer sources. It was found that energy savings were not the only quantifiable means of comparison, but that improved degree of heat control, increased convenience, and an improved working environment were also important criteria when considering radiant heating equipment such as radiant baking ovens. Asselberg et al. (1960) studied the basic application of radiant energy to food processing operations such as blanching of vegetables and braising of meat. They found that infrared processed products usually had superior quality, and stressed that the applied maximum wavelength of the radiant energy, although not measured, affected the extent of radiant energy absorbed by the food. Shuman and Staley (1950) had also come to this conclusion, and noted that depth of radiant energy penetration

depended on both product composition as well as the wavelength spectrum of the energy source. Sandu (1986) reviewed the spectral properties of several food products for radiant heating and noted that food products exhibit spectral peaks of higher absorption dependent on the food's composition. Thus, it was hypothesized that radiant energy sources with an output spectrum preferentially shifted toward the food components' absorption peaks would exhibit superior heating, improved processing, and higher quality.

The importance of the radiant emitter's spectral emission has been the subject of few investigations within food processing applications. Some of the more recent and complete radiant spectral distribution studies have addressed heating thermoplastic injection preforms for making blow-molded bottles. Monteix et al. (2001) studied the infrared spectral distribution of radiant emitters heating semi-transparent polyethylene terephthalate (PET) sheets. They modeled the radiant absorption using an assumed graybody emission of a 1700 K tungsten halogen emitter in a flat PET sheet and found good model agreement. Shelby (1991) studied the factors that affect reheat rate of preforms such as: lamp filament temperature, lamp power output, and spectral absorption characteristics. However, no direct measurement of spectral irradiance was measured at the plastic surface. Maoult (1997) compiled a spectral distribution for a 2100°C tungsten source using the Drude method (Bergmann and Schaefer, 1999) to estimate emitter temperature based on its resistivity.

Few researchers have investigated ways to measure and characterize the radiant emitter's spectral distribution preferentially for food processing applications. Burgheimer et al. (1971) investigated varying the wavelength of near infrared energy using thin glass filters for the freeze drying of beef. Skjöldebrand and Andersson (1986) presented results from infrared baking of bread. They classified the infrared energy as short wavelength (<1.3 μm)

or medium wavelength (≥ 2.7 μm) for radiant emitter banks used in an experimental oven. More recently, Sheridan and Shilton (1999) evaluated cooking of hamburger patties with infrared energy by sources with a maximum wavelength of 2.7 μm and 4.0 μm, based on emitter filament surface temperature. Lentz et al. (1995) implemented a water filter in front of several quartz halogen emitters to heat dough in the selective wavelength range of 0.8 to 1.3 μm without browning the surface; however, the authors never directly measured the irradiance at the dough surface. They assumed irradiance emission resembled a blackbody source filtered through a 3 mm thick layer of water.

The above studies all stress the importance of characterization of radiant energy sources for successful food processing applications. Characterization indices include measuring and understanding overall flux intensity as well as emission spectra incident on the food's surface. Most of the previous work assumes gray or blackbody emission and divides the total spectrum into two sections: short and medium/long wavelength. The purpose of this project was to completely characterize short, medium, and long wavelength radiant emitters typically used in food processing equipment and processes. This characterization included measuring the radiant spatial heat flux intensity, emitter surface temperature, and spectral wavelength distribution.

EXPERIMENTAL PROCEDURES

Infrared Heating Systems

Three separate radiant emitter systems were tested to encompass the various categories of radiant emitters: a short wavelength quartz-halogen bulb system, a medium wavelength heated metal sheath system, and a long wavelength woven quartz fabric system. Each system is described below.

The short wavelength radiant system contained two 500 W quartz halogen bulbs (type T3, General Electric, Cleveland, OH). The bulbs used a 20 ga. tungsten filament wire with a 120 mm lighted length. They operated at 120 VAC at a maximum current load of 7 A. The bulbs were connected to a variable transformer to control power level. The bulbs were backed by a parabolic shaped reflector (Fig. 1) with a polished, gold anodized surface with an estimated emissivity of 0.02 (Siegel and Howell, 2002). The bulbs were mounted 35 mm apart, filament to filament, with a 7 mm gap between the filament and the reflector backing (Fig. 1).

The medium wavelength radiant system consisted of two cylindrical (6.2 mm diameter) metal sheathed emitter elements (Chromalox, Pittsburgh, PA). The metal sheath was made of INCOLOY® alloy, a common alloy used for radiant emitting metal surfaces. The emitters operated at 120 VAC with a maximum current load of 9 A. The cylindrical elements were mounted 35 mm apart (centerline to centerline) and had a heated length of 190 mm. Both emitters were backed by the same reflector material as the short wavelength system described above and similarly mounted at a distance of 7 mm from the reflector backing (Fig. 1).

The long wavelength system consisted of a flat plate (305 x 305 mm) with a woven quartz cloth surface finished with a high temperature black coating (Casso-Solar, Pomona, NY). Resistance wires were embedded in the fabric that heated the flat surface. The system operated at 240 VAC up to maximum power of 2160 W. A reflector was not used with this emitter type.

Spatial Heat Flux Intensity Measurements

Heat flux measurements for all infrared emitters were performed using a water-cooled radiometer (model 9000, Vatell Inc., Blacksburg, VA). The sensor had a zinc selenide lens that prevented any convective heat transfer from affecting radiant heat flux measurements. The detector coating had an emissivity of 0.94 at 2 microns and was considered a graybody during calibration. Sensor sensitivity was determined to be +/- 0.612 W/cm^2 during calibration.

Spatial heat flux mapping was accomplished by placing a 180° grid system directly in front of the emitter face along with a plumb bob attached to the radiometer face (Fig. 2). The grid and plumb bob allowed accurate radiometer placement for each polar position. Heat flux measurements were performed at 50 mm distance intervals from the emitter face and at 15° increments radially from the emitter face. The vertical position of the sensor was maintained at the middle, centerline of each emitter system. The centerline provided the most uniform flux location within the fixture and minimized end effects (Ginzburg, 1969). Each heat flux measurement was recorded after 3 min. of heating to ensure thermal equilibrium and three separate measurements were performed for each spatial location.

Emitter Surface Temperature Measurements

The surface temperature of the short and medium wavelength emitters was measured using a disappearing filament optical pyrometer (MD-7268, Pyrometer Instrument, Northvale, NJ). The pyrometer used a target spot diameter of 0.152 mm to measure the emitter surface temperatures. The instrument was accurate to the nearest 0.5 °C, and measurements were taken at a distance of 61 mm from the target. Surface temperature measurements were taken by increasing power output up to the maximum power level for each emitter system. An additional short wavelength emitter was also included for this measurement, a ruby-coated 250 W incandescent heat lamp (R-40, General Electric, Cleveland, OH). All measurements were done in triplicate and then averaged. Surface temperature of the long wavelength system was measured using a type K thermocouple embedded in the heated fabric surface. The surface temperature was measured at approximately 30 to 90 W increments up to the maximum power level.

Emitter Spectral Distributions

The emitter spectral distributions were also measured for each emitter using a Fourier Transform Infrared Spectrophotometer (FTIR), (Digitech series 3000 Excaliber, Randolph, MA). The FTIR system contained an internal light source, a Michelson interferometer, a radiant energy-transmitting beam splitter, a He-Ne laser for measurement of scan position, and a detector. The system was also equipped with an optional external emission port to analyze an external radiation source (Fig. 3). The housing that enclosed these components was continually flushed with dry nitrogen gas to minimize absorption from normal atmospheric components such as water vapor and carbon dioxide (CO_2). The system's

normal stabilized internal light source was turned off and no sample was placed in the sample port during the emitter spectra measurement.

Each radiant emitter was placed 17.5 cm from the external port, perpendicular to a 4 in. polyvinlychloride (PVC) pipe painted flat black internally. The black PVC pipe minimized indirect radiant emissions from reaching the external port as well as protecting the spectrometer housing from the intense radiant energy of the emitters. The emitters were connected to a variable transformer that allowed measurement of emission spectra at varying power levels. Two different FTIR configurations were used to measure the emission over a wavelength range of approximately 0.67 to 25 μm. Table 1 lists the applicable wavelength ranges with the corresponding spectrometer beam splitters and detectors for each measurement.

RESULTS AND DISCUSSION

Spatial Heat Flux Measurements

The largest heat flux measurements occurred at a maximum value of 5.4 W/cm^2 for the short wavelength emitter (Fig. 4a). This value occurred at a distance of 0 mm from the emitter fixture face (Fig. 1), with an incident angle (θ) of 90°, perpendicular to the source. The medium and long wavelength systems also had a localized maximum at the 0 mm, 90° position. However, the 0 mm distance also had the largest influence of incident (sensor placement) angle (θ). Also known as directivity, the effect of varying (θ) at 0 mm was indicated by the symmetrical exponential decrease in normalized intensity (Fig. 4 a,b,c). This decrease in heat flux was most pronounced at the 0 mm distance because the sensor was directed away from viewing both emitter surfaces as the incident angle (θ) increased or

decreased from the 90° placement. Ginzburg (1969) reported that a single reflector, double radiator system provided a uniform radiation sector arc of approximately 120° although the distance from the emitter was not specified. Uniform intensity independent of (θ) was observed for all three emitter systems at distances of 150 mm and greater. There were large decreases in flux intensity at distances of 200 mm or more from the surface. This change in radiant intensity due to distance was expected and followed Lambert's law of radiant energy diffusion (Eqn 1):

$$I = \frac{r^2}{\cos\theta}\frac{df}{da} \qquad [1]$$

where radiant intensity (I) varies by the square of the distance (r) from the emitting source to the receiving surface and with the differential flux per differential area (*df/da*) and the incident angle (θ) are kept constant. It was noted, however, that the long wavelength source retained 25% of the maximum flux up to 200 mm from the source.

Emitter Surface Temperature Measurements

Emitter surface temperatures increased as the normalized power increased (Fig. 5). The filament-type, short wavelength emitters (quartz halogen and coated incandescent bulb), had a surface temperature increase as much as 1250°C. The surface temperature increase per watt increase was greater for short wavelength emitters than the other two emitter types as indicated by a greater trend slope (Fig. 5). The greater surface temperature ($T_{surface}$) increase could be attributed to the much smaller heated surface area of the filament wires compared to the much larger metal sheaths or flat fabric surfaces of the other emitter types. The higher

surface temperature at a given normalized power load (P_{input}) (Fig. 5) also indicated a greater thermal efficiency:

$$Eff_{thermal} = \frac{T_{surface}}{P_{Input}} \quad [2]$$

A radiant food heating operation with a required heating load would benefit from the higher emitter surface temperature of the short wavelength emitter, which produced greater overall radiant thermal energy. However, the importance of the absorption spectra of the target food material should be determined and compared with the emitter output emission spectra as discussed below.

Emitter Spectral Distributions

Short Wavelength System Emission

Figure 6 shows the short wavelength system emission spectra over the wavelength range of 1.8 to 25 μm. The spectra of the short wavelength system at diffent power levels (300, 460, and 637 W) are presented along with corresponding theoretical blackbody distributions. The blackbody curves closely followed the initial spectra peak that occurred from approximately 1.8 to 3 μm. According to Wien's Law, the maximum peak for a blackbody radiator at any temperature is determined by:

$$\lambda_{\max} = \frac{C_3}{T} \quad [3]$$

where C_3= 2897.8 μm K. Therefore, the maximum peak for 2000 K and 1669 K blackbody temperatures were 1.45 μm and 1.73 μm, respectively. As mentioned, the MCT detector cutoff was higher at approximately 1.8 μm, thus the highest emitter specta peaks were unable to be measured. The central crown of the peak was blunted and corresponded to a water vapor absorption band located at 2.7 μm (Modak, 1979). Also, large emission of long

wavelength energy was noted at each power level beyond 3 μm. To investigate the origin of this energy, an emission spectra was measured immediately after the halogen emitter power at 315 W was shut off. The resulting spectra (Fig. 6) of the heated quartz tube, fixture, and reflector represented the large trailing emission with a peak at approximatley 7 μm. This energy was not predicted by the blackbody spectral distribution of the heated filament, but represented a significant source of long wavelength FIR energy over the range of 5 to 25 μm, herein referred to as a background emission signature. Chu et al. (1999) also measured a large amount of long wavelength emission from halogen emitters.

At the far end of the spectrum, beyond 25 μm, the spectral emission decayed toward zero. The emission spectra in FIR range (not shown) continued the emission decrease beyond 25 μm and was virtually undetectable from background noise by 60 μm.

Medium Wavelength System Emission

The medium wavelength emitter spectral response for the wavelength range of approximately 1.8 to 100 μm is shown in Figures 7 and 8. The range was divided into two sections: 1.8 to 25 μm (MIR) and 18 to 100 μm (FIR) dependent on the FTIR hardware setup (Table 1). Both figures show a baseline signal that allowed the signal to noise ratio to be determined, which as 0.1 V/μm for the mid-IR range and 0.25 V/μm for the far-IR range. As noted, the far-IR range had a higher signal-to-noise ratio, and this range required a reduction in the emission port aperature size to prevent detector saturation.

Figure 7 shows several emitter power level spectral scans for the medium wavelength system along with blackbody distribution curves at corresponding temperatures. The most notable features included among the medium wavelength spectra occur in the wavelength

ranges where water and CO_2 cause aborption features. These peaks recognized by the water 'bands' located at 2.7 and 6.3 μm and CO_2 absorption at 4.3 and 9.4 μm (Edwards, 1976 and Modak, 1979). When compared to the theoretical blackbody distribution curves at temperatures corresponding to the emitter temperatures, it was noted that the medium wavelength spectra were shifted approximately 1.5 μm toward the longer wavelengths. This shift, however was attributed to decreased detector sensitivity at wavelengths less than 2.5 μm. At high power levels, the emitters were emitting some NIR and visible energy, but detector cutoff limited measurable quantities in this part of the spectrum. Also noted, the emitter spectra included large areas of longer wavelength energy that is not indicative of the blackbody curves. This energy was visually estimated to represent 50% of the spectral power as indicated by the area under the spectral curves yet not under the blackbody curves. This energy would be a significant source of longer wavelength energy for any food processing application. Energy of a long wavelength range (>6 μm) would likely become a significant source of surface heating for high moisture content foods according to work done by Sandu (1986), Dagerskog (1979), and Dagerskog and Österström (1979).

At the FIR range from 25 to 100 μm, the detector response increased to the peak response value at approximately 30 μm and decreased thereafter (Fig. 8). Prior to 30 μm, detector sensitivity was not great enough to measure the absolute spectral irradiance, but beyond 30 μm the emission decreased due to the spectral properties of the emitter and was not a function of detector sensitivity. No emission was detected beyond 50 μm above the background signal.

CONCLUSIONS

Thermal radiant emitters were characterized by measuring heat flux intensity, emitter surface temperature, and spectral wavelength distribution. Heat flux measurements showed that incident angle and distance from the emitter both caused decreases in the flux intensity from the maximum, which was located 90° perpendicular to the emitter face. Emitter surface temperature measurements indicated that short wavelength radiant systems had the highest surface temperature for the input electrical power. The emitter spectral distributions for both the short and medium wavelength emitter systems had excess far infrared emission compared to theoretical blackbody curves, which would be a significant source of surface absorption energy for food processing or other heating applications.

ACKNOWLEDGEMENTS

Funding for this project was made possible through the USDA National Needs Grants Program #1999-1583 and the USDA National Research Initiative Competitive Grants Program #9801477.

REFERENCES

Asselbergs, E.A., Mohr, W.P., and J.G. Kemp. 1960. Studies on the application of infrared in food processing. Food Technol. (14):449-453.

Barnes, B.T. and W.E. Forsythe. 1936. Spectral radiant intensities of some tungsten filament incandescent lamps. J. of the Optical Society of America. 26: 313-315.

Bergmann, L. and C. Schaefer. 1999. Optics of Waves and Particles. Walter de Gruyter, Berlin.

Burgheimer, F., Steinberg, M.P., and A.I. Nelson. 1971 b. Effect of near infrared energy on rate of freeze drying of beef, 2. Spectural Distribution . J. of Food Science. 36: 273-276.

Chu, H., Lin, S., Chang, C., Su, C., Yen, C., and J. Tsao. 1999. Emission spectrum measurement of the rapid thermal processing heating source by Fourier transform infrared spectroscopy. J. Chinese Soc. of Mech. Engr. 20(6): 553-562.

Dagerskog, M. 1979. Infra-red radiation for food processing II. Calculation of heat penetration during infra-red frying of meat products. Lebensmittel Wissenschaft Technologie 12(4): 252-257.

Dagerskog, M. and L. Österström. 1979. Infra-red radiation for food processing I. A study of the fundamental properties of infra-red radiation. Lebensmittel Wissenschaft Technologie 12(4): 237-242.

Ginzburg, A.S. 1969. Application of Infra-red Radiation in Food Processing. Cleveland: CRC Press.

Hankins, W. 1989. Infrared process heating in the U.K. J. of Microwave Power and Electromagnetic Energy. 24(4): 236-246.

Lentz, R.R., Pesheck, PS., Anderson, G.R., DeMars, J., and T.R. Peck. 1995. Method of processing food utilizing infrared radiation. U.S. Patent No. 5,382,441.

Maoult, Y. Le, Schmidt, F.M., Laborde, V., El Hafi, M., and P. Lebaudy. 1997. Measurement and calculation of perform infrared heating: a first approach. Proceeedings of the Fourth International Workshop on Advanced Infrared Technology and Applications. Firenze, Sept. 1997.

Monteix, S., Schmidt, F., Le Maoult, Y., Ben Yedder, R., Diraddo, R.W., and D. Laroche. 2001. Experimental study and numerical simulation of perform or sheet exposed to infrared radiative heating. J. of Materials Processing Technol. 119: 90-97.

Sandu, C. 1986. Infrared radiative drying in food engineering: a process analysis. Biotechnology Progress 2(3): 109-119.

Shelby, M.D. 1991. Effects of infrared lamp temperature and other variables on the reheat rate of PET. Proceedings of ANTEC '91: 1420-1424.

Sheridan, P. and N. Shilton. 1999. Application of far infra-red radiation to cooking of meat products. J. of Food Engr. 41: 203-208.

Siegel, R. and J. Howell. 2002. Thermal Radiation Heat Transfer, 4th ed. Taylor and Francis Publ. New York.

Skjöldebrand, and C.G. Andersson. 1986. Baking using short wave infra-red radiation. In Proc. 1st Europ. Conf. On Food Science and Technol., ed I.D. Morton, 364-372. New York, NY.

Table 1. FTIR spectrometer hardware configurations used to measure radiant emission response in select wavelength ranges.

Wavelength Range		**Beam Splitter Substrate**	**Detector**
Mid-IR	1.1 to 20 μm	KBr[‡]	MCT[*]
Far-IR	20 to 100 μm	6.25μ Mylar	DTGS[†]

[*] mercury cadmium telluride, [†] deuterated triglycine sulfate, [‡] potassium bromide

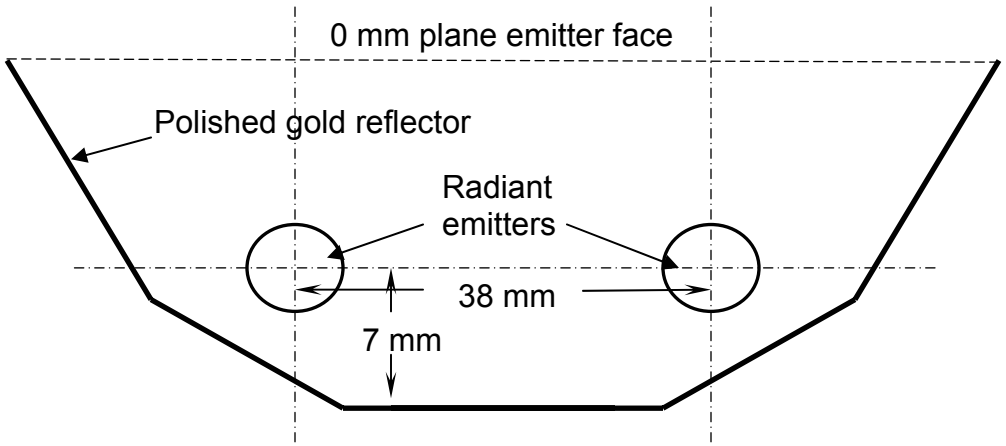

Figure 1. Cross section of the reflector and emitters used in the short and medium wavelength radiant heating systems.

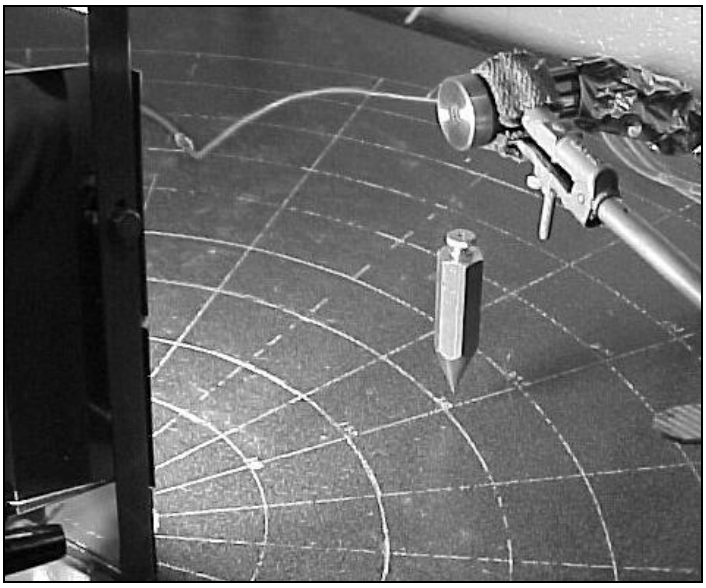

Figure 2. Radiometer used to measure heat flux intensity of each radiant emitter. A 180° grid system was used to measure the distance from the emitter face (r) and the incident angle (θ) of the radiometer position.

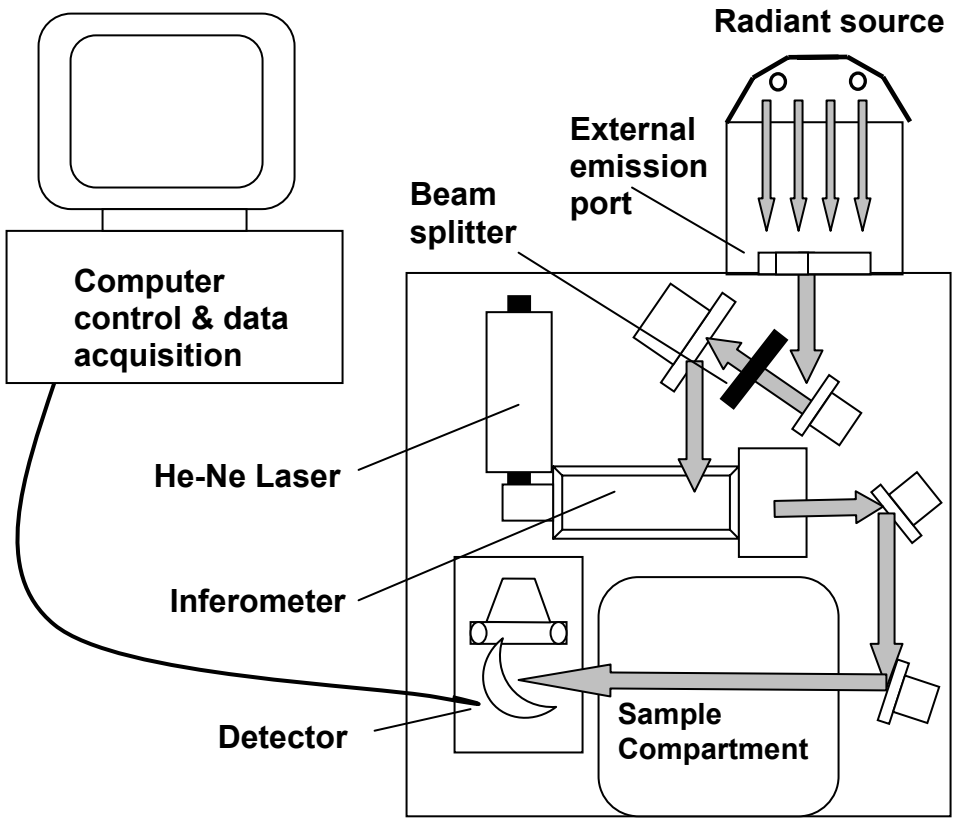

Figure 3. Schematic diagram of the FTIR spectrophotometer used to measure thermal radiant emitter spectral distribution. Grey arrows represent radiant energy emission path through the instrument.

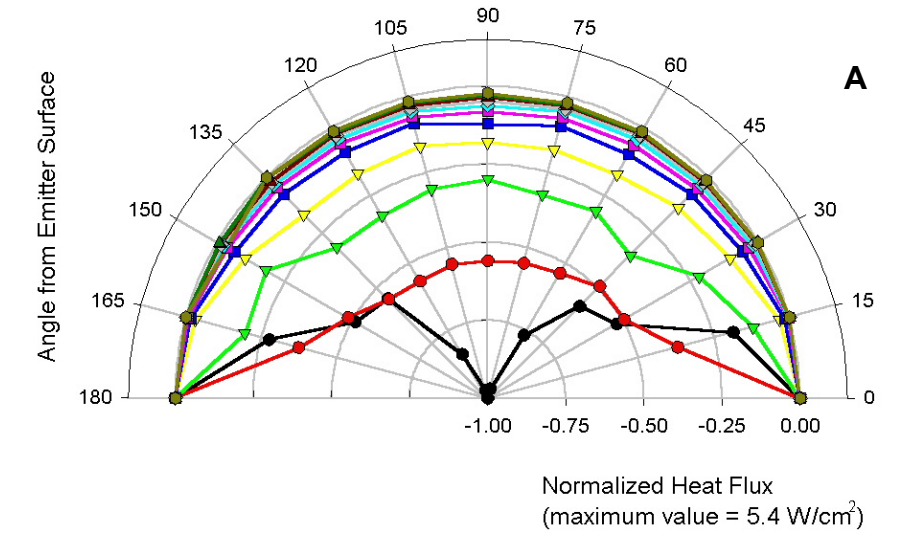
A
90
75
60
45
30
15
0
105
120
135
150
165
180
Angle from Emitter Surface
-1.00
-0.75
-0.50
-0.25
0.00
Normalized Heat Flux
(maximum value = 5.4 W/cm2)

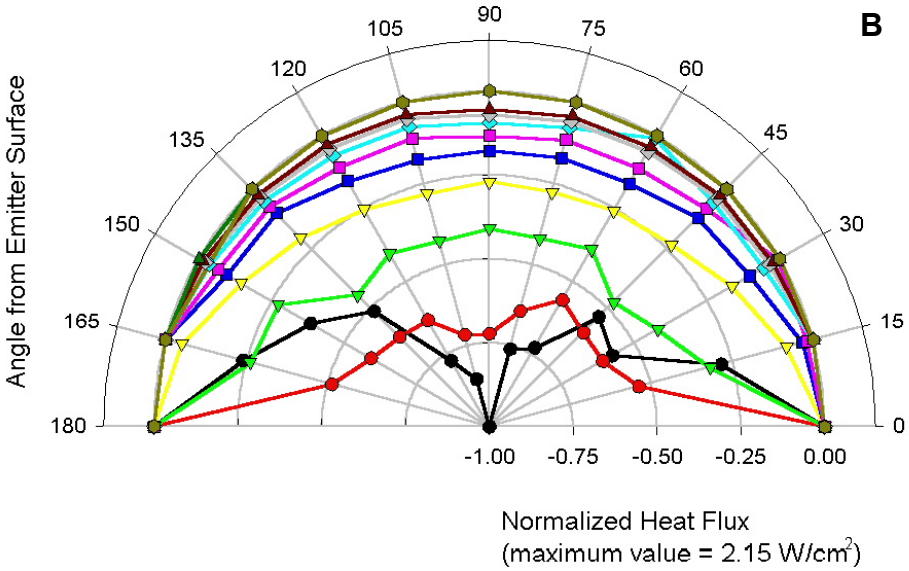
B
90
75
60
45
30
15
0
105
120
135
150
165
180
Angle from Emitter Surface
-1.00
-0.75
-0.50
-0.25
0.00
Normalized Heat Flux
(maximum value = 2.15 W/cm2)

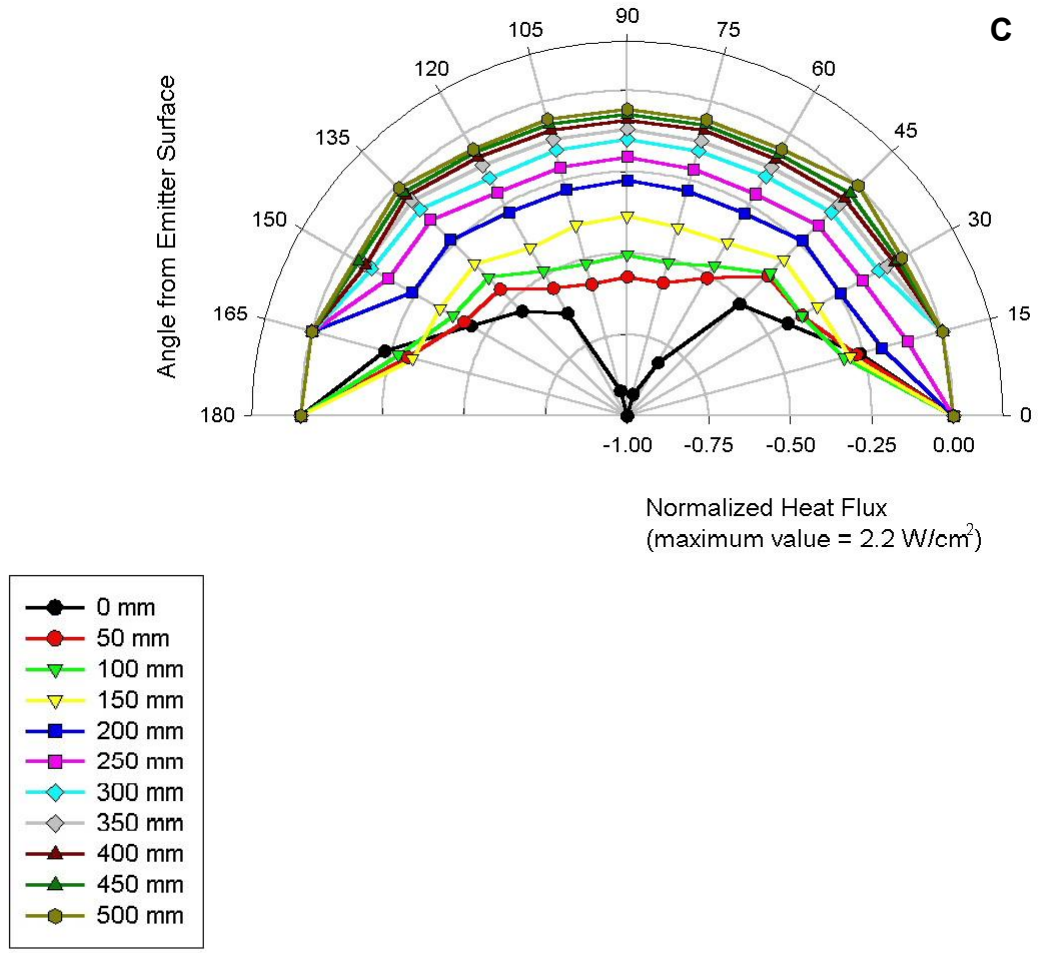

Figure 4. Spatial heat flux intensity measurements for three different radiant heating systems: (A) short wavelength system (B) medium wavelength system (C) long wavelength system. Each line represents the distance (r) from the emitter facing to the sensor, 0 to 500 mm in 50 mm increments. Radial distances represent normalized intensity for each emitter type, and the angles (θ) are the incident angle of the measurement.

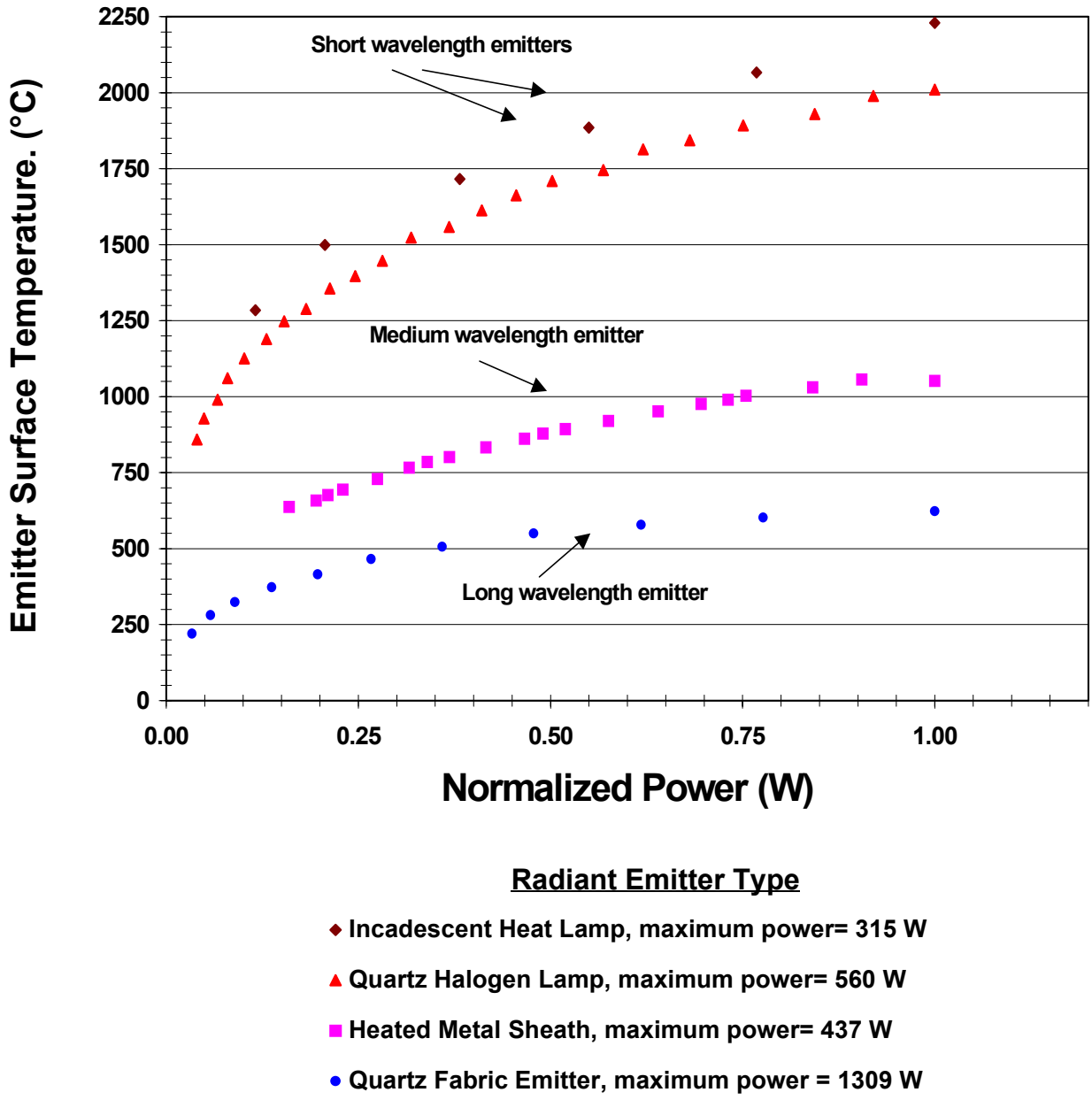

Figure 5. Emitter surface temperature and normalized power for short, medium, and long wavelength emitters commonly used in food processing applications.

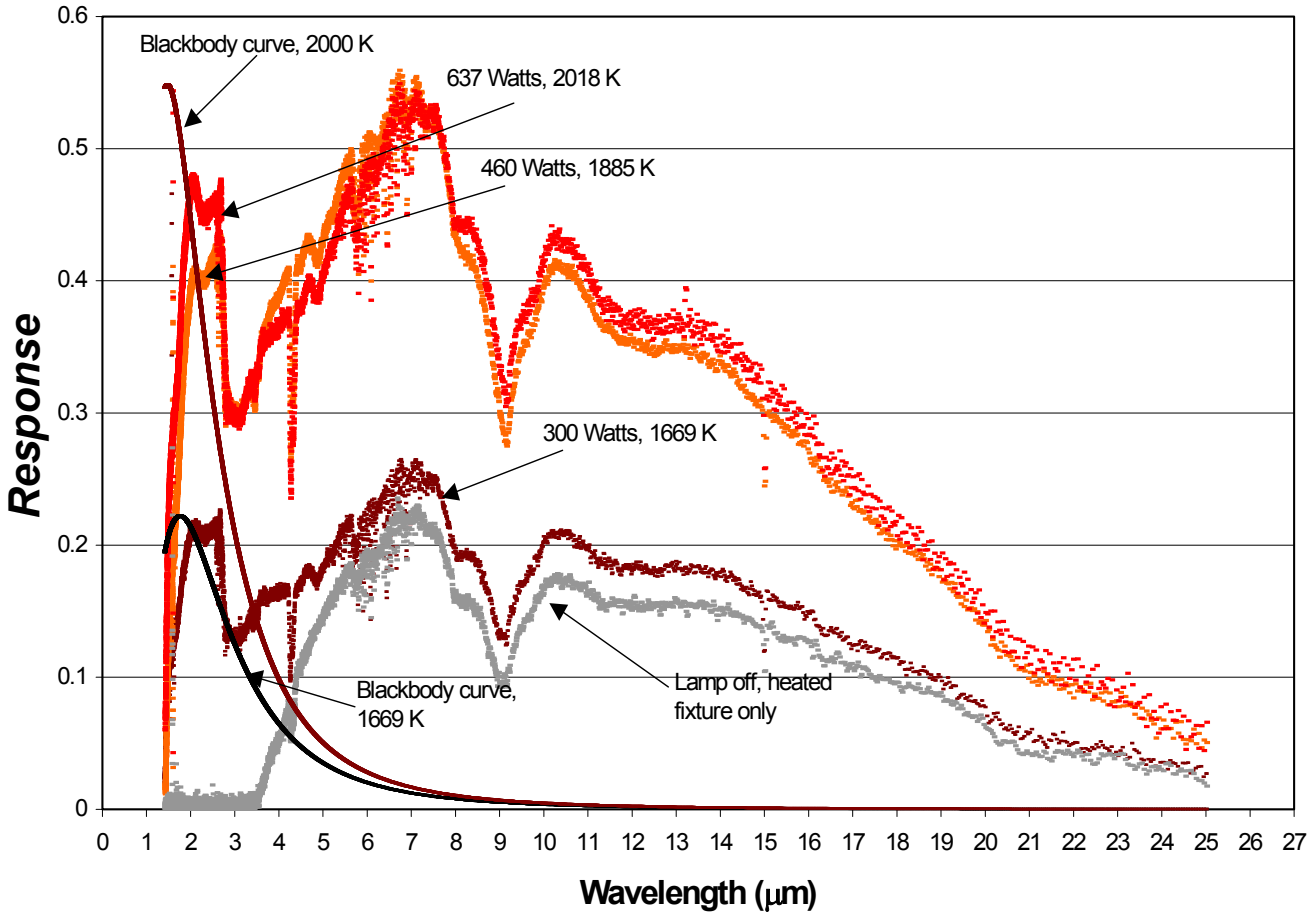

Figure 6. Fourier transform emission spectra from short wavelength radiant heating system at several power levels along with theoretical blackbody curves at corresponding temperatures

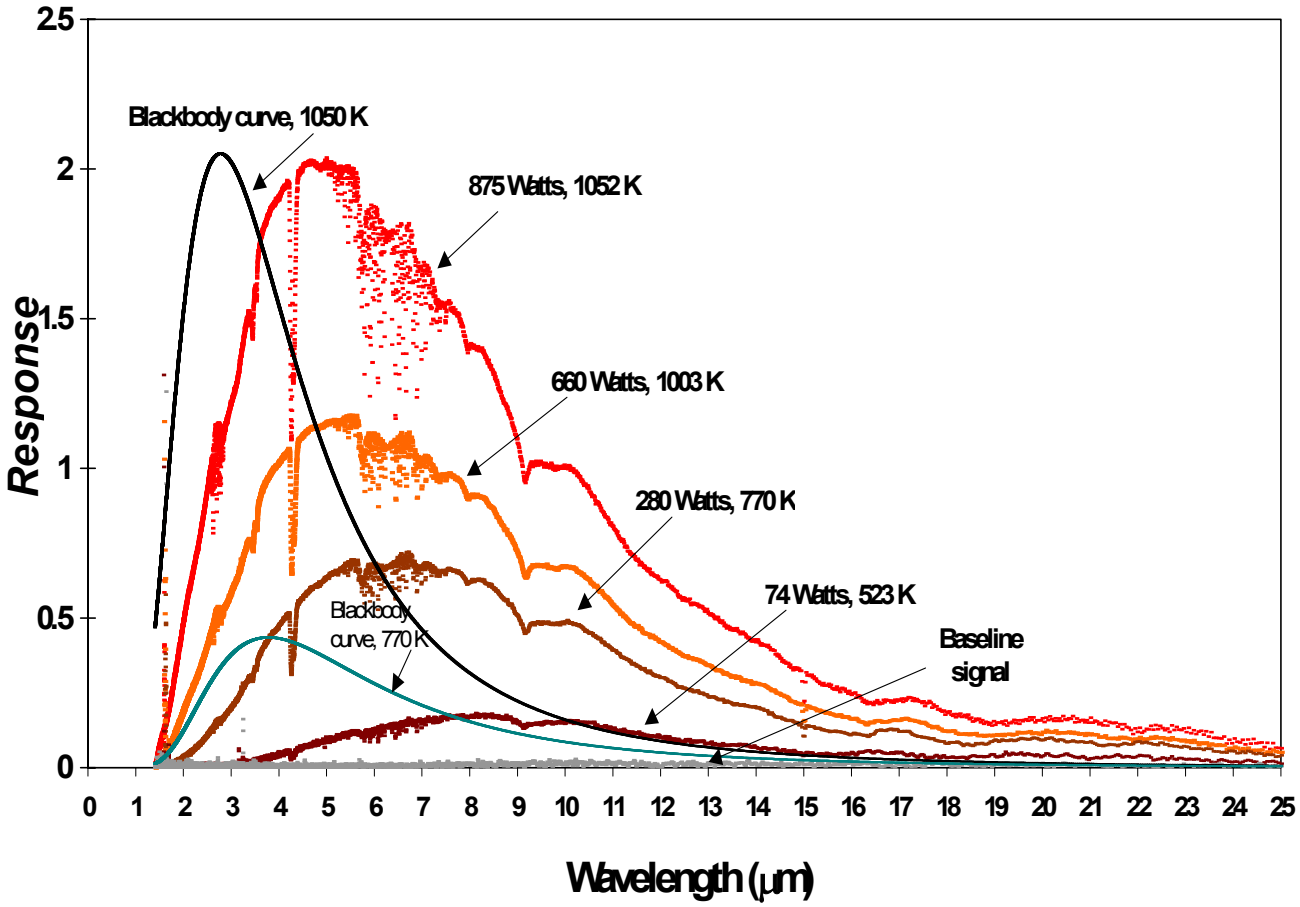

Figure 7. Fourier transform emission spectrum from medium wavelength radiant heating system at several power levels along with corresponding theoretical blackbody curves.

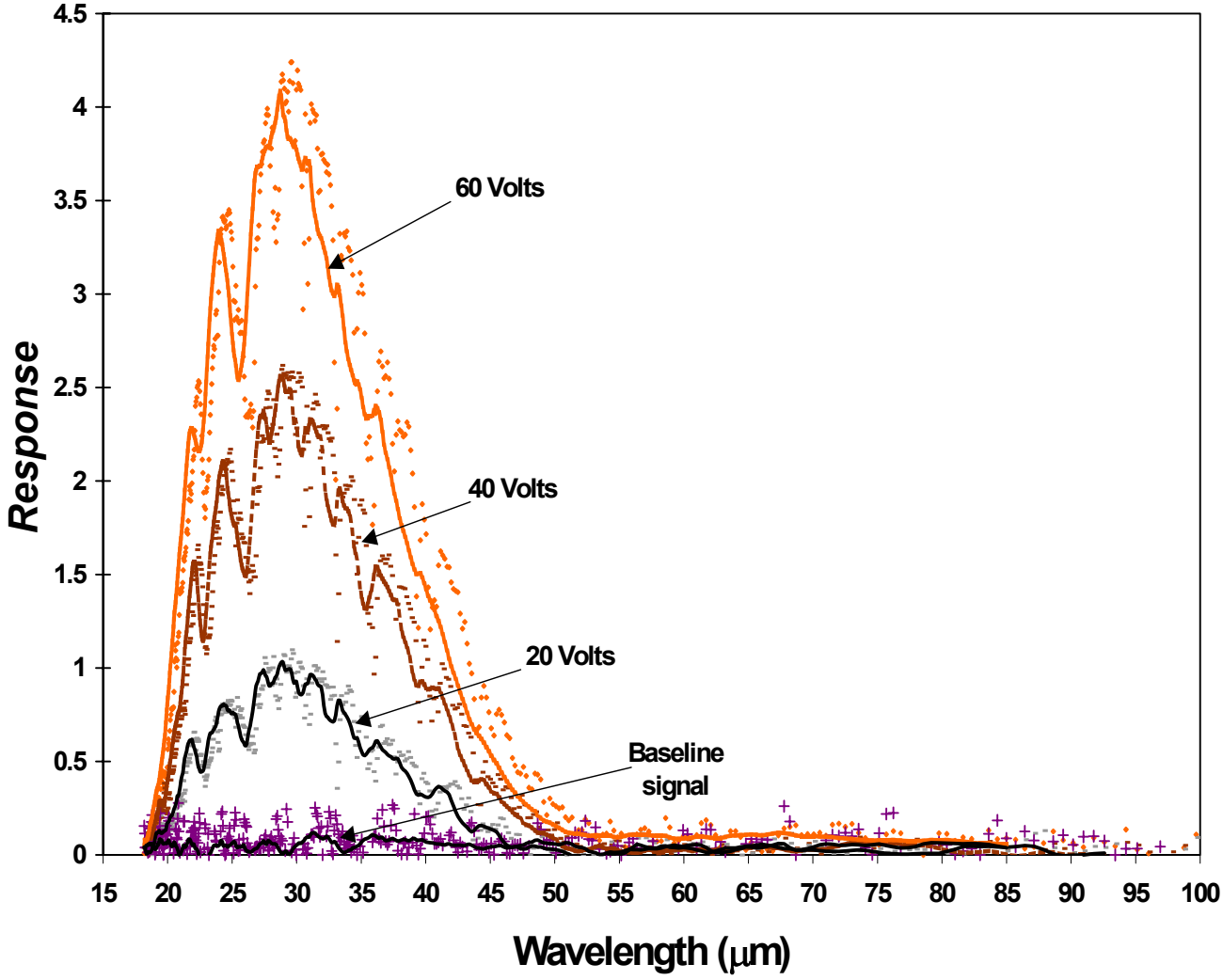

Figure 8. Fourier transform emission spectrum from medium wavelength radiant heating system at several power levels for the wavelength range of 30 to 100 μm. Prior to 30 μm the detector sensitivity limited absolute response values.

II

Comparison of French Fried Potatoes Produced Using Different Finishing Methods

Lloyd, B.J., Farkas, B.E.[1], and K.M. Keener

[1]Corresponding Author

Authors are Brian J. Lloyd, Research Assistant; Brian E. Farkas[1], Associate Professor; and Kevin M. Keener, Associate Professor; all from the Department of Food Science, North Carolina State University, Raleigh, NC 27695.

Submitted to the Journal of Food Processing and Preservation

ABSTRACT

The effect of finish heating method: immersion frying, oven heating or dynamic radiant heating was evaluated for texture, color, and sensory properties of par-fried French fries. Peak breaking force was highest for radiant heated French fry samples. Color analysis revealed equivalent b-value (yellowness) of crust color for immersion fried and radiant heated French fries. Sensory evaluation indicated overall acceptability of radiant heated French fries equivalent to traditional immersion fried French fried potatoes.

INTRODUCTION

Fried foods are a significant source of food products consumed in the United States. The most popular fried food is French fries with over 3.6 million tons consumed annually (USDA, 2001). The majority of French fries are served in quick serve restaurants (QSR) as a side item. A large order of French fries on average contains approximately 540 calories with 26 g of fat (McDonalds, 2003). The FDA recommended daily intake (RDI) based on a 2,000 calorie diet is 65 g of fat (USDA, 2003), thus one large order of French fries approaches 45% of RDI for fat and 27% of total daily calories. American consumers are increasingly becoming more health conscious and finding that fried foods such as French fries should be avoided. United States French fries sales dropped 10 percent from 2001 to 2002, after more than a decade of increasing sales (Myers, 2003). Food products with reduced fat, calories, sodium, etc. were termed 'less-evil' products and identified as the #2 Top Food Trend for 2003 (Sloan, 2003). French fries of lower fat content and equivalent sensory attributes would be expected to be highly accepted by consumers.

Development of lower calorie, lower fat French fries for the QSR may involve product reformulation, changing the finish-frying step, or a combination of each. French fries sold by restaurants and retail establishments generally start with an initial par-frying step. The par-fried potatoes retain 7 to 10% fat, prior to being frozen, packaged and sold (Gould, 1999). Retail QSRs then finish-fry the par-fried potatoes by immersion frying. During immersion finish frying the fat content increases to 15 to 30%. The calories contributed by fat is notably high, constituting over 40% of total caloric contact for French fries. Development of an alternative finish-frying process that would retain the unique

French fry characteristics of golden color, crisp crust, and soft core produced by immersion frying (Hubbard and Farkas, 2000), yet yield a lower oil content product (< 13 %) would be highly desirable to consumers and retail QSRs alike.

The finish frying step is usually accomplished by immersion frying in hot (176°C, 350°F) oil. Another less common method is oven baking at temperatures of 234°C (450°F). However, a new approach to an alternative finish frying process utilizes dynamic radiant heating. Radiant heating broadly includes electromagnetic thermal energy in the wavelength range of approximately 0.4 to 1000 μm (Siegel and Howell, 2002), which is long wavelength ultraviolet to far infrared. Radiant heating is primarily a surface heating technique (Sandu, 1986), although limited subsurface penetration does occur (Dagerskog, 1979).

The controlled dynamic radiant heating technique (CDR) revealed here utilizes the adaptability of radiant energy to reproduce the heat flux intensity (W/m^2) profile that occurs during immersion frying. The immersion frying heat flux of raw Russet potatoes was found to quickly increase to a high maximum value (35,000 W/m^2) then decreasing with time (Hubbard and Farkas, 1999). The uniqueness of the approach incorporates emitter spacing and varying emitter power levels to replicate immersion frying heat transfer without the use of a deep fat fryer, which adds additional oil to a par-fried product. Other methods of heating such as convection cannot deliver the intense heat flux required for crust development without using high air velocities which dries the product and strips out oil.

The CDR approach to mimic immersion frying heat transfer is relatively new although past research has reported on radiant heating of potato and French fry products. Afzal and Abe (1999) reported radiant drying of potatoes to be a falling rate process and moisture removal could be described by a modified exponential function. Masamura et al.

(1988) reported on the drying of potato using far infrared radiation. Radiant drying was shown to require less energy than traditional convective drying processes. Gaon and Wiedersatz (1993) developed an alternative frying process utilizing a microwave section and an infrared heating section to produce potato chips without oil. Radiant heating of potato products is not new, however CDR heating has not been investigated.

An experimental CDR oven was developed to finish fry par-French fries mimicking heat transfer found in traditional immersion frying. In preliminary tests, French fries prepared by this oven had shown comparable appearance and crust texture to traditionally immersion fried product. However, instrumental and sensory methods must be used to objectively measure the quality of CDR heated French fry products compared to other heating methods. The objectives of this research were: (1) to measure texture and surface color properties of French fries produced using three finish heating methods; and (2) to measure consumer acceptance of important French fry attributes for French fries produced by three finish heating methods.

MATERIALS AND METHODS

Finish Heating Methods

Four 32 oz. packages of frozen store brand (Harris Teeter, Matthews, NC) par-fried shoe-string cut potatoes were purchased and mixed into one homogenous batch. The par-fries were made from Russett potatoes and contained 11.2% fat. The par-fried potatoes were stored at -20°C until testing. The par-fries did not contain added colorants that might affect degree of browning measurements. Moisture and fat content was determined for the par-fries

and after each heat treatment using AOAC methods (AOAC, 1995). The three finish heating methods employed were: immersion frying, residential oven heating, and CDR heating.

Immersion Frying

Approximately 35 g of frozen par-fried French fries (about 16 fries) were immersed in partially hydrogenated vegetable oil (FryMax® brand, Ach, Memphis, TN) at 172°C (350°F). The fryer (Rival, model 3, Arpt, KS) had a two-quart oil capacity. The sample was fried for 3.5 minutes then removed from the oil and drained according to package instructions. A 3.5 min. frying time was found sufficient for adequate moisture removal in frozen shoestring French fries as shown by Du Pont et al. (1992). The finished fries were then placed under a 250 W heat lamp. A timer monitored the residence time under the heat lamp, and samples were discarded after four minutes due to a change in texture.

Oven Heating

A 35 g sample of frozen French fries (approximately 16 fries) was placed on an aluminum Teflon-coated cake pan. The pan was placed in a free convection oven (Frigidair, Gallery Series) set at 232°C (450° F) for 8 min. as recommended by the French fry manufacturer. After heating, the fries were placed under a heat lamp (250 W) and discarded after four minutes. Two identical ovens were used for this method, and oven temperature was monitored to insure similar heating in both ovens.

CDR Heating

An experimental CDR oven was used to finish fry frozen par-fried potatoes. The oven used a stainless steel belt to continuously expose samples to a series of 500 W quartz-halogen radiant emitters. Five pairs of emitters were mounted on opposing sides of the belt (Fig. 1). Each pair of emitters was independently controlled and designed to expose the

sample to a heating regime that reproduced the heat flux experienced during traditional oil immersion frying as outlined by Hubbard and Farkas (1999). The samples experienced an overall heating time of 3 min., which was found sufficient for adequate heating. After leaving the oven, French fries were retained under a heat lamp (250W) for a maximum of four minutes.

Texture Analysis

Textural properties were evaluated immediately after each heat treatment using a TA.XT2 Texture Analyzer with a 5 kg load cell (Texture Technologies Corp., Scarsdale, NY/Stable Microsystems, Surrey, U.K.). Data collection and analyses were done using the Texture Expert software of the TA.XT2 analyzer. Two probe types and methods were utilized. For both probe types, 3 batches of 10 fries per batch were evaluated for each heating treatment.

Puncture: A single flat end stainless steel probe of 1 mm diameter was used for crust penetration as outlined by Lima and Singh (2001). Probe speed was maintained at 1.6 mm/s. The maximum puncture force was recorded and each fry sample was tested on opposing sides, i.e. 2 measurements per sample, to minimize localized crust variation from non-uniform heating methods such as the oven heating treatment.

Kramer Shear: The Kramer shear method was noted by Walter et al. (2002) as the most precise texture analysis procedure for a French fry-type product. A single heated fry was placed across the bottom of the five-blade Kramer shear cell. Blades were driven downward at a speed of 1.6 mm/s. The peak force was collected for analysis and comparison.

Color Comparison

Sample color was evaluated after each heat treatment using digital image analysis. A single fry was placed on a black background and a 2272 x 1704 pixel image was acquired using a digital camera (model MVC-CD400, Sony, Tokyo, Japan). The camera was mounted on a copy stand with the focal length, lighting, and camera settings consistent for all samples. The acquired image was analyzed using Adobe Photo Shop (version 6.0, San Jose, CA) to isolate the sample from the background as well as eliminate any shadowing effects. Histogram data was collected for mean and standard deviation of luminosity, lightness, and b-value of the extracted image. Measurement ranges were defined by 0 (completely black) to 255 (pure white) luminosity and lightness. The b-value scale was 0 (blue) to 255 (yellow) (Russ, 1999). The b-value indicated the yellow to orangeness of the sample indicating the degree of browning of a French fry product.

Sensory Analysis

Consumers of French fries were recruited to evaluate the acceptability using the three methods. Consumers (n=53) were volunteers solicited from North Carolina State University Department of Food Science students, staff, faculty, and guests. Consumer testing was conducted with the approval of the NCSU Institutional Review Board (IRB) for human subjects. Each panelist was first presented a consent form and screener to gather demographic information. After the screener was completed, the panelist was presented with a score sheet and each French fry sample monadically. Each panelist received and evaluated a single sample at a time in a predetermined randomized order. Panelists were provided with a score sheet, a pencil, napkin and rinse water. The evaluated attributes included: overall appearance liking, overall acceptability, overall flavor liking, overall texture liking, overall

crispness intensity and liking, and overall oily mouthfeel and liking. The attributes were evaluated on a 9-point hedonic scale anchored on the left with dislike extremely and on the right with like extremely (Meilgaard et al., 1997). After all samples were evaluated, the score sheets were collected and the panelist was given a food treat for his/her participation.

Statistical Analysis

Univariate analysis of variance (ANOVA) was performed for each measured attribute using the GLM (General Linear Model) procedure in SAS (version 8, Cary, NC). LSMEANS tests were used to determine statistical difference between attribute means of each heating treatment as well as the variation due to batch and sample. Frequency histograms of sensory demographic data were performed to reveal notable trends of French fry consumption and consumer information. Pearson correlation analysis was also performed to indicate linear relationships between sensory attributes.

RESULTS AND DISCUSSION

Texture Analysis

Peak force values for each of the three heating methods were determined (Table 2). Punch test values showed that there was not a significant ($p < 0.05$) difference in texture between the heat treatments. The standard deviation was high at 26 to 47% of the mean value. This high variability was also observed by Walter et al. (2002) using the punch test. These authors measured the crust texture of sweet potato French fries as well as Ore-Ida brand French fries and found a coefficient of variation of 38.2%. The high variation was likely due to localized non-uniform crust formation that caused probe placement on the crust surface critical toward repeatable measurements for a given sample. Although there was not

a significant difference in peak force, the CDR heated sample showed the highest mean value as well as the lowest standard deviation.

The Kramer shear test showed that CDR heated French fries had a significantly higher peak force ($p < 0.05$) than immersion fried or oven baked. The Kramer shear method was found superior by Walter et al. (2002). These authors measured a coefficient of variation of the Kramer shear at 3.8%, while the puncture test was 38.2% for Ore-Ida brand French fries. The Kramer shear measurements also showed that the immersion fried and oven baked fries were not significantly different in peak force (Table 2). It was noted that oven baked fries did not have uniform crust on the sides in contact with the pan and the side facing upward. The heated pan surface created a darkened, thicker crust, while the upward facing side usually had under-developed crust.

Color Analysis

Comparison of color indices for finished fries indicated the degree of crust darkening (luminosity and lightness) and yellowness (b-value) could be used to distinguish between heating methods. Luminosity measurements revealed an equivalent degree of darkening among the treatments. However, the lightness (L-value) values showed that the immersion fried and oven cooked samples were equivalent while the CDR heated samples were slightly yet significantly ($p<0.05$) lighter overall color (Table 3). It was also noted that some of the CDR heated product with pointed ends had darkened tips. It was hypothesized that excessive drying of these thinner regions caused darkening from excessive heating.

The degree of yellowness (b-value) for the immersion fried and CDR heated samples were not significantly ($p < 0.05$) different. The oven baked fries were a more orange to dark

red color due to excessive browning at pan contact areas. From observation, the CDR heated fries showed a fairly consistent golden color in the central portions of the fry that resembled traditional immersion fried product; however the immersion fried samples were more uniform in color end-to-end especially noticeable at the thinner, pointed end. Overall, the flux from CDR heating reproduced immersion frying heat transfer on a macroscopic scale for the uniformly-shaped fries, leading to proper coloration. However, localized excessive heating would still sometimes occur at thinner end regions of the CDR heated product. As a possible explanation, immersion frying decreased the localized boiling heat transfer flux of the thinner, sensitive regions tip as these regions lose moisture and dry out (Farkas and Hubbard, 2000). The decrease in heat flux was speculated to prevent any excessive darkening or charring in the immersion fried samples that was sometimes noted in the CDR heated samples.

Sensory Evaluation

The CDR heated fries were equally acceptable to consumers as compared with the other two heating treatments with respect to overall appearance, flavor liking and oily mouthfeel liking (Table 4). The CDR heated French fries received the highest mean hedonic scores for oily mouthfeel liking even though the lipid content was the lowest (Table 1). There were no differences in overall appearance liking among the fries suggesting that darkened tips of the CDR samples did not affect consumers.

As mentioned, the flavor liking scores were not statistically ($p<0.05$) different (Table 4). For flavor liking, the highest standard deviations among all attributes suggested segmentation in the consumer group for French fry flavor. Oil and browning products represent the primary flavoring sources in French fries (Martin and Ames, 2001). The CDR

heated samples had a superior browned surface likely causing the highest mean flavor scores. The immersion-fried samples contained much more oil flavoring due to the higher oil content, which was liked by a segment of the consumer population but not universally as indicated by the higher standard deviation.

CDR heated fries had a significantly different texture than immersion fried (Table 4). Oven baked fries were neither different than either immersion fried or CDR heated. The term 'texture' was not intended to overlap with the crispness attribute although they were highly correlated (Table 5). The oil to lubricate the palate in the immersion fried samples was absent in the oven baked and CDR heated samples, which likely caused decreased mean texture-liking scores.

The crispness intensity and crispness liking scores showed a similar trend with immersion fried fries higher than CDR heated samples. Oven cooked was not significantly ($p<0.05$) different than either other treatment. Crispness intensity was positively correlated with crispness liking. Consumers also indicated crispness as a primary factor of choice of French fries. Increasing the crispness of CDR heated French fries would be a requirement to improve overall consumer acceptance of a reduced fat French fry product.

Oily mouthfeel intensity and liking indicated that both oven cooked and CDR heated fries had a less oily mouthfeel. However, consumers indicated that less oily mouthfeel was preferred, although no liking differences were found. Oily mouthfeel intensity and oily mouthfeel liking showed a negative correlation (Table 5). Consumers rated CDR heated French fries higher than oven baked due to a less oily mouthfeel. There was significant correlation of acceptability with flavor liking and texture liking as well as texture liking with crispness intensity and liking (Table 5).

Finally, overall acceptability of each finish treatment showed that CDR heated fries were not statistically ($p<0.05$) different than traditional, full-fat immersion finished fried French fries. Oven baked fries received a significantly lower acceptance score than immersion fried or CDR heated. These results indicate that consumers did not reject the alternative finish-frying method of CDR heating designed to mimic traditional immersion frying.

CONCLUSIONS

This research demonstrated that CDR heated finish-fried French fries had consistent texture, color, and consumer acceptability when compared to an immersion finished-fried product. Consumer demographic information collected during sensory analysis indicated that consumers were interested in a low/reduced fat French fry as an alternative to traditional immersion fried French fries. Improving crispness intensity is needed for the CDR heated French fry product. The overall acceptability of CDR heated French fries was not statistically different than traditional immersion finish frying. CDR finish heating of par-fried French fries shows promise to produce a lower fat product, as well as an alternative process to traditional immersion finish frying.

ACKNOWLEDGEMENTS

The authors would like to thank Dr. MaryAnne Drake for her contributions to the sensory analysis section. We also wish to acknowledge APW Wyott Inc. Dallas, TX, for donation of equipment supplies. Funding for this project was made possible through the USDA National Needs Grants Program #1999-1583 and the USDA National Research Initiative Competitive Grants Program #9801477.

REFERENCES

Afzal, T.M. and T. Abe. 1999. Some fundamental attributes of far infrared radiation drying of potato. Drying Technol. 17(1,2): 137-155.

AOAC International. 984.25 and 963.15. *Official Methods of Analysis, 16th Ed.* AOAC International, Gaithersburg, MD. 1995.

Dagerskog, M. and L. Osterström. 1979. Infra-red radiation for food processing I. A study of the fundamental properties of infra-red radiation. Lebensmittel Wissenschaft Technologie 12(4): 237-242.

Du Pont, M.S., Kirby, A.R., and A.C. Smith. 1992. Instrumental and sensory tests of texture of cooked frozen French fries. Int. J. Food Sci. and Technol. 27: 285-295.

Fiona, L.M. and J.M. Ames. 2001. Comparison of flavor compounds of potato chips fried in palmolein and silicone fluid. JAOCS. 78(8): 863-866.

Gaon, D. and J. Wiedersatz. 1993. Process for preparing fat free snack chips. U.S. Patent No. 5,202,139.

Gould, W.A. 1999. Potato production, processing, and technology. Timonium, MA: CTI Publ. Inc.

Hubbard, L.J. and B.E. Farkas. 2000. Determination and analysis of oil temperature effects on convective heat transfer coefficients and heat flux in immersion frying. J. of Food Processing and Preservation. 24: 143-162.

Hubbard, L.J. and B.E. Farkas. 1999. A method for determining the convective heat transfer coefficient during immersion frying. J. of Food Process Engr. 22: 201-214.

Lima, I. and R.P. Singh. 2001. Mechanical properties of a fried crust. J. Texture Studies. 32(1): 31-40.

Martin, F.L. and J.M. Ames. 2001. Comparison of flavor compounds of potato chips in palmolein and silicone fluid. J. Am. Oil Chemists Soc. 78(8): 863-866.

Masamura, A., Sado, H., Honda, T., Shimizu, M., Nabetani, H., Nakajima, M., and A. Watanabe. 1988. Drying of potato by far infrared radiation. Nippon Shokuhin Kogyo Gakkaishi. 35(5): 309-314.

McDonalds Corp. June 8, 2003. McDonald's USA nutrition facts for popular menu items. Oak Brook , IL.

Meilgaard M., Civille, G.V., and B.T. Carr. 1997. Sensory evaluation techniques. 3rd ed. Boca Raton, Fla.: CRC Press, Inc.

Myers, M. 2003. USPB to share commitment to improving the potato's nutrition image with top three processors. United States Potato Board press release. Denver, CO July 7.

Russ, J.C. 1999. The image processing handbook. 3rd ed. Boca Raton, Fla.: CRC Press, Inc.

Sandu, C. 1986. Infrared radiative drying in food engineering: a process analysis. Biotechnology Progress 2(3): 109-119.

Sloan, A.E. 2003. Top 10 trends to watch and work on: 2003. Food Technol. 57(4): 30-50.

USDA. 2003. Code of Federal Regulations, Nutrition labeling of food. Title 21. Section 101.9.

USDA. 2001. U.S. agricultural statistics for French fry production and consumption. USDA National Agricultural Statistics Service. www.usda.gov/nass.

Walter, W.M., Truong, V.D., and K.R. Espinel. 2002. Textural measurements and product quality of restructured sweetpotato French fries. Lebensm-Wiss. u.-Technol., 35(3): 209-215.

Table. 1. Fat and moisture content of par-fried French fries heated by three different methods. Reported values are the mean of three samples from three batches. Values in parentheses are the standard deviation. Like letters in each row indicate a significant difference ($p<0.05$) was not found.

Component (%, wet basis)	**Raw Par-Fried**	**Immersion Fried**	**Oven Baked**	**Radiant Heated**
Lipid content	11.2^{a}, (1.44)	19.2^{b}, (0.19)	13.8^{ac}, (0.96)	13.0^{ac}, (0.38)
Moisture content	63.0^{a}, (0.37)	50.4^{b}, (1.64)	37.8^{c}, (1.92)	36.6^{c}, (0.15)

Table 2. Crust texture comparison of French fries prepared using three different heating methods. Like letters in each column indicate that there was not a significant difference ($p<0.05$) between means.

Heat Treatment	Punch test (N)		Kramer shear (N)	
	Mean (N)	**Stnd. dev.**	**Mean (N)**	**Stnd. dev.**
Immersion Fried	0.521[a]	0.245	21.3[a]	6.54
Oven Baked	0.573[a]	0.302	20.0[a]	4.91
Radiant Heated	0.604[a]	0.199	24.5[b]	4.71

Table 3. Color comparison of French fries prepared by three different finish heating methods. Like letters in each column indicate that there was not a significant difference ($p<0.05$) between means.

Heat Treatment	**Degree of Crust Darkening**		**Yellowness**
	Luminosity	**Lightness (L-value)**	**b-value**
Uncooked par-fried	203.4[a]	209.9[a]	145.0[a]
Immersion Fried	172.8[b]	183.7[b]	172.0[b]
Oven Baked	172.6[b]	184.8[b]	178.2[c]
Radiant Heated	177.7[b]	189.7[c]	171.1[b]

Table 4. Mean hedonic scores for par-fried French fries heated using different finishing heat treatments. Like letters in each row indicate that there was not a significant difference ($p<0.05$) between means.

Attribute	Immersion Fried		Oven Baked		Radiant Heated	
	mean	stnd dev.	mean	stnd dev.	mean	stnd dev.
Overall Appearance Liking	6.30[a]	1.38	6.00[a]	1.74	5.92[a]	1.53
Overall Acceptability	5.94[a]	1.82	5.33[b]	1.87	5.67[a]	1.48
Overall Flavor Liking	5.45[a]	2.28	5.23[a]	1.90	5.56[a]	1.64
Overall Texture Liking	5.89[a]	1.89	5.67[ab]	2.01	5.19[b]	1.83
Overall Crispness Intensity	5.28[a]	2.09	5.00[ab]	2.36	4.40[b]	1.73
Overall Crispness Liking	5.53[a]	2.03	5.19[ab]	2.32	4.79[b]	1.96
Oily Mouthfeel Intensity	5.49[a]	1.75	4.83[b]	1.78	4.10[c]	1.80
Oily Mouthfeel Liking	5.49[a]	1.84	5.52[a]	1.80	5.90[a]	1.52

(n=53)

Table 5. Correlation coefficients for French fry attributes. Significant ($p<0.05$) correlations are indicated by *. Attributes are coded by: Appearance liking (A); Acceptability (B); Flavor liking (C); Texture liking (D); Crispness Intensity (E); Crispness liking (F); Oily mouthfeel intensity (G); Oily mouthfeel liking (H).

	A	B	C	D	E	F	G	H
A	--------							
B	0.4805*	--------						
C	0.3408*	0.7861*	--------					
D	0.3368*	0.6283*	0.5478*	--------				
E	0.2544*	0.4567*	0.3293*	0.7459*	--------			
F	0.3463*	0.5878*	0.4749*	0.8299*	0.8562*	--------		
G	-0.0461	-0.1148	-0.1608*	0.0280	0.1072	0.0639	--------	
H	0.2452*	0.3872*	0.4809*	0.3554*	0.1639*	0.2984*	-0.2428*	--------

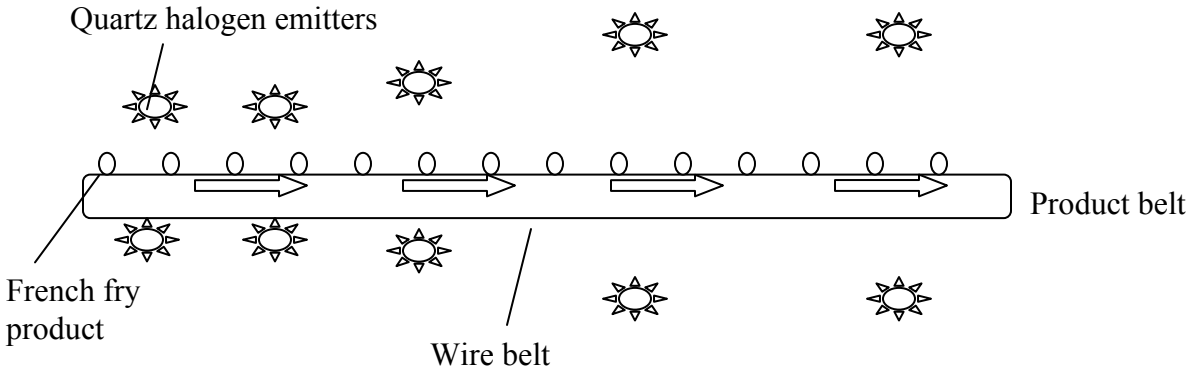

Figure 1. Simplified cross-section schematic of the experimental radiant heated oven. Notice emitter spacing increased along belt length to decrease heat flux impinging on French fries. Not to scale.

III

Numerical Simulation of High Intensity Radiant Heating of Potatoes

Lloyd, B.J., Farkas, B.E.[1], and K.M. Keener

[1]Corresponding Author

Authors are Brian J. Lloyd, Research Assistant; Brian E. Farkas[1], Associate Professor; and Kevin M. Keener, Associate Professor; all from the Department of Food Science, North Carolina State University, Raleigh, NC 27695.

Submitted to the Journal of Food Engineering

ABSTRACT

A numerical simulation of high intensity radiant heating was developed for a potato slab. The simulation predicted the temperature profile throughout in a one-dimensional slab. A surface crust and core region were defined and the increase in crust thickness was tracked during radiant heating. Measured surface and core temperatures showed excellent agreement with simulation results producing an average deviation of less than 3°C during 15,000 and 27,000 W/m^2 constant flux heating. The simulation was used as a tool to evaluate parameters which affect radiant heating of products and to simulate immersion frying and crust formation.

INTRODUCTION

Radiant heating includes electromagnetic thermal energy in the visible and near-, mid-, and far-infrared wavelength ranges approximately 0.6 to 100 μm (Siegel and Howell, 2002). Radiant heating has the advantages of fast response time, high energy conversion, simple equipment design, and adaptability with other heating treatments (Sharples, 1971). Radiant heating of foods has traditionally been used for baking, roasting, and surface drying. New applications of radiant heating of foods are emerging and one area of particular interest is development of surface crusts.

Radiant heating has been used to heat food products where a surface crust is desired. Sheridan and Shilton (1999) reported on the application of infrared radiation to cooking meat products. Crust was developed in areas where the surface temperature exceeded 100°C. An infrared emitter with surface temperature of 1098 K was used. Skjöldebrand and Andersson (1989) compared bread baked using infrared radiation with traditional convection baked bread. The authors concluded that parameters such as radiant power level and spectral intensity could be used to control the crust formation and other product quality indices. Unklesbay and Unklesbay (1985) found that pizza dough color and crust formation was directly related to infrared emitter temperature. Sato et al. (1992) found that rate of crust formation in bread and white flour batter was dependent on the wavelength characteristics of the radiant emitter used.

Products such as French fries that traditionally utilize immersion frying for crust development (Farkas, 1994) have the potential to be produced by radiant heating. Understanding crust development as affected by radiant energy absorption must occur on a

fundamental level. Many factors contribute to crusting such as product surface temperature, moisture content, and energy flux into the product.

One tool to help understand the basic theory of radiant heating of foods has been mathematical modeling. Several approaches of mathematical simulation of radiant heating of foods have been investigated. Fasina et al. (1998) developed a numerical simulation for the infrared heating of barley kernels. The authors used transient heat transfer in spherical coordinates with a surface absorption radiant boundary condition, and diffusion mass transfer with internal resistance. Configuration (view) factors were also calculated between the infrared heaters and the grain bed. Simulation results and measured data were similar although heating time was restricted to less than 16 s. Ranjan et al. (2002) also simulated infrared drying processes. Potato drying was modeled using coupled heat and diffusive moisture transfer equations with infrared energy applied as a surface boundary condition. Results showed good agreement with simulated data for an infrared flux of less than 8000 W/m^2, although the potato product was never heated above 90°C. Datta and Ni (2002) modeled the heating of potato with coupled microwave and infrared heating. The authors showed mathematically that microwave and infrared energy absorbed similarly. An exponential decay term was used for infrared energy absorption. The infrared flux intensities tested were between 2000 to 6000 W/m^2. The numerical simulation penetration depth of the infrared energy into the potato was specified according to Nuri (1984). Dagerskog (1979) mathematically modeled radiant heating of several food products including bread, pork, and potato. A one dimensional radiant heat transfer equation for the surface [1] and interior regions [2] was written using finite difference equations (Dagerskog, 1979):

$$T_{1,k+1} = T_{1,k} + \frac{2a\Delta t}{\Delta x^2}\left(T_{2,k} - T_{1,k}\right) + 2a\frac{\alpha\Delta t}{k\Delta x}\left(T_{air} - T_{1,k}\right) + \frac{2a\Delta t}{k\Delta x}\left[PT\left(1 - P_2\right) + RT\left(R_2 - R_1\right)\right] \quad [1]$$

$$T_{n,k+1} = T_{n,k} + a * \frac{\Delta t}{\Delta x^2}\left(T_{n+1,k} - 2T_{n,k} + T_{n-1,k)}\right) + \frac{a\Delta t}{k\Delta x}\left[PT\left(P_n - P_{n-1}\right) + RT\left(R_{n+1} - R_n\right)\right] \quad [2]$$

In this approach, mass transfer was ignored, material properties were constant, and no attempt was made to incorporate crust development. This approach addressed development of subsurface radiant dissipation. For each node, an exponential radiation dissipation term was introduced as an internal generation term(s) (PT and RT) by the constant radiant energy flux. Subsurface heating was calculated and used to determine the temperature distribution throughout the food material at any time.

Limited research has been conducted on mathematical simulation of radiant heating of foods. Many limitations exist that restrict application of high intensity (>15,000 W/m^2) incident energy. The objectives for this study were to measure the temperature rise and mass loss of raw potatoes from high intensity radiant heating. Secondly, a mathematical simulation of the temperature distribution within a potato slab during radiant heating was developed.

MATERIALS AND METHODS

Sample Preparation and Data Collection

Russet potatoes were purchased from a local supplier. A hand shoestring cutter was used to cut the raw samples into 3/8" X 3/8" standard shoestring size (USDA, 2003). The length of each sample was trimmed to approximately 6 cm. Single samples were prepared immediately prior to radiant heating.

Once the raw samples were cut, they were prepared by inserting a thermocouple into the geometric center. A 20 gauge shielded type T thermocouple was placed into a pre-drilled, central hole approximately 3 cm into the sample from one end. The thermocouple-potato junction was sealed and anchored with a small drop of instant glue (Loctite 401, Loctite Corp. Rocky Hill, CT). The sample was then suspended by the thermocouple wire from an overhead balance to measure mass loss during heating. The sample was suspended between the radiant heating systems (Fig. 1) and exposed to the radiant energy during the duration of each heating regime.

The surface temperature of the potato sample was also measured during heating using an infrared optical pyrometer (model OS65, Omega Engineering, Samford, Conn.). The pyrometer lens had a 24:1 field of view and was focused at a 0.64 cm (¼ in.) diameter circle at a 6 in. distance. The small spot size ensured that only the sample surface temperature was measured.

Radiant Heating System

The radiant heating system was a short wavelength system. The system contained two 500 W quartz halogen bulbs (type T3, General Electric, Cleveland, OH). The bulbs used a 20 gage tungsten filament wire with a 120 mm lighted length. They operated at 120 VAC at a maximum current load of 7 A. The bulbs were connected to a variable transformer to control power level. The bulbs were backed by a parabolic shaped reflector (Fig. 1) with a polished, gold anodized surface with an estimated emissivity of 0.02 (Siegel and Howell, 2002). The bulbs were mounted 35 mm apart, filament to filament, with a 7 mm gap between the filament and the reflector backing (Fig. 2). Additional emitter characteristics are outlined by Lloyd et al. (2003).

Data Collection Analysis

During the heating experiments, data was collected for the center temperature, surface temperature, mass loss, and emitter power. Heat flux was measured prior to sample testing using a water-cooled radiometer (model 900-9, Vatell, Christiansburg, VA). All sensor measurements were simultaneously recorded using a Daqbook data acquisition system (Omega Engineering, Stamford, Conn.) connected to a computer. Measurements were taken at 5 Hz for the duration of the heat treatment. Ten replications of each sample type and system were averaged for each reported measurement. The data was collected and analyzed using a spreadsheet (Microsoft Excel®).

Mathematical Model

Heat transfer within a raw potato was mathematically simulated to determine internal temperature distribution. The simulation did not attempt to model radiant energy transfer between the emitter system and the food surface, thus shape and view factors were not considered. It was assumed that the radiant emission from the potato surface was negligible compared to the incoming flux from the radiant emitter systems.

The simulation separated the problem into two separate regions: crust (I) and core (II) (Fig. 3). A partial differential equation (PDE) for the energy transfer was applied to both crust (I) and core (II) regions:

$$\frac{1}{\alpha}\frac{\partial T}{\partial t} = \frac{\partial^2 T}{\partial x^2} + \frac{I_0\left(e^{-\sigma x_i} - e^{-\sigma x_{i-1}}\right)}{xk} \qquad [3]$$

With initial and boundary conditions,

IC: $T(t,x) = T_0$ $0 \leq x \leq L/2,\ t = 0$

BC1: $-k\frac{\partial T}{\partial x} = h\left[T_\infty - T(t,x)\right]$ x=0, t >0

BC2: $\frac{\partial T}{\partial x} = 0$ x=L/2, t >0

BC3: $T(t,x) = T_{bp}$ x= X, t >0

where BC3 was applied to both regions. Boundary condition one (BC1) was the convective energy losses to the environment equal to conduction at the surface. Development of the radiant heat transfer term in equation [3] was similar to that given by Nissim et al. (1980), which is an application of Beer's law of radiation extinction (Sandu, 1986). As the energy penetrated the product, it is assumed to be absorbed as thermal energy or scattered (Birth, 1978) based on the spectral dissipation coefficient σ_λ:

$$I_\lambda = I_{\lambda 0} e^{(-\sigma_\lambda x)} \quad [4]$$

The spectral dissipation coefficient σ_λ in equation [3] was separated into two radiant flux terms based on the absorption of short wavelength (< 1.4 μm) and long wavelength (>1.4 μm) incoming radiant flux. The separation point approximated Wien's law for maximum wavelength of a heated surface with temperature (T):

$$\lambda_{\max.} = \frac{C_3}{T}$$

The short wavelength emitter system operated at approximately 2000 K (Lloyd et al., 2003), thus 1.4 μm was an appropriate separation approximation for the two radiant flux terms. The approach of individual radiant dissipation terms based on wavelength ranges has been used by Wade (1987), Skjöldebrand and Andersson (1986), and Dagerskog Osterström (1979) for a variety of food products such as bread, pork, and potato. Dissipation coefficient values were chosen based in wavelength depth extinction spectroscopy as outlined by Peirs et al.

(2002) and Lammertyn (2000) for apple tissue as well as Dagerskog and Osterström (1979) for potato tissue.

Initially, there was no crust region and the simulation created the crust region (I) after the surface temperature reached T_{bp} (Califano and Calvelo, 1991). Thereafter, the thickness of the crust region increased as lower nodes reached T_{bp}. An interfacial energy balance (Farkas et al., 1996) was used to determine the energy required for moisture evaporation from the crust region at the crust/core interface, (Fig. 3). This energy balance was written as:

$$\frac{dX}{dt} = \frac{q_{vap}}{A\varepsilon_l \rho_l \Delta h_{vap}} \qquad [5]$$

BC: X=0 t=0

It was assumed that the rate of moisture diffusion to the interface was negligible compared to the rate of moisture evaporated during crust development.

Equation [3] and the ordinary differential equation [5] were solved using explicit finite differences (Smith, 1985) and implemented to model the temperature distribution of the material at any time during the heating process. The node size was 0.01 cm for Δx with a maximum time step of 0.01 s per iteration. The material properties and other engineering parameters are presented in Table 1. The stability criteria for the finite difference equations was satisfied for the surface and subsurface nodes as given by Incropera and DeWitt (1996):

Interior: $Fo \leq ¼$

Surface node: $Fo(2 + Bi) \leq ½$

where Fo and Bi are calculated according to Incropera and DeWitt (1996) as:

$$Fo = \frac{\alpha \Delta t}{(\Delta x)^2} \quad [6]$$

$$Bi = \frac{h \Delta x}{k} \quad [7]$$

The finite difference equations were programmed using Fortran (v 6.0, Absoft Corp., Rochester Hills, MI) and the desired output values were plotted using a spreadsheet (Microsoft Excel®). Program code is given in Appendix 1.

RESULTS AND DISCUSSION

Model Testing and Validation

Temperature, crust thickness, and moisture loss during radiant heating of potato was simulated for up to 5 min. and compared with experimental data for two flux intensity values. The predicted crust and core simulation results compared with the measured experimental data were consistent with a flux intensity of 27,000 W/m^2 impinging on the potato surface. The difference in the numerical internal core temperature and measured data averaged less than 4°C for the entire simulation. The core temperature reached a plateau at 105°C after approximately 100 s of heating, which is higher than the boiling point of water although Califano and Calvelo (1991) routinely measured 103°C in the center of heated potato. The plateau value of T_{bp} was manually set in the simulation. For the surface temperature, the formation of surface crust can be noted to occur at approximately 60 s. The crust formation caused a step-wise increase in the predicted temperature as interior nodes were discretely converted into crust. This conversion changed the nodal physical properties, most importantly the conductive heat transfer value, from core to crust values. Overall, the surface temperature rise during crust formation was in good agreement with the measured surface

temperature. A surface temperature maximum of 160°C was programmed into the simulation.

The numerical simulation results and experimental data for 15,000 W/m^2 constant flux intensity were similar (Fig. 5). It can be seen that the difference in numerical and experimental temperatures was greatest from 50 to 100s. Ranjan et al. (2002) also measured the greatest deviation of simulated and measured temperature rise for infrared heated potato during this approximate time period. As the temperature increased above 100°C, the predicted and measured surface crust temperature averaged less than 3°C difference.

An investigation into the effect of flux intensity using numerical simulation revealed that flux intensity greatly affected surface and core temperatures. The predicted core temperatures for flux intensities of 10,000 to 30,000 W/m^2 revealed an increased rate of core temperature rise (Fig. 6). Core temperature rise to reach T_{bp} was only 100s for 30,000 W/m^2, while over 250s with 10,000 W/m^2. As flux increased, the effect on core temperature rise diminished. The time to reach core T_{bp} would be critical for processors heating other food materials with mandatory internal temperature requirements such as a formed chicken nugget product. Similarly, the predicted surface temperature rise changed as flux intensity increased (Fig. 7). The time required to reach crust formation varied widely although the length of time to crust formation shortened as the flux intensity doubled. Predicted temperatures within the depth of the material (Fig. 8) graphically present the transcient response at 30 s time intervals. The most notable feature of the temperature rise occurred as the moving boundary transitioned surface nodes from the core (II) to the crust (I).

Influence of Dissipation Coefficient on Predicted Temperature

The most widely used mathematical discription of radiant energy absorption within food materials is Beer's law (Sandu, 1986). The exponential decay of radiant energy within a food material is based on a dissipation coefficient exponent (σ) and plays a critical role in subsurface heating during radiant heating. Measurement of the dissipation coefficient of foods has not been thoroughly investigated and few values exist in the literature. It was not the purpose of this project to explore this material property, however the influence of varying the dissipation coefficient in the developed numerical simulation was investigated.

Representative values of σ were used to illicit a predicted temperature response at the surface and the core. The ratio of short to long wavelength surface flux was maintained at 25% short and 75% long wavelength (Table 1). The core temperature profiles (Fig. 9) developed distinct pairs of temperature trends linked by the long wavelength value, σ_L. The effect of varying σ was not as dramatic for the surface temperature profiles (Fig. 10). As expected the surface nodes absorbed more radiant energy, thus the temperature trends were grouped closer as σ changed. Figures 8 and 9 represent realistic radiant heating situations by incorporating the effects of surface reflection, two σ values representing short and long wavelength energy, and a specific ratio of short to long wavelength flux. However, a clearer representation of the effects of varying σ was found by plotting nodal radiant energy extinction for a single σ value (Fig. 11). As shown here, higher σ values result in greater radiant energy absorbed closer to the surface, while lower σ values increased absorbed energy several millimeters into the product. However, the magnitude of this more deeply absorbed energy is not large compared with the subsurface energy absorption.

Predicted Crust Thickness and Measured Drying Profiles

The increase in crust thickness for different flux intensities was predicted by tracking the movement of the crust/core interface, x=X(t). The crust thickness increased by a smooth, almost linear trend up to a maximum time of 300s (Fig. 12). Predicted crust thickness was consistent with measured end crust values at 1.8 mm for the 27,000 W/m^2 intensity flux.

Moisture loss was measured at two flux intensities, 15,000 and 27,000 W/m^2 (Fig. 13). A linear decrease in moisture loss was observed with both flux values yielding nearly identical drying rates. Drying rate did not reach a falling rate period but remained a constant rate process. At the end of each drying experiment, the samples had highly browned crust and additional heating produced charring. It was speculated that drying rate was governed by vapor diffusion from the crust, and additional energy from an increase in flux caused more developed crust browning and not an increase in moisture evaporation rate.

Conclusions

Predicted and measured temperature profile of raw potato was modeled using one dimensional radiant heat transfer and moisture evaporation equations. High intensity radiant heat transfer was simulated by separating the potato into a crust and core region and tracking the development of the crust as surface moisture was evaporated. Measured surface and core temperatures of 15,000 and 27,000 W/m^2 showed excellent agreement with simulation results producing an average deviation of less than 3°C.

Several input variables of the model were also tested for influence on predicted surface and core temperature. Doubling the impinging radiant flux intensity lead to a decrease in the time required to reach T_{bp} at the center. Crust thickness was predicted to

increase by an average of 14% as radiant flux intensity doubled. The dissipation coefficient, σ, caused a greater change in core temperature as shorter wavelength radiant energy (low σ value) penetrated deeper within the product. Finally, the drying rate of raw potato was measured as a constant rate process with flux intensities of 15,000 and 27,000 W/m^2 producing nearly identical drying rates.

ACKNOWLEDGEMENTS

Funding for this project was made possible through the USDA National Needs Grants Program #1999-1583 and the USDA National Research Initiative Competitive Grants Program #9801477.

NOMENCLATURE

Roman Letters

a	thermal diffusivity (m^2/s) (Dagerskog, 1979)
Bi	Biot number (dimensionless)
C_3	radiation constant = 2897.8 μm K (Incropera and DeWitt, 1996)
$\mathcal{D}$	moisture diffusivity (kg/s)
Fo	Fourier number (dimensionless)
h	convective heat transfer coefficient (W/m^2K)
h_{vap}	latent heat of water (J/kg)
I_0	incident radiant flux intensity (W/m^2)
I_λ	spectral radiant flux intensity (W/m^2 μm)
$I_{\lambda 0}$	incident spectral flux intensity (W/m^2 μm)
k	thermal conductivity (W/mK)
L	length (m)
P	distribution of radiant energy (Dagerskog, 1979)
R	distribution of radiant energy (Dagerskog, 1979)
PT, RT	total density of radiation at surface (W/m^2) (Dagerskog, 1979)
q_{vap}	moisture vaporization flux (kW)
T	temperature (°C)
T_{bp}	boiling point temperature (°C)
T_∞	temperature of surround air (°C)
t	time (s)
x	position within potato (m)

X	position of crust core interface (m)

Greek Letters

α	thermal diffusivity (m^2/s)
α	convective heat transfer coefficient (W/m^2K) (Dagerskog, 1979)
ε_l	volume fraction of water (dimensionless)
λ_{max}	maximum wavelength (μm)
ρ_l	liquid density (kg/m^3)
σ_L	long wavelength (>1.4 μm) dissipation coefficient (m^{-1})
σ_λ	spectral dissipation coefficient (m^{-1})
σ_s	short wavelength (<1.4 μm) dissipation coefficient (m^{-1})

Subscripts

k	time increment (Dagerskog, 1979)
n	space increment (Dagerskog, 1979)

REFERENCES

Birth, G.S. 1978. The light scattering properties of foods. J. of Food Science 43: 916-925.

Califano, A.N. and A. Calvelo. 1991. Thermal conductivity of potato between 50 and 100°C. J. Food Sci. 56(2): 586-587, 589.

Dagerskog, M. 1979. Infra-red radiation for food processing II. Calculation of heat penetration during infra-red frying of meat products. Lebensmittel Wissenschaft Technologie 12(4): 252-257.

Dagerskog, M. and L. Osterström. 1979. Infra-red radiation for food processing I. A study of the fundamental properties of infra-red radiation. Lebensmittel Wissenschaft Technologie 12(4): 237-242.

DesRuisseaux, N.R. and R.D. Zerkle. 1970. Temperature in semi-infinite and cylindrical bodies subjected to moving heat sources and surface cooling. J. Heat Transfer 92: 456-464.

Dumas, C. and G.S. Mittal. 2002. Heat and mass transfer properties of pizza during baking. Int. J. of Food Properties 5(1): 161-177.

Farkas, B.E. 1996. Modeling heat and mass transfer in immersion frying. I. model development. J. Food Engr. 29: 211-226.

Fasina, O.O., Tyler, R.T., and M.D. Pickard. 1998. Modeling the infrared radiative heating of agricultural crops. Drying Technol. 16(9): 2065-2082.

Gould, W.A. 1999. Potato production, processing, and technology. Timonium, MA: CTI Publications.

Incropera, F.P. and DeWitt, D.P. 1996. Fundamentals of Heat and Mass Transfer, 4th ed. New York: Wiley.

Lammertyn, J., Peirs, A., De Baerdemaeker, J., and B. Nicolaï. 2000. Light penetration properties of NIR radiation in fruit with respect to non-destructive quality assessment. Postharvest Biology and Technology. 18: 121-132.

Lloyd, B.J., Farkas, B.E., and K.M. Keener. 2003. Characteristics of radiant emitters used in food processing. J. Microwave Power & Electromagnetic Energy. (In review).

Nissim, Y.I., Lietoila, A., Gold, R.B., and J.F. Gibbons. 1980. Temperature distributions produced in semiconductors by a scanning elliptical or circular CW laser beam. J. Applied Physics 43: 577-583.

Peirs, A., Scheerlinck. N., Touchant, K., and B.M. Nicolaï. 2002. Comparison of fourier transform and dispersive near-infrared reflectance spectroscopy for apple quality measurements. Biosystems Engineering. 81(3): 305-311.

Rice, P., Selman, J.D., and Abdul-Rezzak, R.K. 1988. Effect of temperatures on thermal properties of record potatoes. Int. J. Food Sci Tech. 23:281-286.

Sandu, C. 1986. Infrared radiative drying in food engineering: a process analysis. Biotechnology Progress 2(3): 109-119.

Sharples, J.T. 1971. Electroheat in food processing. British Food Journal. Jan./Feb: 14-56.

Sheridan, P. and N. Shilton. 1999. Application of far infra-red radiation to cooking of meat products. J. of Food Engr. 41: 203-208.

Siegel, R. and J.R. Howell. 2002. Thermal Radiation Heat Transfer. New York: Taylor & Francis.

Skjöldebrand, and C.G. Andersson. 1989. A comparison of infrared bread baking and conventional baking. J. of Microwave Power and Electromagnetic Energy. 24(2): 91-101.

Smith, G.D. 1985. Numerical solution of partial differential equations: Finite difference methods. Oxford University Press, N.Y., New York.

USDA. 2003. United States standards for grades of frozen French fried potatoes. CFR 52.2391-2405.

Table 1. Physical property and numerical simulation input data.

Input parameter	Value
Radiant surface flux, I_0 (W/m^2)	15000, 27000
Half thickness, $L/2$ (m)	5x10^{-3}
Time step, (s)	0.01
Node thickness, Δx (m)	1x10^{-4}
Ratio of liquid to solid in Core (II), ε_l (m^3)	0.2
Initial product temperature, T_0 (°C)	24
Latent heat of water, Δh_{vap} (J/kg)	2.257x10^6
Specific heat, Crust (I) (J/kg K)	3500
Core (II) (J/kg K)	3050
Density, ρ_c Crust (I) (kg/m^3)	310
ρ_l Core (II) (kg/m^3)	1000
Thermal Conductivity, k Crust (I) (W/m K)	0.119
k Core (II) (W/m K)	0.6
Convection heat transfer coefficient, h (W/ m^2 K)	20
Surrounding air temperature, T_∞ (°C)	22
Boiling point temperature, T_{bp} (°C)	105
Short wavelength dissipation coefficient, σ_s (m^{-1})	225
Long wavelength dissipation coefficient, σ_l (m^{-1})	1000
Short wavelength reflection	0.3
Long wavelength reflection	0.5
Radiant flux, % short wavelength (< 1.44 μm)	0.75
% long wavelength (>1.44 μm)	0.25

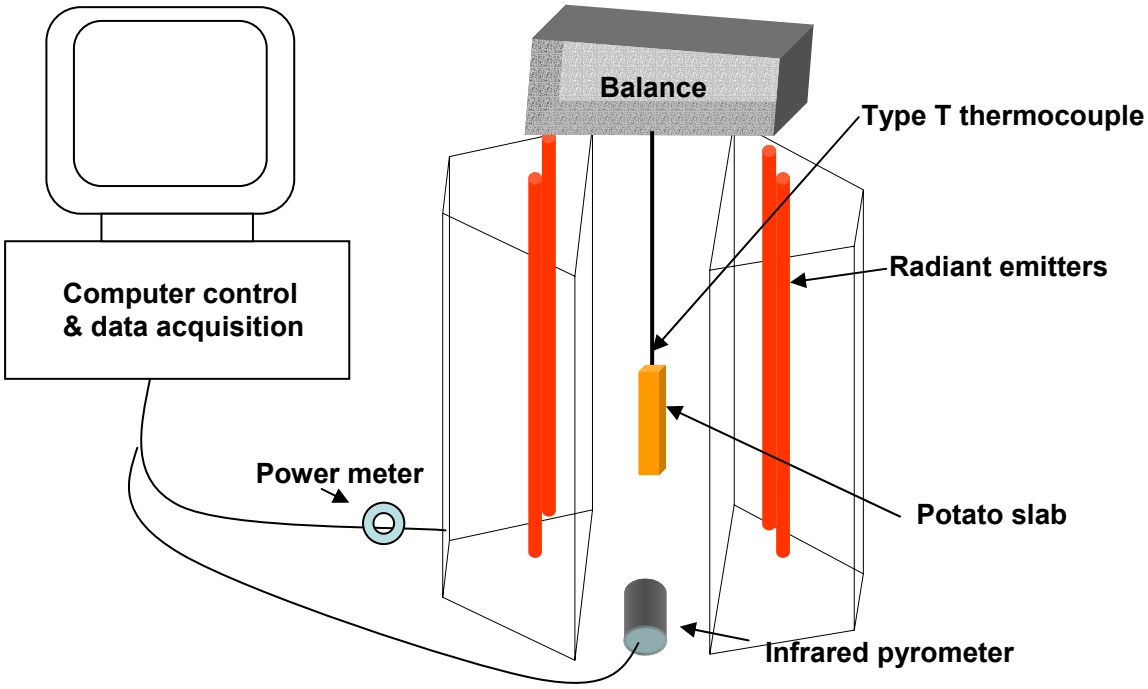

Figure 1. Schematic diagram of the radiant heating system and data acquisition.

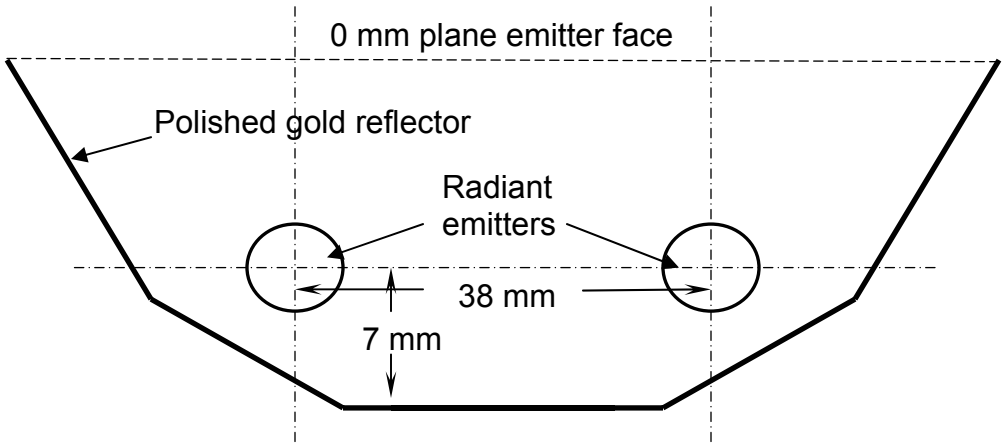

Figure 2. Cross section of the reflector and emitters used in the short wavelength radiant heating system.

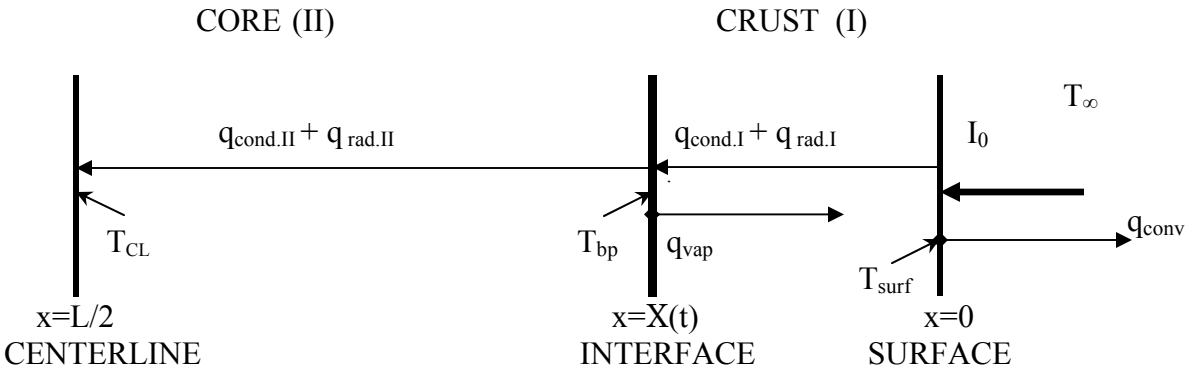

Figure 3. Regions within a potato during radiant heating.

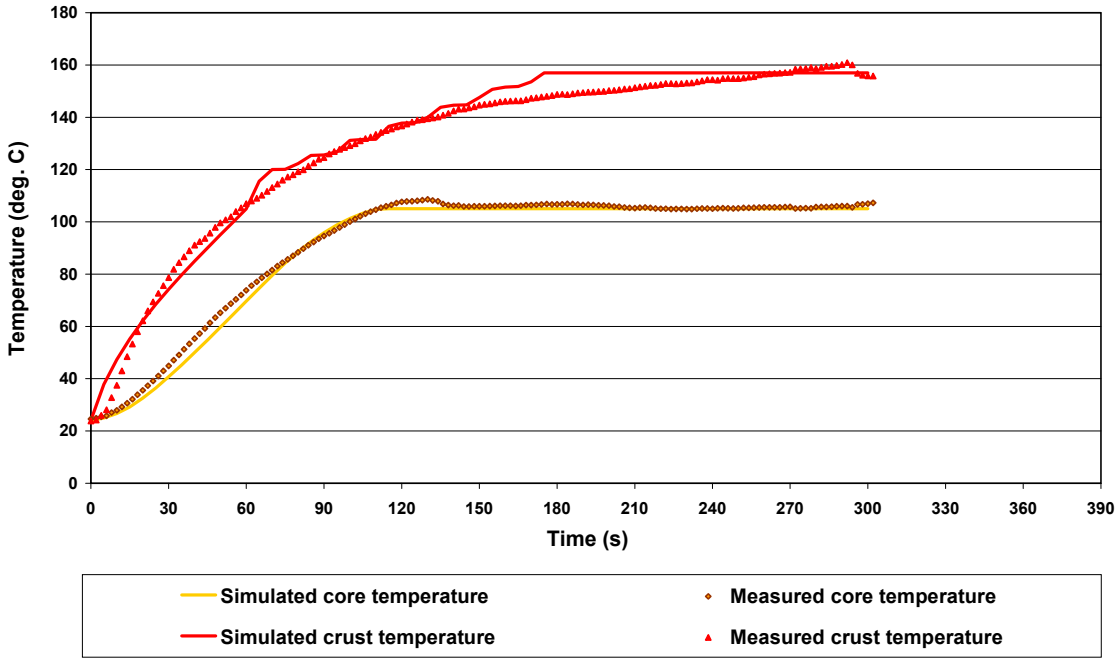

Figure 4. Comparison of predicted and measured high intensity 27,000 W/m^2 radiant heating of raw potato.

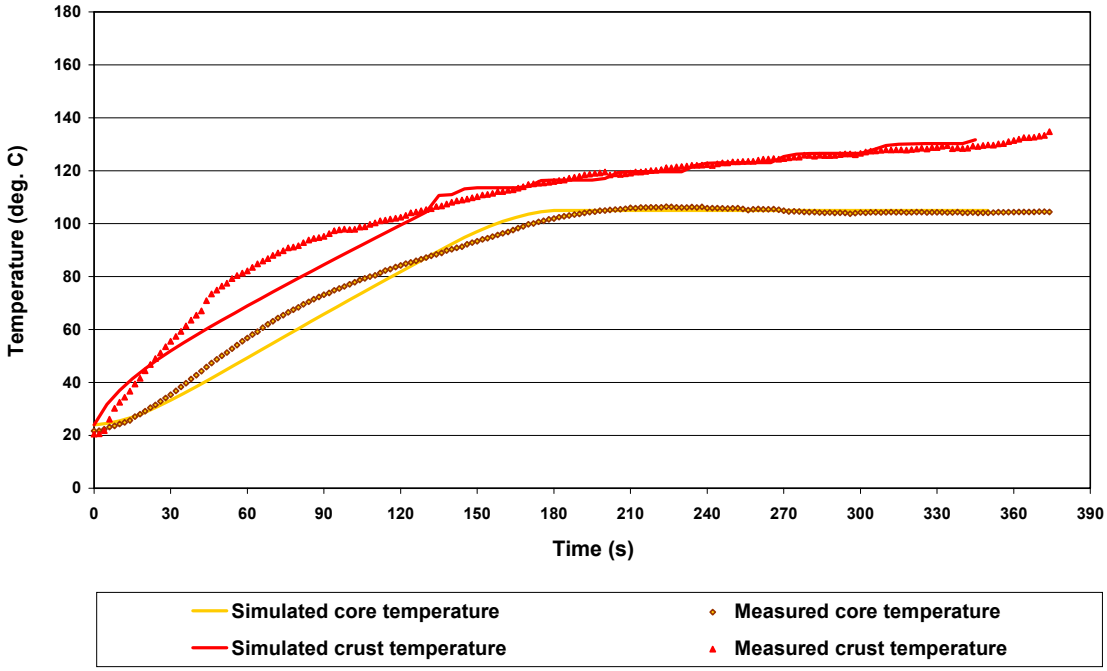

Figure 5. Comparison of predicted and measured high intensity 15,000 W/m^2 radiant heating of raw potato.

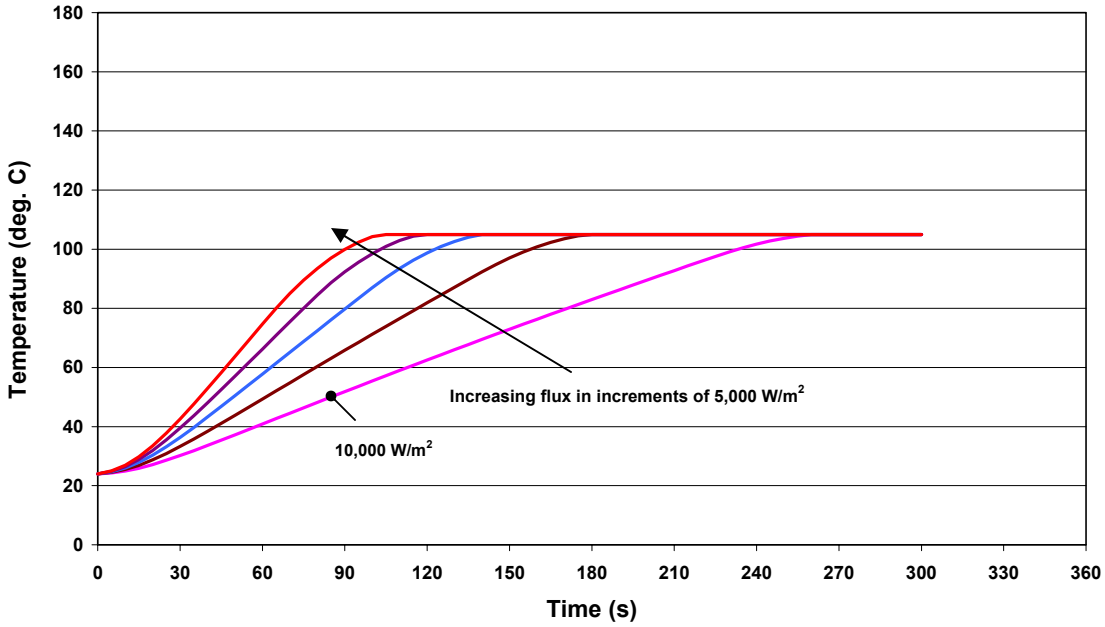

Figure 6. Simulated core temperature profiles of raw potato at different radiant flux intensities.

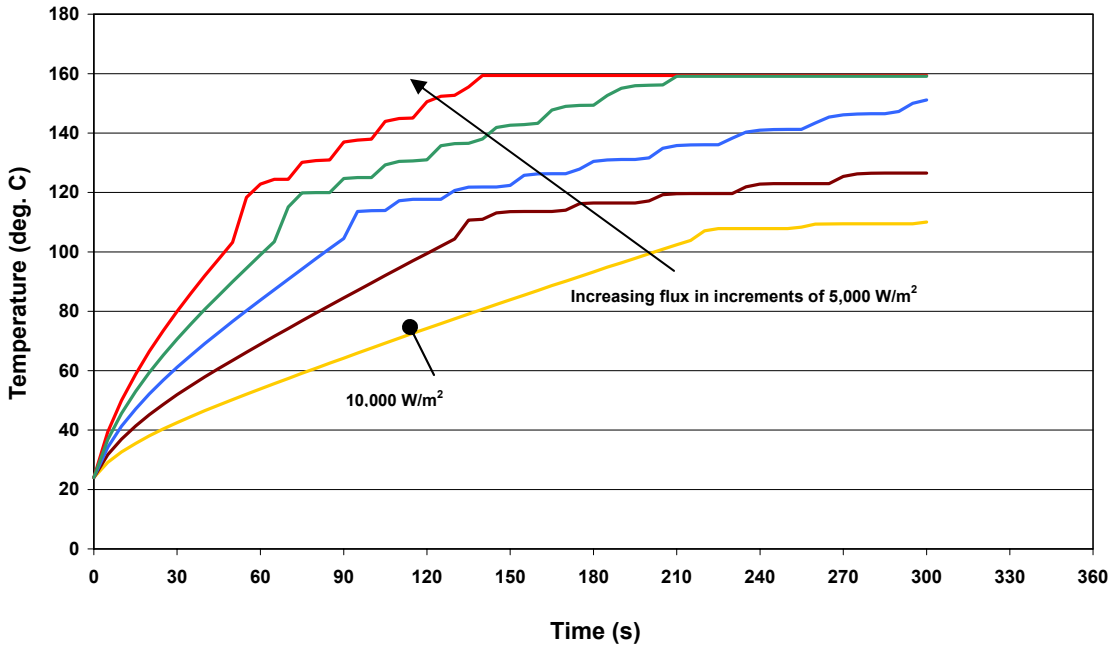

Figure 7. Simulated crust temperature profiles of raw potato at different radiant flux intensities.

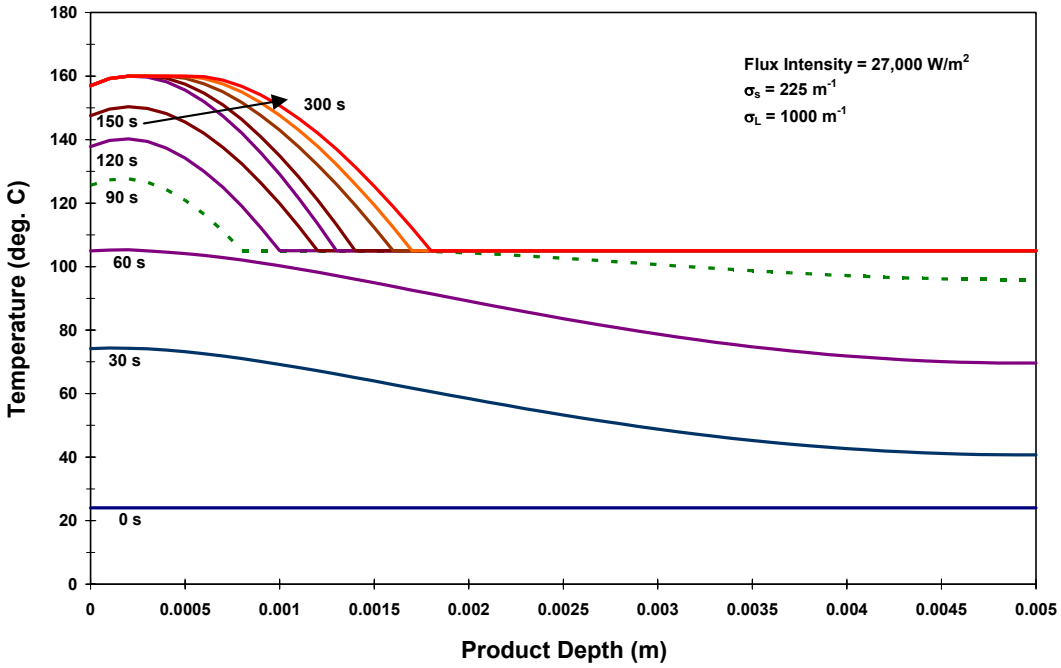

Fig. 8. Predicted temperature response through the depth of potato heated with 27,000 W/m^2 radiant energy every 30 s.

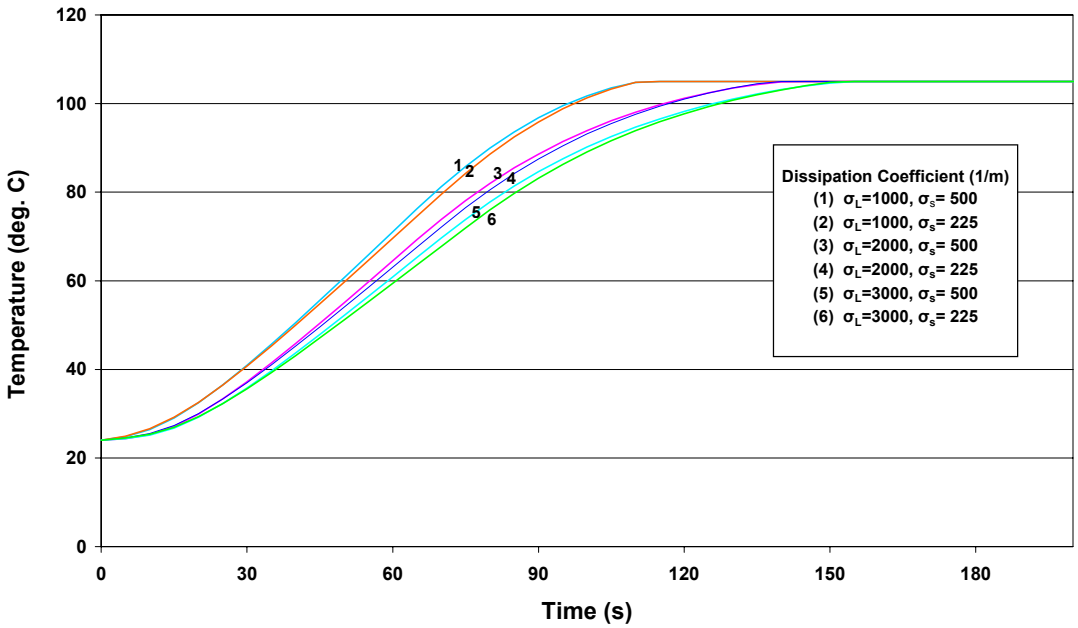

Figure 9. Variation of predicted core temperature with variation in short and long wavelength dissipation coefficients.

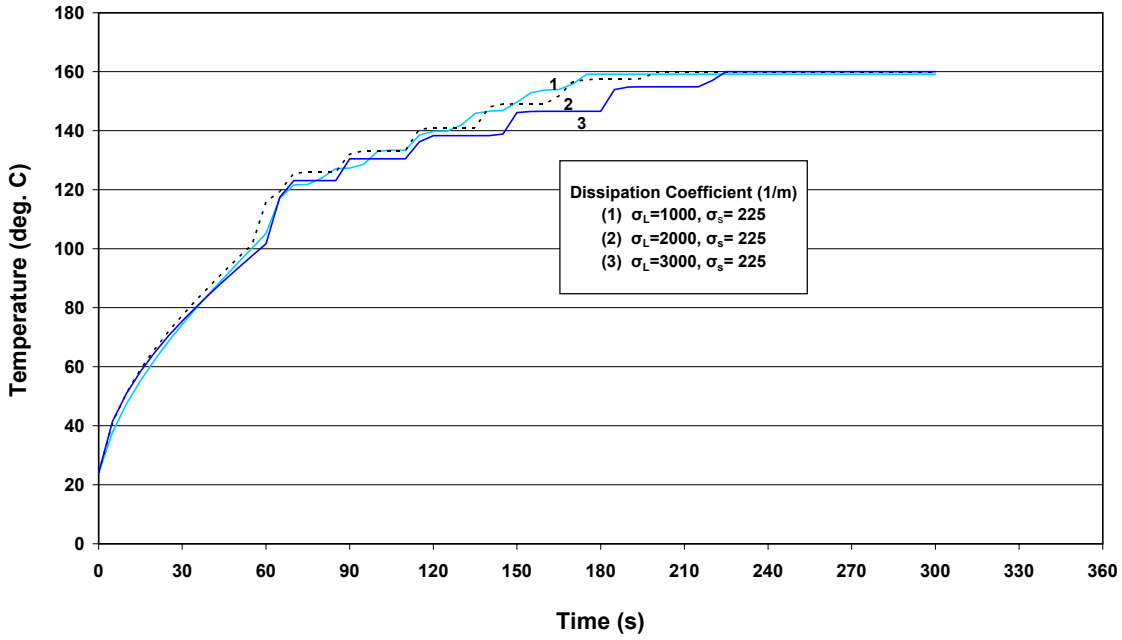

Figure 10. Variation of predicted surface crust temperature with variation in short and long wavelength dissipation coefficients.

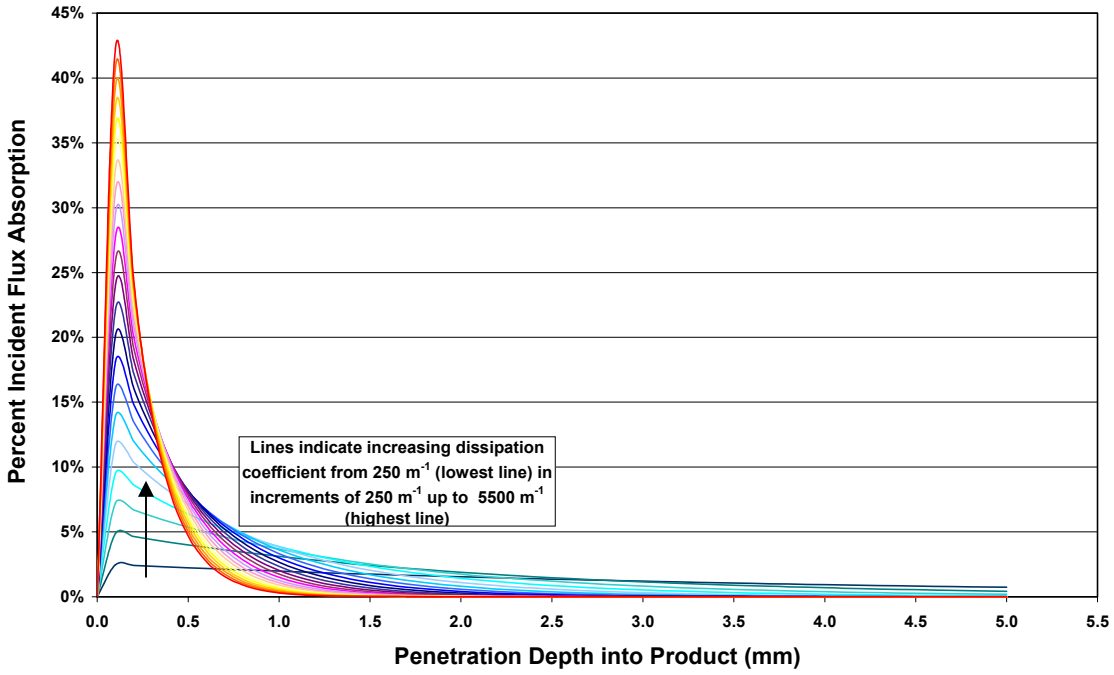

Figure 11. Extinction of incident radiant heat flux as dissipation coefficient increased.

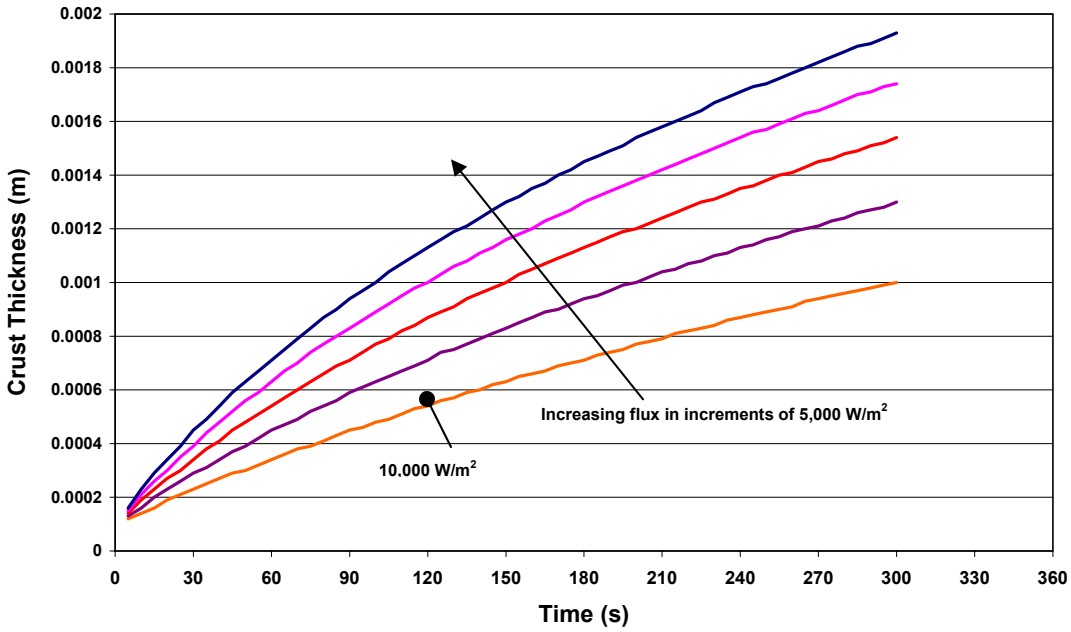

Figure 12. Predicted thickness of the crust region at different radiant flux intensities.

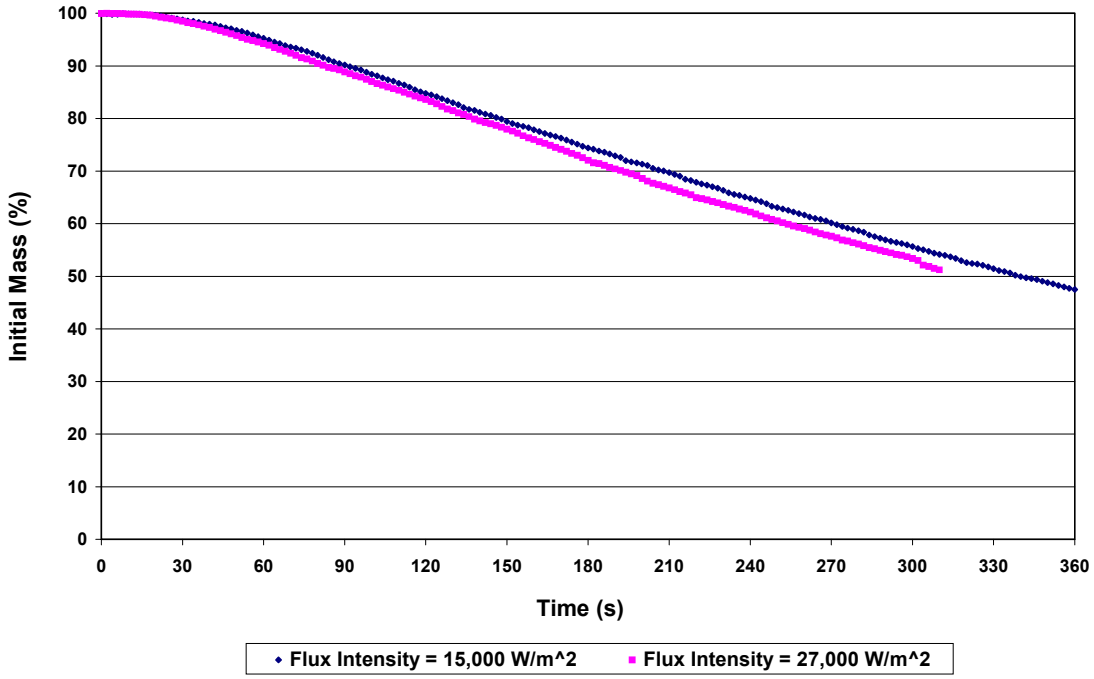

Figure 13. Measured moisture loss of radiant heated raw potato at different flux intensities.

APPENDIX 1

```
      PROGRAM RADSLAB
C     PROGRAM TO CALCULATE SOLUTION FOR TEMPERATURE DISTRIBUTION
C     IN RADIANT HEATED SLAB USING EXPLICIT FINITE DIFFERENCE
C     SCHEME

      REAL KCRUST,KCORE,K,RHOCRUST,RHOCORE,CPCRUST,CPCORE
      REAL DCRUST,DCORE,FCRUST,FCORE
      REAL A,IO,IOS,IOL
      DIMENSION TM(51,2),R(51),DX(2)
      DATA PI/3.14159/

C     DEFINITION OF VARIABLES: VALUES IN [] ARE BASE VALUES

C     A = HALF-THICKNESS OF SLAB [M]
C     CP=CORE SPECIFIC HEAT [3500 J/KG K]
C     D=THERMAL DIFFUSIVITY [M2/S]
C     DR=DISTANCE BETWEEN CALCULATED TEMPERATURES
C     DT=TIME STEP [S]
C     F=FOURIER NUMBER
C     H=CONVECTIVE HEAT TRANSFER COEFFICIENT [20]
C     IOL=TOTAL LONG WAVE IR BEING ABSORBED [W/M2]
C     IOS=TOTAL SHORT WAVE IR BEING ABSORBED [W/M2]
C     KCORE=CORE THERMAL CONDUCTIVITY [0.6 W/MK]
C     KCRUST=CRUST THERMAL CONDUCTIVITY [0.119 W/MK]
C     NDR = NUMBER OF SEGMENTS FOR WHICH TEMPERATURE IS CALCULATED
C     PRCTL=FRACTION OF LONG WAVE IR >1.44uM [0.75]
C     PRCTS=FRACTION OF SHORT WAVE IR <1.44uM [0.25]
C     REFLL=LONG WAVE REFLECTION [0.5]
C     REFLS=SHORT WAVE REFLECTION [0.3]
C     RHO=CORE DENSITY [1000. KG/M3]
C     SIGL=LONG WAVE DISSAPATION COEFICIENT [3100 1/M]
C     SIGS=SHORT WAVE DISSAPATION COEFICIENT [225 1/M]
C     TINF=SURROUNDING TEMPERATURE [22]
C     TMZERO = INITIAL UNIFORM TEMPERATURE OF SLAB [C]
C     TSTOP = FINAL TIME FOR CALCULATION OF SLAB TEMPERATURE [S]


C     OPEN OUTPUT DATA FILE

      OPEN(2,FILE='RadFry.dat',STATUS='NEW')

C     DATA INPUT

  10  PRINT *, 'ENTER 1 FOR t vs. FLUX'
      PRINT *, '      2 FOR t vs. TEMPERATURE'
      PRINT *, '      3 FOR x vs. TEMPERATURE [NEG TO QUIT]'
      ACCEPT *, NFLAG

      IF(NFLAG.LT.0) THEN
      GOTO 550
      ELSE
      ENDIF
```

```
C     SET AND CALCULATE INITIAL PROPERTY VALUES

       H=20.
       TINF=22.
       TMZERO=24.
       A=0.005
       TSTOP=355.
       DT=.01
       NDR=50
       DR=A/NDR
       NP=NDR+1
       NTPR=TSTOP/5

       IO=27000.
       SIGS=225.
       SIGL=1000.
       PRCTS=0.25
       PRCTL=1.-PRCTS
       REFLS=0.35
       REFLL=0.05
       IOS=IO*PRCTS*(1.-REFLS)
       IOL=IO*PRCTL*(1.-REFLL)

       ETAL=0.8
       RHOL=1000.
       HVAP=2257060.
       KCRUST=0.119
       KCORE=0.655
       RHOCORE=1106.
       RHOCRUST=310.
       CPCORE=3450.
       CPCRUST=3050.
       DCORE=KCORE/(RHOCORE*CPCORE)
       DCRUST=KCRUST/(RHOCRUST*CPCRUST)
       FCORE=DCORE*DT/(DR*DR)
       FCRUST=DCRUST*DT/(DR*DR)

C     ****MENU DRIVEN INPUT SECTION****
   12
       WRITE(*,209) IO,SIGS,SIGL
  209 FORMAT(/3X,'1 IR FLUX = ',F8.1,' [W/M2]'//
      2 3X,'2 SHORT WAVE DISSAPATION COEFFICIENT = ',F8.1,' [1/M]'//
      3 3X,'3 LONG WAVE DISSAPATION COEFFICIENT = ',F8.1,' [1/M]'/)

       WRITE(*,*) 'TYPE NUMBER OF VALUE TO CHANGE (0 TO CONTINUE): '
       ACCEPT*, NV
       IF(NV.EQ.0)THEN
       GOTO 13
       ELSE
       ENDIF

   11 IF(NV.EQ.1)THEN
       WRITE(*,*) 'ENTER NEW IR FLUX: '
       ACCEPT*, IO
       IOS=IO*PRCTS*(1.-REFLS)
```

```
      IOL=IO*PRCTL*(1.-REFLL)
      ELSE
      IF(NV.EQ.2)THEN
      WRITE(*,*) 'ENTER NEW SHORT WAVE DISSAPATION COEFFICIENT: '
      ACCEPT*, SIGS
      ELSE
      IF(NV.EQ.3)THEN
      WRITE(*,*) 'ENTER NEW LONG WAVE DISSAPATION COEFFICIENT: '
      ACCEPT*, SIGL
      ELSE

      ENDIF
      ENDIF
      ENDIF

      GOTO 12

   13 CONTINUE

C     *****END OF MENU INPUT SECTION****

C     PRINT OUT INPUTS

      WRITE(9,500) DCORE,DCRUST,A,TMZERO,DR,DT,SIGS,SIGL,IO,H,TINF
      WRITE(2,500) DCORE,DCRUST,A,TMZERO,DR,DT,SIGS,SIGL,IO,H,TINF
  500 FORMAT(3X,'EXPLICIT FINITE DIFFERENCE SOLUTION FOR ',
     1 'TEMPERATURE IN IR HEATED SLAB'//3X,
     2 'CORE DIFFUSIVITY = ',E11.5,' [M2/S]'/3X,
     3 'CRUST DIFFUSIVITY = ',E11.5,' [M2/S]'/3X,'1/2 THICK = ',F8.5,
     4 ' [M]'/3X,'INITIAL TEMPERATURE = ',F8.1,' [C]'/3X,
     5 'DISTANCE STEP DR = ',F8.5,' [M]'/3X,
     6 'TIME STEP USED DT = ',F8.5,' [S]'/3X,
     7 'SHORT WAVE DISP COEFF = ',F8.1,' [1/M]'/3X,
     8 'LONG WAVE DISP COEFF = ',F8.1,' [1/M]'/3X,
     9 'TOTAL IR FLUX = ',F12.1,' [W/M2]'/3X,
     @ 'CONVECT HEAT TRANS COEF = ',F8.1,' [W/M2K]'/3X,
     @ 'SURROUNDING TEMP = ',F8.1,' [C]'//)

C     INITIALIZE ARRAYS

      DX(1)=0.0001
      DX(2)=0.0001

      DO 50 I=1,NP
      R(I)=(I-1)*DR
      TM(I,1)=TMZERO
      TM(I,2)=TMZERO
   50 CONTINUE

C    SET NODES FOR PRINTING

      M1=1
      M2=2
      M3=NDR/2+1
      M4=M3+M3/2
      M5=NP
```

```
      IF(NFLAG.EQ.2) THEN
      WRITE(2,520) R(M1),R(M2),R(M3),R(M4),R(M5)
      WRITE(9,520) R(M1),R(M2),R(M3),R(M4),R(M5)
C      WRITE(9,520) R(1),R(2),R(26),R(38),R(NP)
  520 FORMAT(1X,'POSITION',1X,F7.5,1X,F7.5,1X,F7.5,1X,F7.5,1X,F7.5)
      ELSE
      WRITE(2,525)

      WRITE(9,525)
  525 FORMAT('FLUX AT SURFACE, W/M2',/3X,'TIME[S]',3X,
     1 'IOS',3X,'IOL',3X,'QCRUST',3X,'QINTERFACE',3X,'X(t)')
      WRITE(2,528) T,IOS,IOL,QCRUST,QINTER,DX(1)
      WRITE(9,528) T,IOS,IOL,QCRUST,QINTER,DX(1)
      ENDIF

      T=0
      TPRINT=0
      DTPRINT=TSTOP/NTPR

      IF(NFLAG.EQ.2) THEN
C     WRITE OUT INITIAL TEMPERATURES

      WRITE(2,535) T,TM(M1,1),TM(M2,1),TM(M3,1),TM(M4,1),TM(M5,1)
      WRITE(9,535) T,TM(M1,1),TM(M2,1),TM(M3,1),TM(M4,1),TM(M5,1)
  535 FORMAT(1X,F6.1,1X,F6.2,1X,F6.2,1X,F6.2,1X,F6.2,1X,F6.2)

      ELSE
      ENDIF

C     TIME LOOP

  100 T=T+DT
      TPRINT=TPRINT+DT
      IF(T.GT.TSTOP) THEN
      WRITE(9,600)
  600 FORMAT(///3X,'PRESS RETURN TO CONTINUE'/)
      PAUSE
      GO TO 10
      END IF

C     SOLVE FINITE DIFFERENCE EQUATION FOR INTERIOR POINTS

      DO 120 I=2,NDR

      IF(I*DR.LT.DX(1).AND.TM(I,1).GT.105.) THEN
      K=KCRUST
      F=FCRUST
      ELSE
      K=KCORE
      F=FCORE
      ENDIF


      TM(I,2)=TM(I,1)+F*(TM(I+1,1)-2*TM(I,1)+TM(I-1,1)
     1  +(IOS*DR*(EXP(-1*SIGS*(I-1)*DR)-EXP(-1*SIGS*I*DR))/K)
     2  +(IOL*DR*(EXP(-1*SIGL*(I-1)*DR)-EXP(-1*SIGL*I*DR))/K))
```

```
  120 CONTINUE

      DO 125 I=2,NDR

      IF(I*DR.LT.DX(1).AND.TM(I,2).GT.160.) THEN
      TM(I,2)=160.
      ELSE
      ENDIF

      IF(I*DR.GT.DX(1).AND.TM(I,2).GT.105.) THEN
      TM(I,2)=105.
      ELSE
      ENDIF
  125 CONTINUE

C     USE BOUNDARY CONDITIONS TO CALCULATE CENTER AND EDGE TEMPERATURES


      IF(TM(1,1).GT.105.) THEN
      K=KCRUST
      ELSE
      K=KCORE
      ENDIF

      TM(1,2)=1/(K/DR+H)*(H*TINF+K*TM(2,2)/DR)

      IF(TM(1,2).GT.160.) THEN
      TM(1,2)=160.
      ELSE
      ENDIF

      TM(NP,2)=TM(NP-1,2)

      IF(TM(NP,2).GT.105.) THEN
      TM(NP,2)=105.
      ELSE
      ENDIF

C     CALCULATE FLUXES AND CRUST THICKNESS

      DO 127 I=2,NP

      IF(TM(I,2).GT.105.)THEN

      QCRUST=-1.*KCRUST*(105.-TM(1,2))/DX(1)
      QINTER=QCRUST+IOS*EXP(-1*SIGS*DX(1))+IOL*EXP(-1*SIGL*DX(1))

      ELSE
      QINTER=IOS*EXP(-1*SIGS*DX(1))+IOL*EXP(-1*SIGL*DX(1))
      ENDIF

  127 CONTINUE

      DX(2)=DX(1)+QINTER*DT/(ETAL*RHOL*HVAP)
      DX(1)=DX(2)

C     RESET TEMPERATURES
```

```
      DO 130 I=1,NP
      TM(I,1)=TM(I,2)
  130 CONTINUE

C     WRITE OUT THE RESULTS FOR THIS TIME STEP

      IF(TPRINT.GE.DTPRINT) THEN

      IF(NFLAG.EQ.1)THEN
      WRITE(2,528) T,IOS,IOL,QCRUST,QINTER,DX(1)
      WRITE(9,528) T,IOS,IOL,QCRUST,QINTER,DX(1)
  528 FORMAT(1X,F6.1,1X,F8.0,1X,F8.0,1X,F8.0,1X,F8.0,1X,F8.5)

      ELSE
      IF(NFLAG.EQ.2)THEN
      WRITE(2,530) T,TM(M1,1),TM(M2,1),TM(M3,1),TM(M4,1),TM(M5,1)
      WRITE(9,530) T,TM(M1,1),TM(M2,1),TM(M3,1),TM(M4,1),TM(M5,1)
  530 FORMAT(1X,F6.1,1X,F6.2,1X,F6.2,1X,F6.2,1X,F6.2,1X,F6.2)

      ELSE
      IF(NFLAG.EQ.3)THEN
C     PRINT OUT DATA FOR X VS T PLOTS
      WRITE(2,964) T
      WRITE(9,964) T
  964 FORMAT(3X,F8.1,3X)

       DO 973 I=1,NP
       WRITE(2,965) R(I),TM(I,2)
       WRITE(9,965) R(I),TM(I,2)
  965  FORMAT(3X,F8.4,3X,F6.2)
  973  CONTINUE

      ENDIF
      ENDIF
      ENDIF

      TPRINT=0.

      END IF

      GO TO 100
  550
      END
```

APPENDIX 2

DYNAMIC RADIANT FOOD PREPARATION PROCESSES AND SYSTEMS

FIELD OF THE INVENTION

[0001] The present invention relates generally to the preparation of food and, more particularly, to dynamic radiant food preparation processes and systems.

BACKGROUND OF THE INVENTION

[0002] Deep fat frying, or immersion frying, results in food products that typically have a fried, crusty exterior that is generally pleasing to consumers. However, such food products may be high in fat content. Cooking such foods also presents difficulties in commercial establishments. The quality of the oil tends to decrease with use, which leads to inconsistent food product quality. The oil from immersion fryers may also result in accidents to workers.

SUMMARY

[0003] According to embodiments of the present invention, a continuous oven includes a conveyor having a first end and a second end and a plurality of infrared emitters spaced apart along the conveyor. The emitters are spaced to provide a decreased heat flux to a product on the conveyor at the second end of the conveyor as compared to the first end of the conveyor.

[0004] In further embodiments according to the present invention, a continuous method of cooking a food product in a oven includes:

(a) exposing the product to electromagnetic radiation such that the resulting heat flux is sufficient to produce a crust matrix on a surface of the product; and then

(b) exposing the product to electromagnetic radiation such that the resulting heat flux sufficient to heat an interior of the product.

BRIEF DESCRIPTION OF THE DRAWINGS

[0005] **Figure 1** is cross sectional view of an oven according to embodiments of the present invention; and

[0006] **Figures 2-4** are graph diagrams illustrating the heat flux of a sensor along an oven according to further embodiments of the present invention.

DETAILED DESCRIPTION OF THE INVENTION

[0007] The present invention now will be described more fully hereinafter with reference to the accompanying drawings, in which preferred embodiments of the invention are shown. This invention may, however, be embodied in many different forms and should not be construed as limited to the embodiments set forth herein; rather, these embodiments are provided so that this disclosure will be thorough and complete, and will fully convey the scope of the invention to those skilled in the art. Thicknesses and dimensions of some components may not be drawn to scale and may be exaggerated for clarity.

[0008] The present invention is directed to food preparation using radiant heating. Radiant electromagnetic energy can be used to provide a heat flux to a food product at a wavelength and penetration depth such that the resulting product may have characteristics similar to that of immersion fried products.

[0009] An oven **10** according to embodiments of the present invention is shown in **Figure 1**. The oven **10** includes a conveyor belt **16** that provides movement from a front end **18** to a back end **20** of the belt **16**. A food product **14** can be placed on the conveyor belt **16** and moved by the belt **16** from the front end **18** to the back end **20**. A plurality of emitters **12a-12e** are placed near the belt **16** to provide radiant electromagnetic energy to the food product **14**.

[0010] Electromagnetic radiation incident on the product **14** in the oven **10** can be controlled using various techniques. In some embodiments, radiant heat flux is selected to approximate heat flux in an immersion frying process. Immersion frying processes are generally characterized by a substantial increase in heat flux when a food product is immersed in oil followed by a declining heat flux. Moreover, the penetration depth of the radiation can be selected to achieve certain results. For example, a crust matrix may be formed by relatively long wave radiation, which does not penetrate significantly into the surface. Subsequently, a shorter wave radiation may be applied, which generally penetrates more deeply into a food product to cook and/or heat the interior.

[0011] As shown in **Figure 1**, the oven **10** includes emitters **12a-12e** that are spaced to vary the electromagnetic radiation incident on the food product **14** as it progresses between the front end **18** and the back end **20** of the conveyor belt **16**. For example, the distance from each of the emitters **12a-12e** to the conveyor belt **16** is successively greater from the front end **18** to the back end **20** of the belt **16**. In addition, the distance between each successive one of the emitters **12a-12e** is greater from the front end **18** to the back end **20** of the belt **16**. For example, the distance between the emitters **12b** and **12c** is greater than the distance between the emitters **12a** and **12b**. As illustrated, the emitters **12a-12e** include a top set and a bottom set of emitters **12a-12e** positioned above and below the belt **16**.

[0012] In this configuration, the heat flux incident of the food product **14** varies as the product **14** progresses from the front end **18** to the back end **20** of the belt **14**. After an initial rapid increase in heat flux near the front end **18**, the heat flux generally decreases as the food product **14** travels along the belt. The decreasing heat flux may be a result of the placement of the emitters **12a-12e**, and may include intervening increases in heat flux. Moreover, the power of the emitters **12a-12e** can be controlled to vary the energy and wavelength of the emitted radiation. The heat flux incident on the product **14** decreases as the distance of the product **14** increases. Distances between the emitters **12a-12e** can be uneven and/or range from between a fraction of a centimeter to about 10, 20, 50 or 100 cm. For example, the heat flux when the product **14** is near emitters **12a-12b** towards the front end **18** of the belt **16** can increase to above about 2.5 W/cm^2 or 3.0 W/cm^2 or more. As the product travels past emitters **12c-12e**, the heat flux generally decreases due, for example, to the increased distance between emitters **12c-12e** and the product **14**. Other parameters may be used to decrease the heat flux along the belt **16**, such as decreasing power or increasing the distance between the emitters **12a-12e** and the belt **16**.

[0013] The frequency of the electromagnetic radiation emitted by the emitters **12a-12e** can also be controlled. Without wishing to be bound by theory, the frequency of the emitted radiation is a function of the temperature of the emitter, which, in turn, is proportional to the emitter power. The frequency distribution of the emitted radiation can be modeled according to blackbody radiation and

calculated by equations relevant to blackbody radiation, for example, Planck's equation:

$$u(\lambda) = \frac{8\pi hc\lambda^{-5}}{e^{hc/\lambda kT} - 1}$$

where λ is the wavelength, *T* is the temperature in Kelvin, *h* is the Planck's constant, *k* is Boltzmann's constant, and *c* is the speed of light. The wavelength and temperatures of exemplary emitters is discussed in the "Characterization of Radiant Emitters Used in Food Processing," which is attached hereto as **Appendix A** and is to be considered a part of the current application. For example, short wavelength emitters, such as quartz halogen emitters and incandescent lamps, typically have temperatures between about 1900°C to about 3000°C. Medium wavelength emitters, such as metal sheaths and nickel chromium wires, typically have temperatures between about 900°C to about 1800°C.

[0014] The frequency distribution can be controlled by adjusting the power to the emitters. Lower power generally results in relatively longer wavelength radiation, and higher power generally results in relatively shorter wavelength radiation. Longer wavelength radiation does not penetrate as deeply into a food product as shorter wavelength radiation. As would be understood by those of skill in the art, various filters and/or reflectors can also be used to produce a desired wavelength. For example, wavelengths can be between about 0.4μm to about 100μm and heat flux can be between about 0-10 W/cm^2.

[0015] Accordingly, as shown in **Figure 1**, a crust matrix on the product **14** may be achieved by operating the emitters **12a-12b** towards the front end **18** of the belt **16** at a lower power than the emitters **12c-12e** towards the back end **20** of the belt **16**. The relatively lower power at which emitters **12a-12b** are operated can result in longer wavelength light, which heats the surface of the product **14** when the product is towards the front end **18** of the belt **16**. The lower wavelength radiation can result in the formation of a crust matrix. Moreover, the relatively short distance between the product **14** and the emitters **12a-12b** can result in a high heat flux relative to subsequent emitters **12c-12e**. In this configuration, the emitters **12a-12e** can emit longer wavelength radiation and high heat flux to the product **14** towards the front end **18** of the belt **16** (to form a crust matrix) compared with shorter wavelength radiation and lower heat flux to the product **14**

towards the back end **20** of the belt **16** (to heat the product interior). The speed of the conveyor belt **16** can be adjusted to expose the product **14** to a given wavelength and heat flux for a sufficient period of time to achieve desired results such as a surface crust matrix without burning and/or heating without over cooking. In some embodiments according to the invention, shorter wavelength radiation can be used to produce relatively high heat flux incident on the product and to form the crust matrix. The shorter wavelength radiation can be followed by longer wavelength radiation (for example, at a greater distance from the product) to cook the interior of the product. Other combinations of can be used.

[0016] The change in heat flux, power, frequency distribution and the like can be controlled along the conveyor to produce various results in preparing the food product **14**. The changes in heat flux may be gradual or may have intervening increases and decreases between the front end **18** and the back end **20** of the belt **16**. For example, as a food product **14** passes directly beneath or above one of the emitters **12a-12e**, the intensity of the radiation and heat flux will generally increase. Radiation from the emitters can also be controlled by selectively turning an emitter on and off, for example, half as much heat flux could be achieved by setting an emitter to be on for three seconds and off for three seconds. In some embodiments according to the invention, a sensor can be sent along a conveyor, such as conveyor belt **16**, to detect the heat flux and/or wavelength of the radiation at successive points along the conveyor. Various parameters, such as emitter distances, emitter powers, speed of the conveyor belt, and the like, can be adjusted to achieve desired food preparation characteristics. For example, to approximate immersion frying, parameters can be selected to produce high heat flux radiation followed by lower heat flux and radiation. The wavelength of the radiation can also be adjusted to control the penetration depth of the energy.

[0017] Examples of "infrared frying" (e.g., radiant food preparation using parameters to approximate the results of immersion frying) are discussed in the "Overview of Infrared Frying", which is attached hereto as **Appendix B** and is to be considered a part of the current application. **Appendix B** includes a graph illustrating an example of heat flux v. time for an oven, such as the oven **10** shown in **Figure 1**. As shown in the graph of **Appendix B**, the measured heat flux may increase and decrease along the conveyor as time progresses. The fluctuations

shown are the result of heat fluctuations as the sensor passes from one emitter to the next, and each emitter causes a spike in the sensed heat flux. However, the smoothed heat flux profile illustrates an initial increasing heat flux from about 0 to about 50 seconds followed by a decreasing heat flux. In some embodiments according to the invention, the heat flux increases to above about 2.5 W/cm^2 in about 75 seconds or 50 seconds or less. The formation of a crust matrix on a surface of the product can have a duration of about 300 seconds, and in some embodiments, the crust matrix can be formed in about 200 seconds, 100 seconds or less. Additional examples of heat flux v. time are given in **Figures 2-4**. Further examples of radiant heating methods and systems are given in the "Comparison of Different Finish Frying Methods of French Fries for Consumer Acceptability" and "Development of an Alternative Finish Frying Process Using Dynamic Radiant Heating", which are attached hereto as **Appendix C** and **Appendix D**, respectively, and are to be considered a part of the current application.

[0018] Any suitable emitter and emitter configuration can be used as the emitters **12a-12e** in **Figure 1**. For example, emitters may be positioned on only one side of a conveyor belt or on all sides of the conveyor belt. Emitters can be point source emitters, elongated in a straight line, or elongated in an arch shape. The emitters can infrared emitters and, more preferably, quartz halogen emitters, such as commercially available 500W quartz halogen emitters. Emitters having various wattages can be used, including 100W emitters, emitters greater than 500W, and two or more emitters joined in parallel arrangements. Any suitable emitter can be used, such as metal sheath emitters, nickel-chromium wires, heated ceramic surfaces, and incandescent heaters, and including the emitters discussed in **Appendix A**. The wavelengths of the electromagnetic radiation emitted by the emitters are typically between about 0.4μm and 300μm. Visible wavelength radiation can also be used, such as between 0.4μm and 0.7μm.

[0019] Moreover, various oven configurations may be used to achieve a desired prepared food product. For example, a batch type oven having emitters configured to produce selected heat flux and/or radiation frequency to a food product could be used. The distance of the food product to an emitter could be controlled by a mechanical controlling mechanism such as an arm or lever. Ovens according to embodiments of the present invention can also be used with other

cooking sources such as microwave radiation sources, convection ovens, and the like.

[0020] Various food products can be prepared according to embodiments of the present invention, such as a par fried food product. Moreover, coating of the food product before or after processing may be used to enhance the taste and/or texture of a food product, for example, by controlling the moisture dissipation through the surface of the product.

[0021] Without wishing to be bound by a particular theory, it is believed that radiant heating systems and processes can be used as an alternative to immersion frying by approximating the heat transfer characteristic of immersion frying. Immersion frying may be characterized by four stages: 1) initial heating, 2) surface boiling, 3) falling rate, and 4) bubble end point. Briefly, when a food product is immersed in frying oil, heat is initially transferred from the oil to the food by free convection and through the food by conduction with little water vaporization (stage 1). During stage 2 (surface boiling), moisture at the surface is suddenly lost, which increases surface heat transfer and results in crust formation. Stage 3 (falling rate) is characterized by decreased heat transfer and a steady decrease in vapor mass transfer from the food product. The bubble end point (stage 4) can be characterized by the apparent cessation of moisture loss from the food during frying. Heat transfer characteristics during immersion frying are discussed in Hubbard, L.J. and B.E. Farkas. 1999. *A method for determing the convective heat transfer coefficient during immersion frying.* J. of Food Process Engr. 22: 201-214 and is attached hereto as **Appendix E** and is a part of the current application.

[0022] Radiant heating utilizes electromagnetic energy in the visible, near, and/or far infrared wavelength regions. As discussed herein, electric radiant emitter sources allow control of power level, incident radiation intensity, and spectral distribution, all of which affect product heating rates and temperature profiles. Accordingly, radiant heat emitters can be used to approximate the heat transfer of immersion frying, for example, as described in **Appendix E**.

[0023] Radiant heating of food products may be studied and/or mathematical models used to simulate temperature change as a function of heat flux and material spectral properties. Process parameters, including spectral properties of food materials and spectral wavelength emissions from radiant emitter sources, may be

used in simulating radiant heating of foods. Such process parameters may be used to provide radiant heating of a product that can simulate an immersion frying process. For example, some mathematical models for radiant heating of foods are a constant radiant heat flux upon one-dimensional flat surfaces. Two dimensional mathematical models of the internal temperature profile of a food product, such as a French fry, may provide additional information. Mathematical modeling and/or experimental information, for example, of a food product during an immersion fat frying process and/or of the food product during radiant heating, may be used to set process parameters of radiant heating systems to produce a food product with some of the characteristics of an immersion fried product.

[0024] For example, the explicit finite difference method may be used for a solution of the transport equations. Temperature distributions can be calculated for a particular shape, such as a square two-dimensional parallelepiped simulation of a shoestring cut French fry. Radiant energy may be assumed incident upon the food surface uniformly, which neglects shape factor considerations between the radiant emitter and the food product surface. Penetration of radiant energy within the food material surface may be assumed to have an exponential decay following Beer's Law. Heat transfer equations can include an internal generation term for absorbed radiant energy as well as conduction and convection heat transfer terms. Simulations may be carried out for both steady and unsteady state heat flux conditions. Experimental data may be collected so that simulated temperature profiles for radiant heating of a product, such as a shoestring French fry, can be calculated and compared with experimental data. Input variables that may impact on output can include radiant energy surface reflection and internal dissipation coefficients. The simulation may serve as a tool for determination of the heating effects of radiant processing parameters and material temperature profiles. Manipulation of model input variables, such as radiant intensity spectral distribution, and food composition, may be done to optimize product heating.

[0025] As described herein, electronically controlled radiant emitters may be used to reproduce heat flux profiles that occur during the boiling phase of immersion frying. Drying rates, and core and surface temperatures of par-fried products, such as French fries, may be measured during radiant heating to

reproduce immersion frying heat transfer. Heat flux measurements may be recorded through the oven using a water-cooled radiometer.

[0026] Embodiments of the present invention are described herein with reference to an initial high heat flux followed by a decreasing heat flux stage. However, the heat flux distribution can be controlled to obtain various heating and/or cooking profiles including an initial low heat flux followed by an increasing heat flux. The frequency of radiation can also be adjusted to obtain various profiles of energy penetration, for example, to heat the surface of a product before or after cooking the internal portion of the product. Moreover, embodiments according to the present invention may be used in various applications including drying processes and curing processes, such as for plastic, paper, and/or chemical manufacturing.

[0027] The foregoing is illustrative of the present invention and is not to be construed as limiting thereof. Although a few exemplary embodiments of this invention have been described, those skilled in the art will readily appreciate that many modifications are possible in the exemplary embodiments without materially departing from the novel teachings and advantages of this invention. Accordingly, all such modifications are intended to be included within the scope of this invention as defined in the claims. Therefore, it is to be understood that the foregoing is illustrative of the present invention and is not to be construed as limited to the specific embodiments disclosed, and that modifications to the disclosed embodiments, as well as other embodiments, are intended to be included within the scope of the appended claims. The invention is defined by the following claims, with equivalents of the claims to be included therein.

That which is claimed:

1. A continuous oven comprising:

a conveyor having a first end and a second end; and

a plurality of infrared emitters spaced apart along the conveyor, the emitters being spaced to provide a decreased heat flux to a product on the conveyor at the second end of the conveyor as compared to the first end of the conveyor.

2. The oven of Claim 1, wherein a distance between each one of the emitters and the conveyor is successively generally greater from the first end of the conveyor to the second end of the conveyor.

3. The oven of Claim 1, wherein a distance between each successive emitter is generally greater from the first end of the conveyor to the second end of the conveyor.

4. The oven of Claim 1, wherein the plurality of emitters comprise a first set of emitters on a side of the conveyor and a second set of emitters on an opposing side of the conveyor.

5. The oven of Claim 1, wherein the decreasing heat flux is preceded by an increasing heat flux.

6. The oven of Claim 1, wherein the emitters are quartz halogen emitters.

7. The oven of Claim 1, wherein the emitters emit electromagnetic radiation in the visible to near-infrared wavelength range.

8. The oven of Claim 1, wherein the emitters emit electromagnetic radiation from between about 0.4μm to about 300μm.

9. The oven of Claim 1, wherein electromagnetic radiation from successive emitters generally increases in wavelength.

10. The oven of Claim 1, wherein the electromagnetic radiation from successive emitters generally decreases in wavelength.

11. The oven of Claim 1, wherein the emitters towards the first end of the conveyor are configured to emit longer wavelength radiation than the emitters towards the second end of the conveyor.

12. The oven of Claim 1, wherein the emitters towards the first end of the conveyor are at a generally lower power level than the emitters towards the second end of the conveyor.

13. The oven of Claim 1, wherein the emitters are configured to approximate a heat flux transfer from the first end of the conveyor to the second end of the conveyor that approximates heat flux during immersion frying.

14. The oven of Claim 1, wherein heat flux from the first end of the conveyor to the second end of the conveyor increases to above about 1.5 W/cm^2 towards the first end of the conveyor and decreases towards the second end of the conveyor.

15. The oven of Claim 1, wherein a heat flux transfer from the first end of the conveyor to the second end of the conveyor increases to above about 3.0 W/cm^2 towards the first end of the conveyor and decreases towards the second end of the conveyor.

16. The oven of Claim 1, further comprising a controller configured to control the speed of the conveyor.

17. The oven of Claim 16, wherein the speed of the conveyor is set such that a heat flux measured at a point on the conveyor increases to above about 2.5

W/cm^2 within less than about 75 seconds.

18. A continuous method of cooking food product in a oven, the method comprising:

(a) exposing the product to electromagnetic radiation such that the resulting heat flux is sufficient to produce a crust matrix on a surface of the product; and then

(b) exposing the product to electromagnetic radiation such that the resulting heat flux sufficient to heat an interior of the product.

19. The method of Claim 18, wherein the heat flux sufficient to produce a crust matrix is above about 1.5 W/cm^2.

20. The method of Claim 18, wherein the heat flux sufficient to produce a crust matrix is above about 3.0 W/cm^2.

21. The method of Claim 18, wherein the electromagnetic radiation to produce a crust matrix on a surface of the product comprises longer wave radiation than the electromagnetic radiation to heat an interior of the product.

22. The method of Claim 18, wherein the electromagnetic radiation to produce a crust matrix is between about 1.4 and 100μm.

23. The method of Claim 18, wherein the electromagnetic radiation to heat an interior of the product is between about 0.4 and 14 μm.

24. The method of Claim 18, wherein the heat flux sufficient to produce a crust matrix and the heat flux sufficient to heat an interior of the product together approximates a heat flux of immersion frying the product.

25. The method of Claim 18, wherein step (a) further comprises exposing the product to a quartz halogen emitter.

26. The method of Claim 18, wherein step (a) has a duration of less than about 300 seconds.

27. The method of Claim 18, wherein steps (a) and (b) are carried out sequentially on the product by placing the product on a continuously advancing conveyor.

28. The method of Claim 18, wherein step (a) further comprises placing the product a conveyor proximate a quartz halogen emitter, the conveyor and quartz halogen emitter configured to produce a variable heat flux at successive points along the conveyor.

29. The method of Claim 28, wherein the variable heat flux increases to above about 2.5 W/cm^2 in a duration of less than about 50 seconds.

ABSTRACT

A continuous oven includes a conveyor having a first end and a second end and a plurality of infrared emitters spaced apart along the conveyor. The emitters are spaced to provide a decreased heat flux to a product on the conveyor at the second end of the conveyor as compared to the first end of the conveyor.

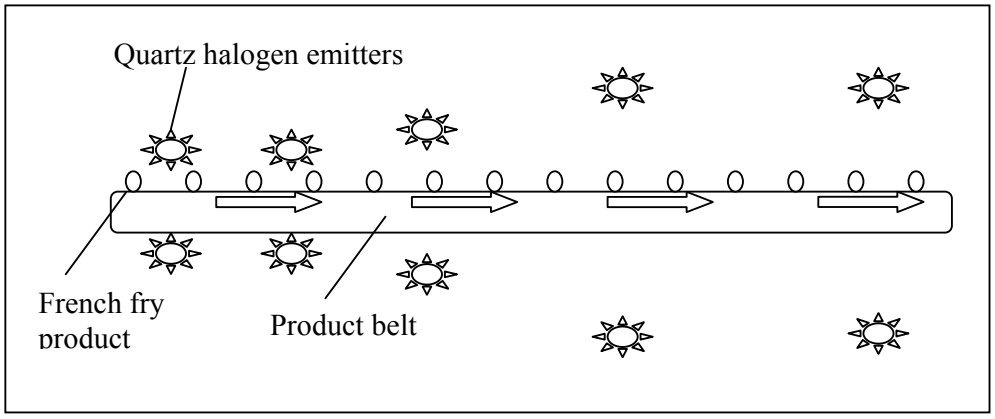

Fig. 1 Simplified cross-section schematic of the experimental radiant heated oven. Notice emitter spacing increased along belt length to decrease heat flux impinging on French fries.

APPENDIX 3

International Conference on Engineering and Food, ICEF 9, Montpellier France, 7-11 March 2004 (submitted).

Development of a Radiant Heating Process to Mimic Immersion Frying

Farkas, B.E., North Carolina State University, Raleigh, NC, USA, 27695. befarkas@ncsu.edu.

Lloyd, B.J., North Carolina State University, Raleigh, NC, USA, 27695. bjlloyd@unity.ncsu.edu.

Keener, K.M., North Carolina State University, Raleigh, NC, USA, 27695. Kevin_keener@ncsu.edu.

Abstract

Dynamic radiant heating was shown as an alternative process to immersion frying to produce foods with fried-like color, texture, and sensory attributes. Immersion frying was reproduced using electronically controlled radiant emitters positioned to simulate the heat flux that occurred during the boiling phase of immersion frying. Results showed an equivalent finish fried product could be produced using this method.

Keywords

dynamic radiant heating, infrared, French fries, immersion frying

Introduction

Fried foods are a significant source of food products consumed worldwide. The most popular fried food is French fries. Frozen potato fry exports from the three major exporting countries: the United States, the Netherlands, and Canada, were a record 2.3 million tons in 2001, (1). The majority of French fries are served in quick serve restaurants (QSR) as a side item. A large order of French fries contains approximately 540 calories with 26 g of fat (2). The FDA recommended daily intake (RDI) based on a 2,000 calorie diet is 65 g of fat (3), thus one large order of French fries approaches 45% of RDI for fat and 27% of total daily calories. American and European consumers are increasingly becoming more health conscious and finding that fried foods such as French fries should be avoided. United States French fries sales dropped 10 percent from 2001 to 2002, after more than a decade of increasing sales (4). Food products with reduced fat, calories, sodium, etc. were termed 'less-evil' products and identified as the #2 Top Food Trend for 2003 (5). French fries and

other fried products with a lower fat content and equivalent sensory attributes would be expected to be highly accepted by consumers.

Development of lower calorie, lower fat French fries for the QSR may involve product reformulation, changing the finish-frying step, or a combination of each. French fries sold by restaurants and retail establishments generally start with an initial par-frying step. The par-fried potatoes retain 7 to 10% fat, prior to being frozen, packaged and sold (6). Retail QSRs then finish-fry the par-fried potatoes by immersion frying in batch fryers. During immersion finish frying the fat content increases to 15 to 30%. Development of an alternative finish-frying process that would retain the unique French fry characteristics of golden color, crisp crust, and soft core produced by immersion frying, yet yield a lower oil content product (< 10%) would be highly desirable to consumers and retail QSRs alike.

Hubbard and Farkas (7) measured the heat flux to potatoes that occurred during immersion frying. The authors found that the heat flux to the product increased quickly to a high level approximately 35, 000 W/m^2, then decreased over time. Reproducing immersion frying heat flux was hypothesized as a critical step for an alternative frying process.

For this project, an experimental oven was developed to reproduce the immersion frying heat flux to replace the finish frying stage. This oven utilized dynamic electromagnetic radiant heating to reproduce the heat flux that occurred during immersion frying. Preliminary tests showed French fries prepared by this oven had comparable appearance and crust texture to the immersion fried product. However, instrumental and sensory methods must be used to objectively measure the quality of alternative radiant heated products compared with other heating methods. The objectives of this research were: (1) to measure texture and surface color properties of French fries produced using dynamic radiant heating, (2) measure consumer acceptance of important French fry attributes heated using radiant heating and other traditional methods, and (3) measure the crust and core temperature of raw potatoes during controlled radiant heating.

Materials and Methods

Four 32 oz. packages of frozen store brand (Harris Teeter, Matthews, NC) par-fried shoe-string cut potatoes were purchased and mixed into one homogenous batch. The par-fries were made from Russett potatoes and contained 11% fat. The par-fried potatoes were stored at -20°C until testing. The par-fries did not contain added colorants that might affect degree of browning measurements. Moisture and fat content was determined for the par-fries and after each heat treatment using AOAC methods (8). The three finish heating methods employed were: immersion frying, residential free convection oven heating, and radiant heating.

Immersion Frying

Approximately 35 g of frozen par-fried French fries (about 16 fries) were immersed in partially hydrogenated vegetable oil (FryMax® Ach Inc., Memphis, TN) at 172°C (350°F). The fryer (Rival, model 3, Arpt, KS) had a two-quart oil capacity.

The sample was fried for 210 s then removed from the oil and drained according to package instructions.

Oven Heating

A 35 g sample of frozen French fries (approximately 16 fries) was placed on an aluminum Teflon-coated cake pan. The pan was placed in an electric home oven (Kenmore) set at 232°C (450° F) for 480 s as recommended by the French fry manufacturer.

Radiant Heating Process

An experimental radiant heating oven was used to finish fry frozen par-fried potatoes. The oven used a stainless steel belt to continuously expose samples to a series of 500 W quartz-halogen radiant emitters. Five pairs of emitters were mounted on opposing sides of the belt (Fig. 1). Each pair of emitters was independently controlled and designed to expose the sample to a heating regime that reproduced the heat flux experienced during traditional oil immersion frying as outlined by Hubbard and Farkas (1999). The samples experienced an overall heating time of 180 s, which was found sufficient for adequate heating. The heat flux was measured in the oven by a optical radiometer, (model 900-9, Vatell, Christiansburg, VA), (Fig. 2). After leaving the oven, French fries were retained under a heat lamp (250W) for a maximum of four minutes.

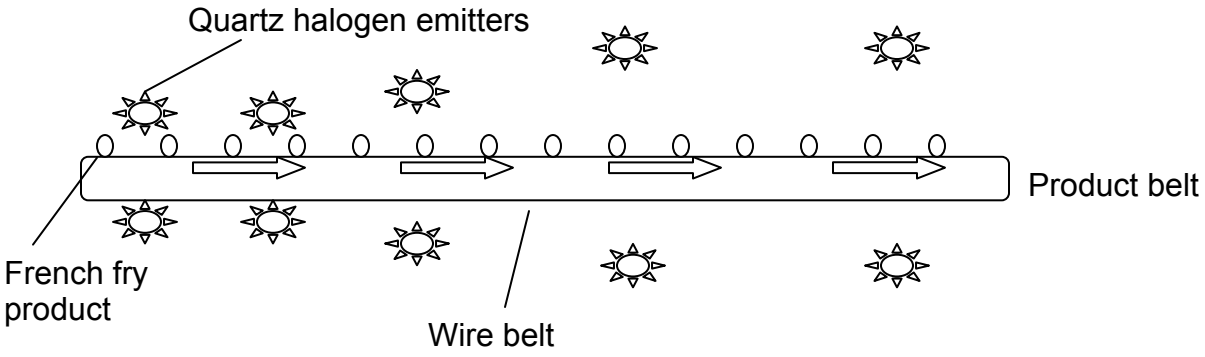

Figure 1. Simplified cross-section schematic of the experimental radiant heated oven. Notice emitter spacing increased along belt length to decrease heat flux impinging on French fries. Not to scale.

Product Quality Measurements: Texture, Color, Sensory Evaluation

French fry quality attributes were measured to evaluate the new dynamic radiant oven with other finish heating methods. Texture was measured using a TA.XT2 Texture Analyzer with a 5 kg load cell (Texture Technologies Corp., Scarsdale, NY/Stable Microsystems, Surrey, U.K.). The probe was a five blade Kramer shear cell. The Kramer shear method was found superior by Walter et al. (9) for a fried potato product.

French fry color was evaluated after each heat treatment using digital image analysis. A single fry was placed on a black background and a 2272 x 1704 pixel image was acquired using a digital camera (model MVC-CD400, Sony, Tokyo, Japan). The camera was mounted on a copy stand with the focal length, lighting,

and camera settings consistent for all samples. Histogram data was collected for mean and standard deviation of luminosity, lightness, and b-value of the extracted image. Measurement ranges were defined by 0 (completely black) to 255 (pure white) luminosity and lightness. The b-value scale was 0 (blue) to 255 (yellow). The b-value indicated the yellow to orangeness of the sample indicating the degree of browning of a French fry product.

Consumers of French fry were recruited to evaluate the acceptability of French fries using the three methods. Consumers (n=53) were volunteers solicited from North Carolina State University Department of Food Science students, staff, faculty, and guests. Each panelist was presented with a score sheet and each French fry sample monadically. Each panelist received and evaluated a single sample at a time in a predetermined randomized order. The evaluated attributes included: overall appearance liking; overall acceptability; overall flavor liking; overall texture liking; overall crispness intensity and liking; and overall oily mouthfeel and liking. The attributes were evaluated on a 9-point hedonic scale anchored on the left with dislike extremely and on the right with like extremely.

Temperature Measurements and Drying Rates

Raw Russet potato fries were cut into the 3/8" X 3/8" standard shoestring size (6). The length of each sample was trimmed to approximately 6 cm. Individual samples were prepared by inserting a thermocouple into the center. A thin 20 gauge shielded type T thermocouple was placed into a pre-drilled, central hole approximately 5 cm into the length of the sample. The thermocouple potato junction was sealed and anchored with a small drop of instant glue. The potato slice was then suspended by the thermocouple wire to an overhead balance to measure mass loss during heating. The sample was suspended in a quartz radiant heating system similar to the radiant oven.

The surface temperature of the potato sample was measured during heating using an infrared optical pyrometer (model OS65, Omega Engineering, Samford, Conn.). The pyrometer lens had a field of view of 24:1 and was focused at a 0.64 cm (¼ in.) diameter circle at 6 in. The small spot size ensured that only the sample surface temperature was measured.

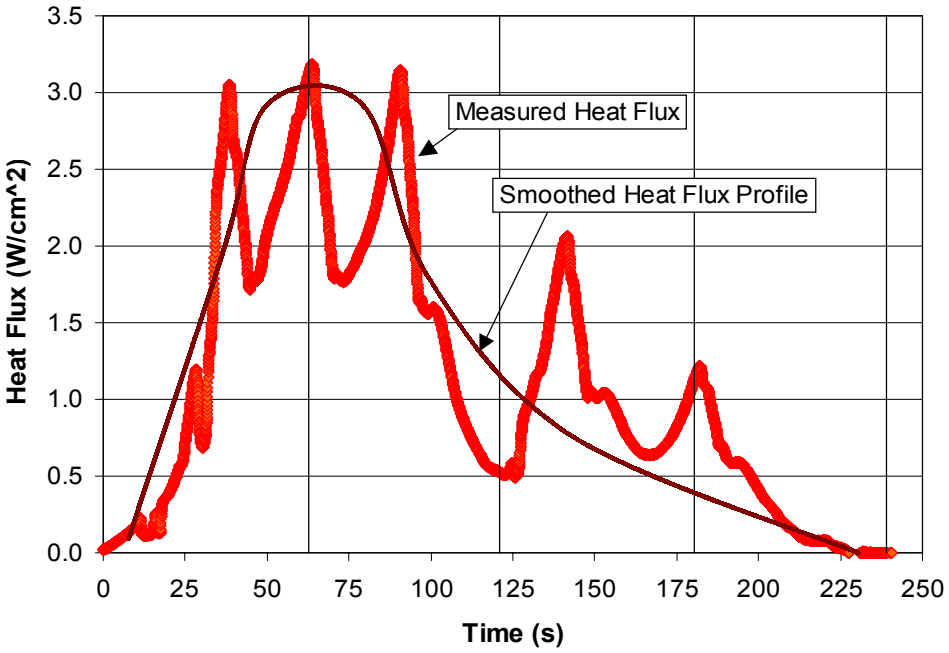

Fig. 2 Heat flux profile measured through experimental radiant oven.

Results and Discussion

Comparison of color measurements for finished samples indicated the degree of crust darkening (luminosity and lightness) and yellowness (b-value) could be used to distinguish between heating methods. Radiant heated product was equivalent to immersion fried in b-value, (Table 1). The Kramer shear test showed that radiant heated French fries had a significantly higher peak force ($p < 0.05$) than immersion fried or oven baked, (Table 1).

Table 1. Texture and color comparison of French fries prepared by three different finish heating methods. Presented values are the mean of 30 samples averaged from 3 batches. Like letters in each column indicate that there was not a significant difference ($p<0.05$) between means.

Heat Treatment	Peak Force (N)		Degree of Crust Darkening		Yellowness
	Mean	Stnd dev.	Luminosity	Lightness (L-value)	b-value
Uncooked par-fried	*	*	203.4[a]	209.9[a]	145.0[a]
Immersion Fried	21.3[a]	6.54	172.8[b]	183.7[b]	172.0[b]
Oven Baked	20.0[a]	4.91	172.6[b]	184.8[b]	178.2[c]
Radiant Heated	24.5[b]	4.71	177.7[b]	189.7[c]	171.1[b]

The radiant heated samples were equally acceptable to consumers as compared with the other two heating treatments with respect to overall appearance, flavor liking and oily mouthfeel liking (Table 2). Overall acceptability of each finish treatment showed that radiant heated fries were not statistically ($p<0.05$) different than traditional, full-fat immersion finished fried French fries.

Table 2. Mean hedonic consumer scores for par-fried French fries heated using different finishing heat treatments. Each value is the mean of 30 samples averaged from 3 batches. Like letters in each row indicate that there was not a significant difference ($p<0.05$) between means.

Attribute	Immersion Fried		Oven Baked		Radiant Heated	
	mean	stnd dev.	mean	stnd dev.	mean	stnd dev.
Overall Acceptability	5.94[a]	1.82	5.33[b]	1.87	5.67[a]	1.48
Overall Appearance Liking	6.30[a]	1.38	6.00[a]	1.74	5.92[a]	1.53
Overall Flavor Liking	5.45[a]	2.28	5.23[a]	1.90	5.56[a]	1.64
Overall Texture Liking	5.89[a]	1.89	5.67[ab]	2.01	5.19[b]	1.83
Overall Crispness Intensity	5.28[a]	2.09	5.00[ab]	2.36	4.40[b]	1.73
Overall Crispness Liking	5.53[a]	2.03	5.19[ab]	2.32	4.79[b]	1.96
Oily Mouthfeel Intensity	5.49[a]	1.75	4.83[b]	1.78	4.10[c]	1.80
Oily Mouthfeel Liking	5.49[a]	1.84	5.52[a]	1.80	5.90[a]	1.52

(n=53)

The surface and core temperature measurements (Fig. 3) of radiant heated raw French fries reveal radiant energy caused rapid temperature increase. The core temperature reached a plateau at approximately 105°C after approximately 100 s of heating, which is higher than the boiling point of water although Califano and Calvelo (10) routinely measured 103°C in the center of heated potato. The surface temperature increased to 160°C, which caused adequate crust formation.

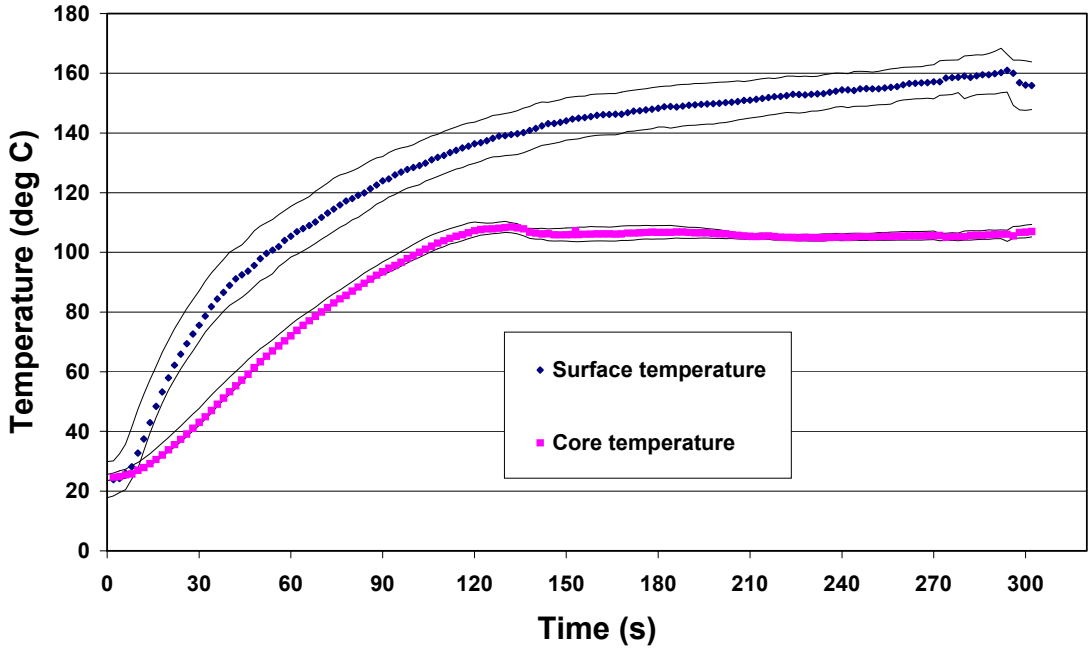

Fig. 3. Surface and core temperature of raw potato heated with constant 30,000 W/m^2 radiant energy. Included are 90% confidence intervals indicating measurement variability of ten sample measurements.

This research demonstrated that radiant finish heating of par-fried French fries shows promise to produce a lower fat product, as well as an alternative process to traditional immersion finish frying with equivalent quality indices.

References

1. USDA. Agricultural statistics for French fry production and consumption. USDA National Agricultural Statistics Service. www.usda.gov/nass. 2001.
2. McDonalds Corp. June 8, 2003. McDonald's USA nutrition facts for popular menu items. Oak Brook , IL.
3. USDA. Code of Federal Regulations, Nutrition labeling of food. Title 21. Section 101.9. 2003.
4. Myers, M. USPB to share commitment to improving the potato's nutrition image with top three processors. United States Potato Board press release. Denver, CO July 7, 2003.
5. Sloan, A.E. Top 10 trends to watch and work on: 2003. Food Technology, 57, 4, 30-50, 2003.
6. Gould, W.A. Potato production, processing, and technology. Timonium, MA: CTI Publ. Inc. 1999
7. Hubbard, L.J. and B.E. Farkas. A method for determining the convective heat transfer coefficient during immersion frying. J. of Food Process Engineering, 22, 201-214, 1999.
8. AOAC International. 984.25 and 963.15. *Official Methods of Analysis, 16th Ed.* AOAC International, Gaithersburg, MD. 1995.
9. Walter, W.M., Truong, V.D., Espinel, K.R.. Textural measurements and product quality of restructured sweetpotato French fries. Lebensm-Wiss. u.-Technol., 35, 3, 209-215, 2002.
10. Califano, A.N. and A. Calvelo. Thermal conductivity of potato between 50 and 100°C. J. Food Sci. 56, 2, 586-587, 589, 1991.